University of Alberta

Engineering Surface-tethered Bacteriocins for Studying Peptide-bacteria Interactions

By

Hashem Etayash

A thesis submitted to the Faculty of Graduate Studies and Research

in partial fulfillment of the requirements for the degree of

Master of Science

In

Pharmaceutical Sciences

Faculty of Pharmacy and Pharmaceutical Sciences

Spring 2013

Edmonton, Alberta

Dedications

I would like to dedicate my thesis to my precious parents, ***My Dad,*** ***Rajab,*** *and My* ***Mom, Azeza****. They were always here for me side by side with their supports, encouragements and prayers. Also I dedicate it to All My brothers and sisters who always been here with their love, compassions and inspirations.*

Abstract

Identification and quantification of pathogenic bacteria has become one of the key elements in biodefense, food safety, diagnostic and drug discovery. The aim of the thesis is to investigate interactions between bacteria and peptides in order to utilize the potential of antimicrobial peptides (AMPs) in specific recognition of pathogenic bacteria. Leucocin A (LeuA) is an AMP that exhibits specific activity against *L. monocytogenes* at nanomolar concentrations. Here, we have synthesized full length LeuA and a shorter fragment using solid phase peptide synthesis. The peptides were characterized and individually immobilized on gold substrate. The bacterial specificity of the anchored peptides was tested against various strains and the results reveal that the adsorbed AMPs display significant binding towards Gram-positive bacteria with various binding affinities from one strain to another. Further, molecular dynamics simulation studies were conducted to provide atomistic insight on the mechanism of peptide-peptide and peptide lipid interactions in a membrane mimicking environment.

Acknowledgements

I would like to acknowledge all the people, who have been always here for me throughout my Master's program, and who have helped me in many different ways to reach my goal.

First of all, tremendous acknowledgment and much-much appreciation go to my thesis advisor Dr. Kamaljit Kaur for giving me this opportunity to work in this exciting project. Thanks for her fabulous support, guidance, and affection which helped me being focused on my research. ***Next,*** I would like to express my gratitude and thankful to Dr. Thomas Thundat for his valuable discussion, encouragement and guidance throughout my project. Collaboration with him has motivated me to focus in my research and to address my future research direction. ***To the same group***, many thanks to my excellent collaborator Dr. Lana Norman; her help, support, cooperation has assisted me finishing my thesis-project and doing most of the work I have done. Thanks so much Lana☺. ***Also,*** acknowledgments and gratefulness go to my advisory committee members Dr. Lavasanifar and Dr. Carlos Velázquez for their guidance, their support and their treasured discussions. ***Much gratitude*** goes to CanBiocin members for allowing me to use their facilities to perform the antimicrobial studies and providing me with the bacterial indicators. To Dr. Liru Wang in particular many-many thanks for all valuable discussion and advises all through my project. ***I would also*** like to show my gratitude to my current and previous lab members, Dr. Rania Soudy, Dr. Sahar Ahmed, Dr. Wael Soliman, and Dr. Krishna Bodapati for the great support and useful discussion they have given me all the way through my program. Their help and support always have been a great inspiration. ***I will never forget to*** acknowledge Libyan Government for the financial support during my program. And Libyan-North American Scholarship Program, **CBIE**, for their support, magnificent coordination, and assistance. NSERC and the Faculty of Pharmacy and Pharmaceutical Sciences, University of Alberta have all the acknowledgement and thankfulness.

Table of Contents

List of Tables

List of Figures

Schemes

List of Abbreviations

AA	Amino acid
AMP	Antimicrobial peptide
AMPs	Antimicrobial peptides
BOP	Benzotriazol-1-yloxy-tris (dimethyl amino)-phosphonium hexafluorophosphate
CD	Circular dichroism
CDC	Centre for Disease Control
Cl^-	Chloride ion
DCM	Dichloromethane
DdH_2O	Double distilled water
DIC	1, 3-diisopropylcarbodiimide
DMF	*N*,*N*-dimethylformamide
DIPEA	N,N-diisopropylethylamine
DMSO	Dimethylsulfoxide
DNA	Deoxyribonucleic acid
DPC	Dynamic poly conjugates
FDA	Food and drug administration
Fmoc	9-Fluorenylmethoxycarbonyl
GIT	Gastrointestinal tract
GROMACS	Groningen-MAchine for Chemical Simulations
HBTU	*O*-Benzotriazole-*N*,*N*,*N*,*N*-tetramethyl-uranium hexafluorophosphate
HCTU	1H-Benzotriazolium 1-[bis(dimethylamino)methylene] -5chloro-,hexafluorophosphate (1-),3-oxide

HOBt	N-Hydroxybenzotriazole
HPLC	High Performance Liquid Chromatography
IPA	Isopropyl alcohol
K	Kelvin
L	Liter
LAB	Lactic acid bacteria
LeuA	Leucocin A
LINCS	Linear Constraint Solver
M	Molar
MALDI	Matrix-assisted laser desorption/ionization
Man-PTS	Mannose -phosphotransferase System
MD	Molecular dynamic simulations
MDR	Multi Drug Resistance
Mg	Milligram
Min	Minute
mL	Milliliter
mM	Milimolar
Mpt	Mannose phosphotransferase
MS	Mass spectrometry
Na^+	Sodium ion
NaCl	Sodium chloride
NCL	Native chemical ligation
Nm	Nanometer
NMM	N-methylmorpholine
NMP	N-methyl-2-pyrrolidinone

NMR	Nuclear magnetic resonance
Ns	Nanosecond
PBS	Phosphate buffer saline
PDB	Protein Data Bank
PI	Peptide interaction
PIs	Peptide interactions
PLIs	Peptide lipid interaction
PPIs	Peptide-peptide interactions
PRIs	Peptide receptor interactions
RNA	Ribonucleic acid
SPPS	Solid phase peptide synthesis
TFA	Triflouroacetic acid
TFE	Triflouroethanol
TOF	Time of flight
UV	Ultraviolet
Vis	Visible
VMD	Virtual Molecular Dynamics

Chapter 1: Introduction

1.1 Bacteriocins

1.1.1 Definition and significance

Bacteriocins are cationic, ribosomally synthesized antimicrobial peptides (AMPs), exported and secreted by both gram-positive and gram-negative bacteria [1-6]. Various bacteriocins are produced by food-grade Lactic acid bacteria (LAB), which offers the possibilities of manipulating food microbial ecosystems in a deliberate fashion-for instance, by using these AMPs to prevent foods from contamination, and/or inhibit growth of specific microorganisms. LAB is a gram-positive organism that produces a large variety of bacteriocins with molecular masses ranging from 2500 to 6000 Da [1]. These self-defense AMPs are synthesized together with a cognate immunity protein that renders the bacteriocins-produced bacteria the immunity to defense against their own bacteriocins [7, 8]. Bacteriocins have shown a substantial promise as antibacterial agents and safe alternative therapy of antibiotics [9]. The use of bacteriocins as food preservatives was reported for the first time in 1950 [10]. Nisin (class I bacteriocin) was the first LAB-AMP approved for marketing as a food preserving product [1].

Food processors nowadays face a huge challenge concerning shelf-life of the products, as well as, risks associated with concomitant use of chemical products such as preservatives and additives. Bacteriocins in this manner are

considered an attractive choice as a food-grade preservative that could provide at least part of the solution. Bacteriocins can inhibit various strains of food pathogenic bacteria, and kill several spoilage organisms that might cause food contamination and decrease the shelf-life of the processed products. At the present time, Nisin and Pediocin PA-1 are the only bacteriocins that are applied as bio-preservatives in food industry; the former was approved in over 40 countries for use as food additives [1]. The term Nisin was used most widely in food as Nisaplin (Danisco)®, which is a preparation that contains 2.5% Nisin with NaCl (77.5%), and non-fat dried milk (12% protein and 6% carbohydrate). On the other hand, pediocin PA-1 has a commercial name ALTA 2431 (Quest) ®, which is based on LAB fermentates generated from PA-1 produced strain *Pediococcus acidilactici* [11, 12].

Bacteriocins can also be used to promote value and quality of the foods, rather than just simply preventing spoilage or safety problems [13]. Furthermore, in the near future food might simply act as a vehicle for the delivery of bacteriocin-producing probiotic bacteria. The production of antimicrobials by a probiotic culture is a desirable trait as they are thought to contribute to the inhibition of pathogenic bacteria in the gut, whereas bacteriocins in food are degraded by the proteolytic enzymes of the stomach [14, 15]. Probiotic bacteria might be ingested in a form that facilitates gastric transit, allowing the *in vivo* production of the bacteriocin in the small or large intestine. It has also been speculated that recombinant probiotic strains that can be induced to produce

bacteriolysin could be developed to facilitate the *in vivo* delivery of bioactive compounds that are produced intracellularly [16].

The hot spot for application of bacteriocins for food safety could be using bacteriocins for specific detection of bacteria in contaminated foods. We are addressing here in this thesis a preliminary study towards detection of gram-positive bacteria and specifically for detection of *Listeria monocytogenes* using Leucocin A, a listeria-sensitive AMP. Class IIa bacteriocin, Leucocin A will be the focus of this approach, and the detection system will be based on applying Leucocin A or Leucocin A fragment as a sensitive molecular recognition element.

1.2.2 Classification of bacteriocins

Several classifications have been proposed for bacteriocins according to their biochemical and genetic properties [1, 6, 17, 18], Class I peptides are the Lantibiotics (lanthionine-containing peptides), class II peptides, which will be our focus in this study, are unmodified peptides except for the disulfide bridge. Class III peptides are high molecular weight, thermo-sensitive antimicrobial agents [17].

Class I bacteriocins, are small antimicrobial peptides (19-38 amino acids in length) known as Lantibiotics. They contain either lanthionine or *β*-methyllanthionine residues in their structures as a result of a post-translational processing which form covalent bridges between specific amino acid residues in their amino acids sequences [19]. Furthermore, Lantibiotics can also contain other unusual residues by post-translational modifications of D-alanines for L-serines

[20, 21]. Lantibiotic has been classified into two sub-classes according to their chemical structures, and modes of action, **(A)** elongated Lantibiotics are amphiphilic cationic peptides, with molecular weight < 4KDa, act by pore formation in the cellular membrane of the target cells (for example, Nisin). **(B)** Globular Lantibiotics (for example, mersacidine) were defined as AMPs with molecular masses ranging from 1.8 to 2.4 KDa that act through enzyme inhibition [2, 22, 23].

Class II bacteriocins *(non-lanthionine-containing bacteriocins),* are small < 10 KDa, cationic, heat stable AMPs. Unlike class I bacteriocins, they are not subjected to post-translational modifications. The majority of these peptides act at nano-molar ranges by inducing a membrane permeabilization on the target cell membrane. Several sub-groups have been suggested for class II bacteriocins [6, 18, 24]; however, the main two types that are common in all classification systems are class IIa (pediocin–like or antilisterial bacteriocins), and class IIb (two-peptide bacteriocins) [2].

Class IIa bacteriocins *(pediocin-like bacteriocins or antilisterial AMPs)*: Since past few years, class IIa bacteriocins have gained a great interest as the most significant class of LAB produced antimicrobial peptides for their use in food preservations and medicine [25]. Class II peptides complement antibiotics in treating infectious diseases [26] and have antiviral properties [27]. Class IIa bacteriocins target a narrow spectrum of bacteria; nevertheless, they exhibit high level of activity against *Listeria monocytogenes*, one of the most fatal foodborne pathogens [28]. The sequence alignment of class IIa bacteriocins reveals that the

peptides consist of two domains, a conserved N-terminal domain with a YGNGV sequence, and disulfide bridge, while a C-terminal domain showing more variability in their amino acid sequences, ending with a structurally extended C-terminal tail (hairpin-like structure) [12, 25, 29, 30]. **Table 1.1** lists amino acid sequences of some class IIa bacteriocins, and highlights the conserved residues.

Despite the differences in Class II bacteriocins amino acid sequences, their C-termini preserve an amphiphilic α-helical structure, which has been found to play a very crucial role in bacteriocins' antimicrobial activity [31-33]. Moreover, the hydrophobic surface of the helix is believed to interact with a lipid membrane of the target cell and ultimately binds to a specific membrane-bound receptor [31-34].

Table 1.1. Amino acid Sequences of several AMPs of class IIa bacteriocins. Underlined cysteine residues are those involved in disulfide bond formation. Conserved residues are shown on bold [2].

Peptides	***Amino acid sequence***
	1 10 20 30 40
Mesentericin Y105	K**YYGN**GVHCTKSGCSVN**W**GEAASAGIHRLANGGNGFW
Leucocin A	K**YYGN**GVHCTKSGCSVN**W**GEAFSAGVHRLANGGNGFW
Sakacin P	K**YYGN**GVHCGKHSCYVD**W**GTAIGNIGNNAAANWATGWNAGG
Curvacin A	ARS**YGN**GVYCNNKKCWV**N**RGEATQSIIGGMISGWASGLAGM
Carnobacteriocin	V**NYGN**GVSCSKTKCSVN**W**GQAFQERYTAGINSFVSGVASGAGSIGR
Pediocin PA-1	**KYYGN**GVTCGKHSCSVD**W**GKATTCIINNGAMAWATGGHQGNHKC

The structural features of four pediocin-like bacteriocins have been elucidated by NMR spectroscopy, Leucocin A [35], carnobacteriocinB2 [36], sakacin P [30], and curvacin A [37] (**Figure. 1.1**). The NMR solution structures

of class IIa bacteriocins reveal that, the peptides consist of N-terminal β-sheet stabilized by conserved disulfide bridges between two amino acid cysteines. Few of class IIa bacteriocins have β-sheet-like structure on the C-terminal region such as pediocin PA-1, sakacin G, plantaricin 423, and enterocin A. These AMPs contain an additional C-terminal disulfide bridge which plays an important role in stabilizing the three dimensional structure of the C-terminal domain [29, 30]. Also it was suggested that structurally stabilized bacteriocins display higher antimicrobial potencies than those containing only one disulfide bridge, especially at higher temperature [38, 39].

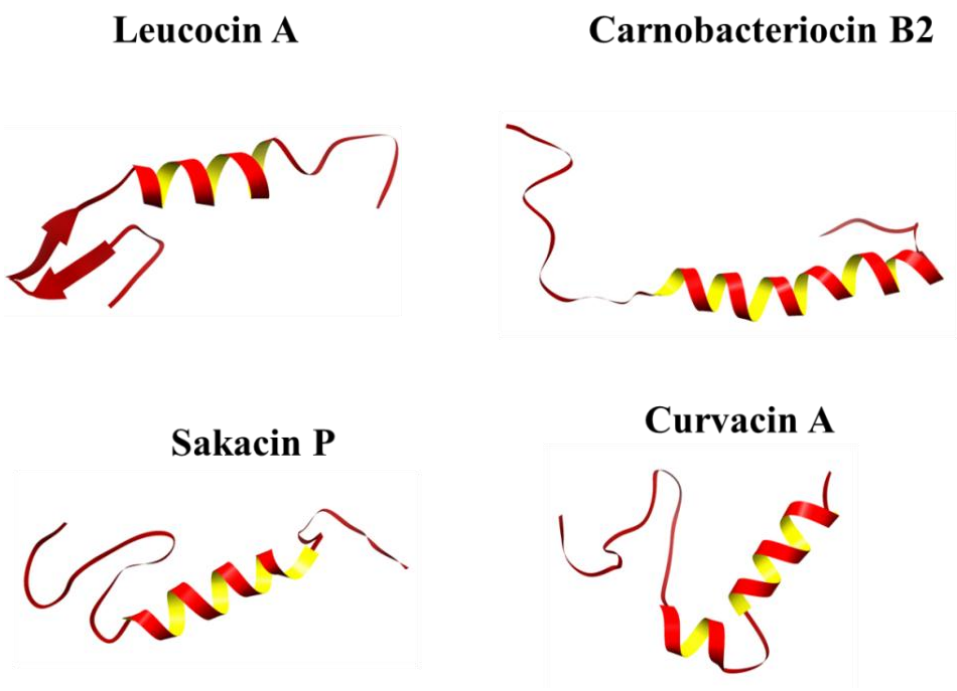

Figure 1.1. Three dimensional NMR structures of four representative peptides of class IIa bacteriocins. Leucocin A [35], Carnobacteriocin B2 [36], Sakacin P [30], and Curvacin A [37].

Class IIb two-peptide bacteriocins, are cationic antimicrobial peptides, consisting of two different peptides which act synergistically, and the genes

producing them are placed next to each other on the same operon. The optimal antimicrobial activity is achieved by presence of these peptides together and in equal amounts, and generally the peptides act at pico to nano molar range of concentrations. Low or no biological activity was detected when those peptides was assayed individually even at micro-molar concentrations [8]. Molecular dynamic simulation studies [40] and gene encoding studies of these peptides showed that the synergistic action of these two peptides is due to the fact that they interact with each other and form a single antibacterial unit rather than individually act on the target cell membrane [8, 41, 42]. Technically, class IIb two-peptide bacteriocins act by disrupting the membrane potential of the target bacterial cell [41-43].

Table 1.2. Amino acid sequences of some unmodified (class-IIb) two-peptide bacteriocins. The GxxxG and AxxxA motifs are shown in bold with grey shading.

Peptide	Abb.	Amino acid sequence
Lactococcin G	LcnG-α	GTWDDI**GQGIG**RVAYWV**GKAMG**NMSDVNQASRINRKKKH
	LcnG-β	KKWGWLAWVDPAYEFIK**GFGKG**AIKEGNKDKWKNI
Plantaricin E/F	PlnE	FNRG**GYNFG**KSVRHVVDAI**GSVAG**IRGILKSIR
	PlnF	VFHAYSARGVRNNYKSAVGPADWVISAVR**GFIHG**
Plantaricin J/K	PlnJ	GAWKNFWSSLRK**GFYDG**EAGRAIRR
	PlnK	RRSRKNGI**GYAIGYAFG**AVERAVLGGSRDYNK
Plantaricin S	Pls-α	RNKLAYNM**GHYAG**KATIFGLAAWALLA
	Pls-β	KKKKQSWYA**AAGDA**IVSFGEGFLNAW

Several AMPs of class IIb two-peptide bacteriocins have been isolated and characterized (**Table. 1.2**), and the first isolated peptide was Lactococcin G

(LcnG) in 1992 [44]. CD studies have shown that these AMPs interact and structure themselves in membrane-mimicking environments such as liposomes and/or triflouroethanol (TFE) [45]. However, they attend to be unstructured in water. In other words, CD experiments have elucidated that when those complementary peptides were mixed and then exposed to membrane-simulating entities, an additional structure will be acquired i.e. peptide-peptide communication to form one functional unit. Result emphasizes that the peptides are in structure-inducing manners upon contact with the membrane of the target cell [45]. So far, the direct interaction between the two complementary peptides has not been clarified by NMR. The three dimensional structures were reported only for three peptides of class IIb two-peptide bacteriocins, Lactococcin G [46], plantaricin JK [47], and plantaricin EF [48]. In addition, the homology structure of plantaricin S was reported by our lab in 2011 [40], see **Figure 1.2**.

Class IIc (cyclic bacteriocins), these bacteriocins are characterized by unique features such that, the N and C termini are covalently linked together to form cyclic AMP [49, 50]. Although few peptides of this class have been identified, the most well-known class IIc bacteriocins are enterocin AS48, circularin A, and gassericin A [49].

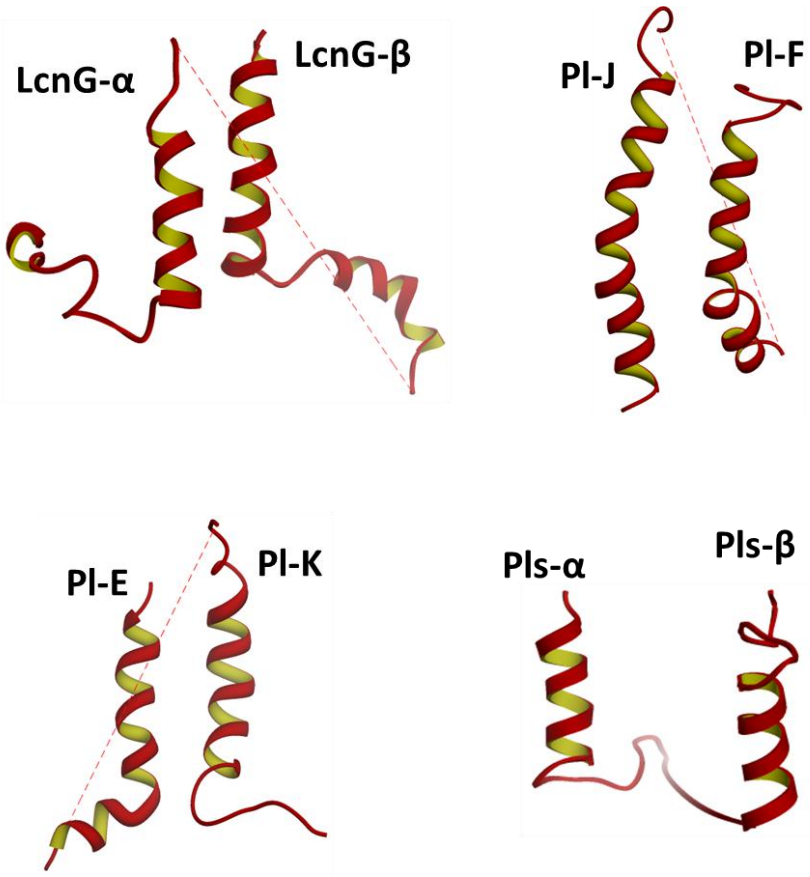

Figure 1.2. NMR solution structures in DPC of three AMPs of class IIb two-peptide bacteriocins, Lactococcin G (LcnG-, and LcnG-), Plantaricin EF (Pl-E, and Pl-F), Plantaricin JK (Pl-J, and Pl-K) and Plantaricin S (Pls-α and Pls-β).

Class III bacteriocins (Non-bacteriocins-lytic proteins), are also known as bacteriolysins. They are very large, sensitive, thermo-labile antimicrobial peptides produced by LAB and non-LAB microorganisms. Only four of LAB-bacteriolysins have been reported and characterized [51, 52], although others which are non-LAB produced have been identified and studied [43, 53, 54]. Interestingly, those peptide bacteriocins are distinctive from true bacteriocins as they function through lysis of the sensitive cells by catalyzing the cell-wall

hydrolysis. Furthermore, unlike other bacteriocins, they do not always have the immunity genes that accompanied bacteriocins structural genes [51, 52].

1.1.3 Spectrum of Activity

Bacteriocins in general have wide spectrum of activity against various bacterial strains, gram-positive and gram-negative bacteria. The activity has been illustrated against bacteria, viruses, and cancer cells [27, 55-57]. Interestingly, certain classes of bacteriocins have shown very narrow spectrum of activity; class IIa bacteriocins for instance, have quite limited spectrum of activity against bacteria compared to other bacteriocins produced by gram-positive bacteria. However, they express very high level of activity at pico-nano molar concentrations [58, 59]. Early studies have suggested that this might be related to the interaction of the peptides with specific molecules at the surface of the target cells [60, 61]. Moreover, with respect to their spectrum of activity, class IIa bacteriocins have shown very strong potencies against *Listeria monocytogenes* in nano to pico molar scales [26, 28, 58, 59]. Despite their structural similarities, class IIa bacteriocins differ markedly in their spectrum of activity, and that has been suggested as a result of their interactions with specific receptors on the target cell membrane. These receptors were revealed to be the mannose phosphotransferase (man-PTS) subfamily, which is suggested to act as membrane-bound receptors on the target cell [34, 58, 61]. The MIC values of some AMPs of class IIa bacteriocins are demonstrated on **Table 1.3**.

The antibacterial activity of bacteriocins depends on at least two steps for its *in vivo* functionality. In the first step, bacteriocins interact with bacterial surface through immediate contact with the membrane, and/or via membrane bound receptor. In the second step, permeabilization of the target membrane occurs by pore formation [2]. The initial binding might be influenced by envelope composition of the target cells, envelope charges, presence, availability, and structure of the putative target molecule (receptor). The secondary step is likely relying on membrane composition and immunity proteins [2].

Table 1.3. Activities of some class IIa bacteriocins toward various indicator strains.

Indicator strains	Sensitivity (MIC, μg/ml)			
	Pediocin PA-1	Curvacin A	Sakacin P	Enterocin
C. divergens NCDO 2306	0.0027	0.017	0.0015	0.0017
L.monocytogenes				
LMG 2801	0.0033	0.040	0.0034	0.0005
LMG 2802	0.0013	0.028	0.0034	0.0002
LMG 2650	0.0047	*0.049*	*0.0073*	0.0008
LMG 2651	0.0029	0.028	0.0036	0.0006
LMG 2652	0.0050	0.030	0.0068	0.0004
LMG 2653	0.0050	0.049	0.0068	0.0008
L. innocua LMG 2654	0.0031	0.026	0.0057	0.0003
L. ivanovii LMG 2803	0.0006	0.0092	0.0002	0.0001

1.1.4 Peptide Interaction (PI)

1.1.4.1 Peptide-lipid interaction (PLI)

Peptide-lipid interaction is defined as influence of the peptide on the state characteristic of the lipid and/or vice versa. Studying protein and/or peptide interactions with lipid-membranes has also been one of the main challenges due to the difficulties encountered in different experimental settings. In peptide-lipid interaction, specific binding sites are always involved; however, the non-specific binding cannot be excluded. In the last decades, studying lipid interactions with the peptide/proteins have received a great attention due to their importance; therefore, several modeling systems have been investigated and designed to mimic the lipid-membrane of the living cells. Many lipid bilayers were designed and elaborated to have the same properties, characteristic and atmosphere of the live cells [62-64].

1.1.3.2 Peptide-peptide interaction (PPI)

Peptide-peptide interaction is a physical phenomenon by which molecular docking between two or more peptides/parts of proteins take place. This interaction could take place *in vivo* (living cells) in common, and/or *in vitro* (experimentally such as in membrane-mimicking environments). Peptide-peptide and/or peptide/protein interactions were proved to play a pivotal rule in almost all the biological processes in the body. PPI interaction might occur as a part of protein complex formation and to obtain a new compound. In case of

peptide/protein transportation for instance, PPI could act as a carrier to transport peptides and/or proteins between the biological organs in the living cells [65, 66].

PPI, interestingly, observed in the antimicrobial peptides to enhance or produce a new biological active polypeptide. In class IIb two-peptide bacteriocins for instance, two peptides interact with each other in equal amounts to produce one functional unit antimicrobial peptide (Lactococcin G) [8, 41]. In general, PPI is very fundamental process in many biological, physiological, and pathological processes in the living cell. Studying and understanding the mechanisms of PPI and its role in many biological processes helps us to improve our knowledge and understanding of different diseases and provides new approaches for developing novel therapeutic [67].

1.1.4.3 Peptide-receptor interaction

The fact that bacteriocins display a well-defined inhibitory spectrum strongly suggests that individual bacteriocin recognize specific receptor on the target cells. Previous studies have shown that several AMPs of class I (Lantibiotics) and other non-Lantibiotics Lactococcin 972 employ a specific precursor in cell wall synthesis (lipid II) as a docking molecule and/or a binding receptor. Attachment of bacteriocins with lipid II leads to inhibition of cell wall synthesis, and/or pore formation [68-70]. Likewise, several studies have elucidated that; one protein known as mannose phosphotransferase permease (man-PTS) could serve as a primary target receptor for class IIa bacteriocins based on some observations of

mutagenesis studies [71-74]. For example, direct mutagenesis of *mpt* operons of both *L.monocytogenes* and *E. faecalis* led to resistance of these bacteria to class IIa bacteriocins [71, 75]. Furthermore, high-level resistance to mesentericin Y105 and other class IIa bacteriocins results from the loss of *mpt* expression either in defined mutants or in spontaneous resistant strains [72]. It is well-known that man-PTS is a transporter family responsible for transport sugars (mannose and glucose), as well as, concomitant phosphorylation process inside the bacteria [76]. It has been classified into four subclasses or domains, cytoplasmic domains include class IIA and IIB, which involved in the phosphorylation. Membrane domains include class IIC and IID and they are involved in membrane transportation [76]. Expression of the genes encoding these four subunits is coordinated, as they are commonly clustered in one operon [77].

In a comparative two-dimensional gel study, results revealed that Leucocin A-resistant cells are generated from Leucocin A-sensitive listerial strains lacked the MptA subunit of this protein [72]. Moreover, heterologous expression of the MptC subunit of the mannose phosphotransferase permease in an insensitive strain of Lactococcus lactis rendered the strain sensitive to several class IIa bacteriocins [74]. A more recent study showed that pediocin-like bacteriocins in fact bind to a part of the mannose phosphotransferase permease (the MptC and/or MptD subunit) that is embedded in the cell membrane [78]. Same studies have also shown that immunity proteins that protect cells from being killed by pediocin-like bacteriocins bind strongly to the man-PTS complex and thereby prevent death of the bacteria. Interactions between pediocin-like

bacteriocins and the man-PTS thus apparently alter the conformation of the permease in a manner that results in membrane leakage, and this leakage may be blocked on the cytosolic side of the membrane by the binding of an immunity protein to the bacteriocin-permease complex. **Figure 1.3** shows a cartoon depiction of protein-receptor and immunity protein receptor interaction.

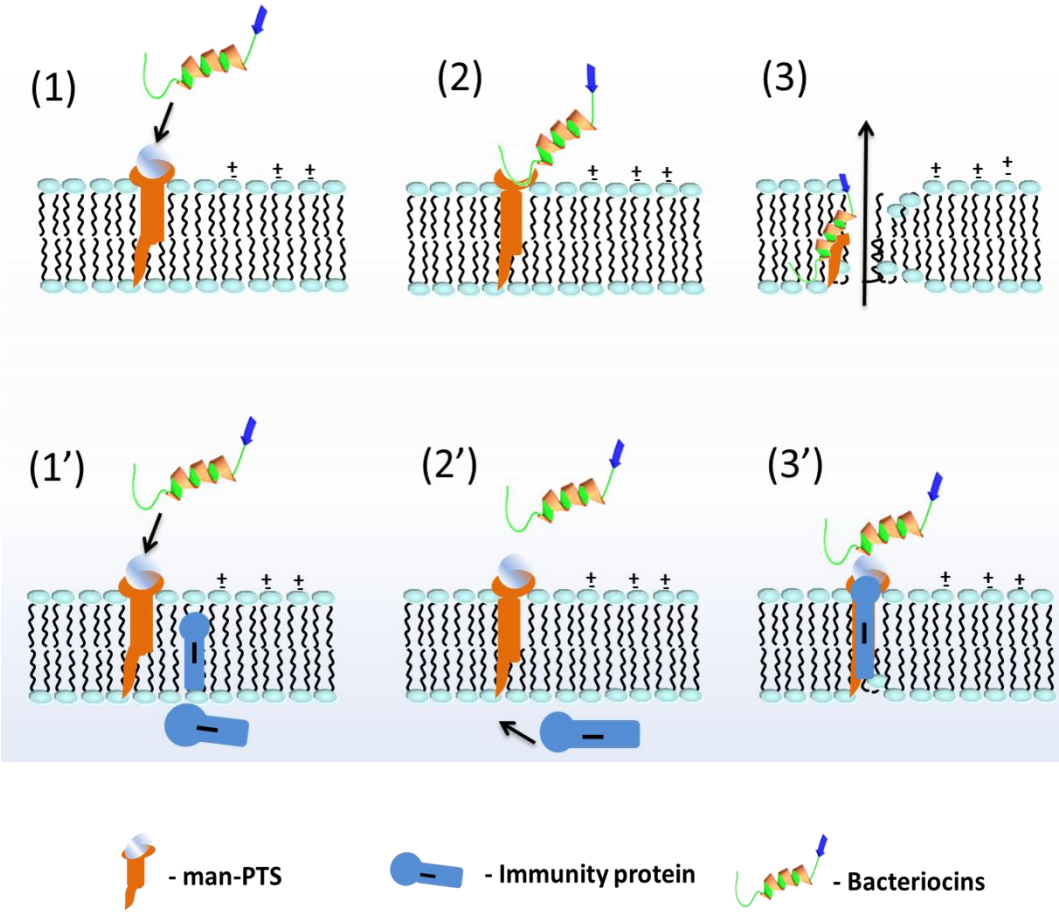

Figure 1.3. A Cartoon depiction of peptide-man-PTS, and immunity protein-man-PTS interactions for pediocin-like bacteriocins **(A)** the bacteriocin employs IIC and IID of the man-PTS as a receptor on target cells (states 1 and 2). After binding, the bound bacteriocin somehow triggers permeabilization of the membrane (state 3), causing leakage of cellular components and, eventually, cell death. **(B)** In immune cells without bacteriocin production, the immunity protein (I) is not tightly associated with the man-PTS (state 1'). Only when exogenous bacteriocin is added to the culture medium (state 2'), the immunity protein approaches and binds strongly the target proteins (IIC and IID).

The cells are thereby protected, probably through the blocking of the bound bacteriocin molecules, from advancing to the subsequent steps that lead to cell death (state 3') [78])

1.2 Chemical Synthesis

Availability of bacteriocins and their analogues in pure forms and in large quantities is one of the main drawbacks that hinder their application as potential antibiotics and as food preservatives. In this regard, extensive studies and several methods have been performed and designed to chemically synthesize these peptides.

Methods of peptide synthesis have been divided mainly into two categories, solution (classical) method and solid phase peptide synthesis (SPPS). The classical method was introduced in the early twentieth century; it was described amply in several reviews and books "Wunsch, 1974; Finn and Hofmann 1976; Coodman et al 2001" [79]. Solution synthesis retains value in large-scales manufacturing and for special laboratories applications; however, the need to optimize the reaction conditions, yields, and purification difficulties render this classical technique quite difficult, time consuming, inconvenient, and labor intensive [80-82]. SPPS, on the other hand, was conceived and elaborated by R. B. Merrifield beginning in 1960s [83] and has some advantages over the classical method. It gives higher yield, low racemization, and easy handling [83]. The concept of SPPS (**Scheme 1.1**) based on covalent anchoring of monomer amino acid to insoluble polymeric support (resin) by specific reactions (protection scheme). The anchored peptide then extended "elongated" by series of addition

(deprotection, coupling) cycles. Once the desirable chain elongation is achieved the crude peptide is released (cleaved) from the supporting polymer under certain conditions. It is necessary to release (cleave) the crude peptide from the support under conditions that are minimally destructive towards sensitive residues in the peptide sequence [84, 85].

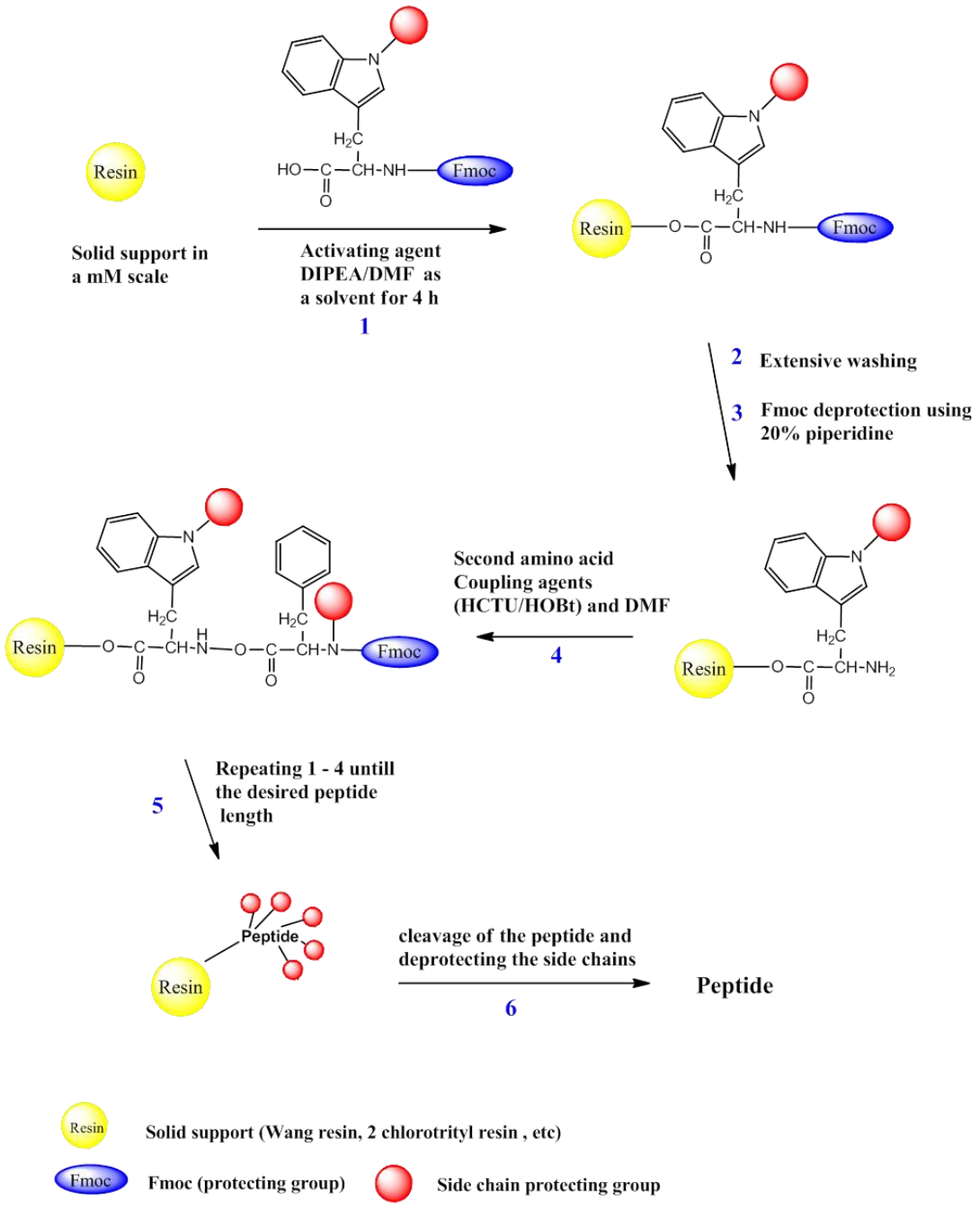

Scheme 1.1. General protocol for solid phase peptide synthesis (SPPS) based on Fmoc-chemistry.

Although SPPS is very effective, efficient, and easy method for peptide synthesis, it has its own limitations and the most severe disadvantage of SPPS is

that only small protein molecules that are comprised of a maximum of approximately 50 amino acids in length can be efficiently synthesized [85].

To overcome these limitations Dawson et al [86] proposed a new strategy for synthesizing long peptides that is known as native chemical ligation (NCL). This technique is based on assembling of two or more unprotected peptide segments to construct a larger polypeptide (**Scheme. 1.2**). NCL has several advantages over stepwise SPPS such as higher purity, yields, and low aggregation/truncations as well as very low racemization [86]. Simply, mechanism of NCL involves a reversible transthioesterfication as a first step (chemo-selective reaction). In this reaction, a thiolated group of an N-terminal cysteine of unprotected fragment attaches a C-terminal thioester of another unprotected fragment, and this leads to form a thioester intermediate. This thioester intermediate will rearrange by *S*, *N*-acyl shift/or migration that results in the formation of a native amide bond (**Scheme 1.2**).

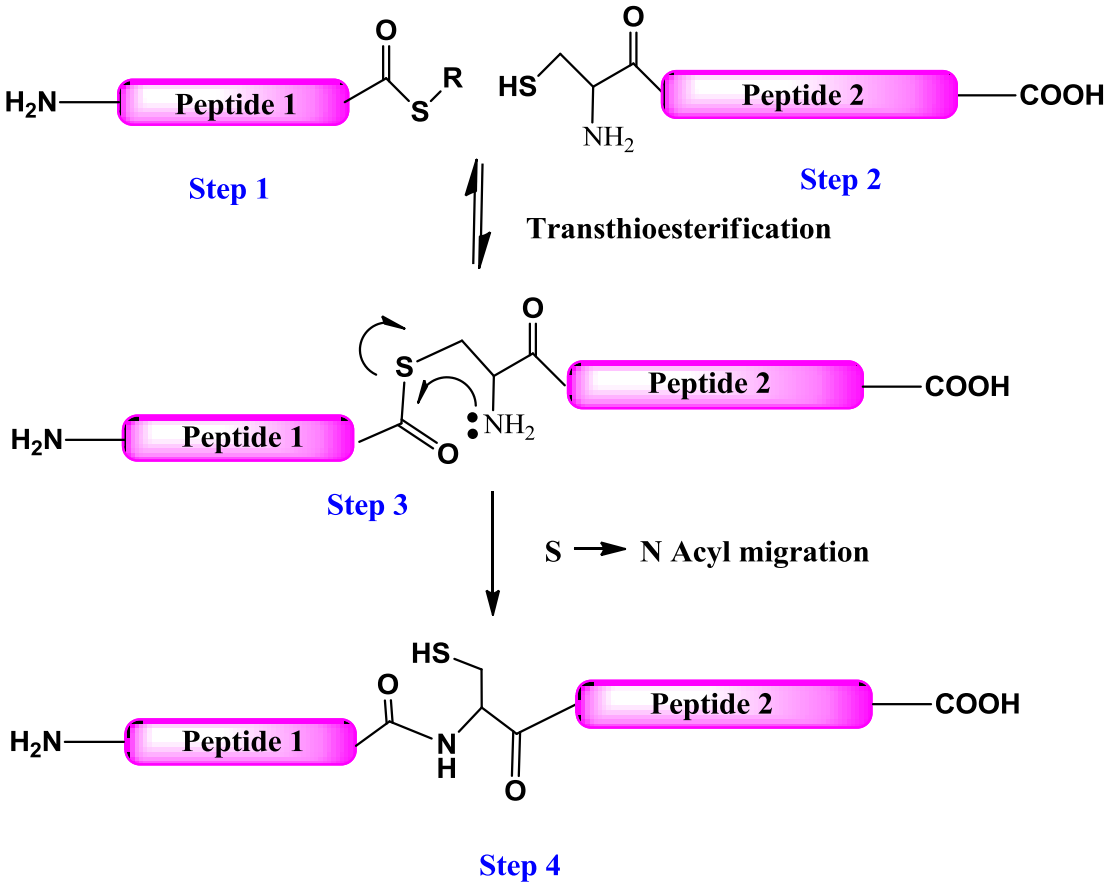

Scheme 1.2. Schematic representation of the mechanism of native chemical ligation; **(1)** first peptide (thiolated N-terminal cysteine) attacks **(2)** the second peptide (C-terminal thioester) in thioesterfication process. (3) Intramolecular N, S-acyl shift. **(4)** Formation of the ligated peptide.

1.3 Detection of Foodborne Pathogens

In recent years, diseases and productivity losses caused by foodborne pathogenic bacteria have attracted substantial attention. Thousands of foodborne pathogenic bacteria were found to affect the health and safety of the world's populations of humans, animals and plants. Among these bacteria, *Campylobacter*, *Salmonella, Listeria monocytogenes, Escherichia coli (E. coli) O157:H7, Staphylococcus aureus*, and *Bacillus cereus* are the major foodborne pathogen bacteria, which are

responsible for the majority of foodborne illness outbreaks [87-91]. Therefore, it is of great importance to develop methods for early detection of foodborne pathogenic bacteria.

1.3.1 Techniques Used for Detection of Bacteria in Foods

The rapid detection of bacteria and other pathogens contaminants in food is crucial for ensuring the safety of consumers. Traditional methods to detect foodborne bacteria often rely on time-consuming growth in culture media, followed by isolation, biochemical identification, and sometimes serological studies.

Recent advances in technology; however, make detection and identification faster, more convenient, more sensitive, and more specific than conventional assays. These new methods are often referred to as "rapid methods", a subjective term used loosely to describe a vast array of tests that includes miniaturized biochemical kits, antibody and DNA-based tests, and assays that are modifications of conventional tests to speed up the analysis [92-95]. Some of these assays have also been automated to reduce hands-on manipulations. With few exceptions, almost all assays used to detect specific pathogens in foods require some growth in an enrichment medium before analysis.

Miniaturized biochemical kits for the identification of pure cultures of bacteria isolated from food. Mostly, consist of a disposable device containing 15 - 30 media or substrates specifically designed to identify a bacterial group or species. With the exception of a few kits where results can be read in 4 hrs, most

require 18-24 hrs incubation. In general, miniaturized biochemical tests are very similar in format and performance, showing 90−99% accuracy in comparison to conventional methods [96]. However, kits that have been in use longer may have a more extensive identification database than newer tests.

During the 1980s, major progresses in basic research were conveyed rapidly to applied areas, as "biotechnology" in the diagnostic field [97].

DNA and antibody-based assays for numerous microbes or their toxins are now available commercially [98]. There are many DNA-based assays, but only probes, polymerase chain reaction (PCR) and bacteriophage have been developed commercially for detecting foodborne pathogens. Probe assays generally target ribosomal RNA (rRNA), taking advantage of the fact that the higher copy number of bacterial rRNA provides a naturally amplified target and affords greater assay sensitivity [99, 100].

DNA hybridization is also being utilized in other technologies, such as the polymerase chain reaction (PCR) assay, where short fragments of DNA (probes) or primers are hybridized to a specific sequence or template, which is then enzymatically amplified by Taq polymerase using a thermocycler [101, 102]. Theoretically, PCR can amplify a single copy of DNA by a million fold in less than 2 hrs; hence it's potential to eliminate, or greatly reduce the need for cultural enrichment. However, the presence of inhibitors in foods and in many culture media can prevent primer binding and diminish amplification efficiency [103], so that the extreme sensitivity achievable by PCR with pure cultures is often reduced

when testing foods. Therefore, some cultural enrichment is still required prior to analysis.

The enzyme-linked immunosorbent assay (ELISA) is the most prevalent antibody assay format used for pathogen detection in foods [104]. Usually designed as a "sandwich" assay, an antibody bound to a solid matrix is used to capture the antigen from enrichment cultures and a second antibody conjugated to an enzyme is used for detection. The walls of wells in microtiter plates are the most commonly used solid support; but ELISAs have also been designed using dipsticks, paddles, membranes, pipet tips or other solid matrices [98].

Antibodies coupled to magnetic particles or beads are also used in immunomagnetic separation (IMS) technology to capture pathogens from pre-enrichment media [105]. IMS is analogous to selective enrichment, but instead of using antibiotics or harsh reagents that can cause stress-injury, an antibody is used to capture the antigen, which is a much milder alternative. Captured antigens can be plated or further tested using other assays [106].

Almost all rapid methods are designed to detect a single target, which makes them ideal for use in quality control programs to quickly screen large numbers of food samples for the presence of a particular pathogen or toxin. A positive result by a rapid method however, is only regarded as presumptive and must be confirmed by standard methods [97]. Although confirmation may extend analysis by several days, this may not be an imposing limitation, as negative results are most often encountered in food analysis. Most rapid methods can be

done in a few minutes to a few hours, so they are more rapid than traditional methods. But, in food analysis, these methods still lack sufficient sensitivity and specificity for direct testing; hence, foods still need to be culture-enriched before analysis [98]. Although enrichment is a limitation in terms of assay speed, it provides essential benefits, such as diluting the effects of inhibitors, allowing the differentiation of viable from non-viable cells and allowing for repair of cell stress or injury that may have resulted during food processing.

The specificity of DNA based assays is dictated by short probes; hence, a positive result, for instance with a probe or primers specific for a toxin gene, only indicates that bacteria with those gene sequences are present and that they have the potential to be toxigenic. But, it does not indicate that the gene is actually expressed and that the toxin is made. Likewise, in clostridial and staphylococcal intoxication, DNA probes and PCR can detect only the presence of cells, but are of limited use in detecting the presence of preformed toxins [98].

Biosensors, a technique that combine biological materials such as antibodies, peptides, and nucleic acids with a physicochemical transducer, have become an important tool for the rapid, sensitive, and selective detection of microorganisms. Biosensors can be classified according to the transducing system as optical, electrochemical, thermometric, piezoelectric, or magnetic [107]. Another option for the rapid and label-free detection of bacteria is surface plasmon resonance (SPR) biosensors. SPR sensors are a type of optical sensors that measure the changes of the refractive index at the sensor surface [108].

1.3.2 Principle of Bacteria Detection Using AMPs

The principle of bacterial detection using AMPs is based on AMPs-labeled biosensor. Generally the principle of biosensor is that the detector molecules (AMPs) are attached to a solid surface in such a way that a specific signal is obtained from the sensor when the detector molecules (AMPs) selectively react, or/bind to the microorganism (bacteria). In other words, the detection relies on the bio-recognition between the predesigned AMP and the unknown sample molecules (bacterial strains). **Figure 1.4** shows the common principle of AMP-sensor technique.

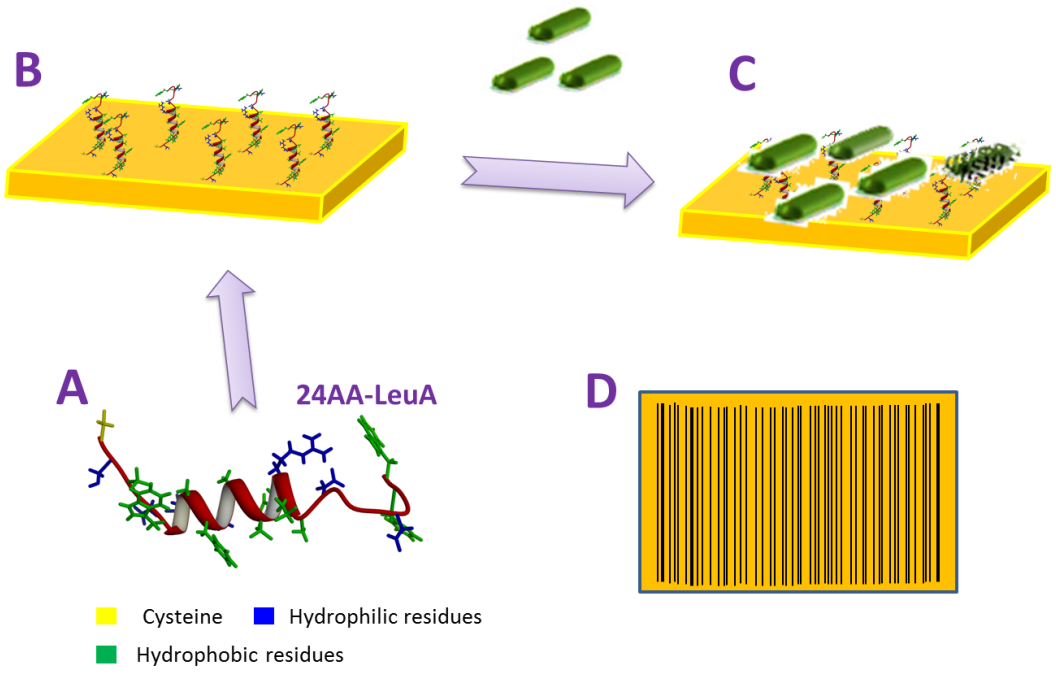

Figure 1.4. AMP-based detection platform **(A)** Magnified image of (24-AA LeuA) in a helical form shows the N-terminal cysteine (yellow) hydrophobic chains (Green) and hydrophilic face (blue). **(B)** Schematic representation of AMP immobilized on interdigitated microelectrode array. **(C)** Bacterial detection via binding to the immobilized AMP. (**D)** Magnified image of the interdigitated microelectrode array (scale bare: 50 μm) [109].

A number of methods based on biosensor have been successfully used for bacterial detection, including nanomechanical cantilever sensing [110, 111], surface-enhanced Raman spectroscopy [112], and quartz crystal microbalance-based sensors [113]. Similarly, recent trials have utilized AMPs as biorecognition elements in fluorescent-based microbial detection with achievable detection limits of 5×10^4 cells⁄mL [114, 115]. Recent studies have reported a label-free electronic biosensor based on the hybridization of the antimicrobial peptide (magainin I) with interdigitated microelectrode arrays for the sensitive and selective detection of pathogenic bacteria via impedance spectroscopy [109]. AMPs-biosensors can develop "all-in-one" solution that combines a high degree of portability, robustness, sensitivity, and selectivity toward detection of foodborne pathogens.

1.4 Thesis Proposal

1.4.1 Thesis Rationale

Identification and rapid detection of bacteria in food, water and pharmaceutical products remains a challenging task that faces researchers nowadays. Rapid and early detection of bacteria plays a vital role when it comes to food safety, drinking water, combating infectious diseases and preventing bio-terrorisms. Effective testing for bacteria requires analytical methods that have to obey a series of restrictive criteria. The most important limitations are the time required for

analysis and the sensitivity of the detective tools. It is also highly desirable to have available analytical methods as selective as possible.

Biosensor techniques that combine biological materials such as antibodies, peptides, and nucleic acids with a physicochemical transducer, have become an important tool for the rapid, sensitive, and selective detection of microorganisms. Electrochemical biosensor has proved to be a promising method for detection of foodborne pathogens due to rapidity, sensitivity as well as the possibility of use on-one-spot detection.

Bacteriocins are now being used for coating different surfaces to create disinfecting antimicrobial surfaces [62, 116]. Class IIa bacteriocin Leucocin A, is one of the most effective AMP that exhibits high activity and significant specificity towards *Listeria monocytogen*es. The nano scale activity of Leucocin A beside its specificity renders it an interesting candidate to be used as a detective molecule for *Listeria monocytogenes*.

Due to the complex nature of the AMPs, their interaction with membranes, receptors and/or with other complementary peptides remains a huge challenge that needs to be resolved. Such insight on PIs will be invaluable for future rational design of new peptide-based therapeutic agents or diagnostics.

1.4.2 Thesis Hypothesis

Class IIa bacteriocin Leucocin A (LeuA) has great distinguishing properties that make it particularly interesting candidate as a molecular recognition element for detection of pathogenic bacteria. In the current thesis, we hypothesize that LeuA and/or a shorter fragment of LeuA (C-terminal 24-AA) can be used for specific detection of pathogenic bacteria, which can be exploited in the future on an electronic biosensing platform for specific detection of *Listeria monocytogenes*.

We also theorizes that studying the peptide-peptide interaction of a representative class IIb two-peptide bacteriocin, LcnG, will provide invaluable insight for future rational studies of peptide-receptor interaction of LeuA as well as design of a new peptide-based therapeutic agents and/or diagnostics.

1.4.3 Thesis Objectives

The main objective of this thesis is to study peptide-bacteria interactions using surface tethered AMPs. The results from this study will guide us in developing future portable AMP-platforms for quantification of foodborne pathogens in contaminated food samples.

Specific objectives of this thesis are:

- (i) Synthesis of antimicrobial peptides LeuA (37 AA) and a shorter fragment of LeuA (24-AA LeuA) using stepwise SPPS and NCL. (Chapters 2 and 3)

- (ii) Immobilization of AMPs on a gold interface using direct immobilization technique and chemical bio-conjugation method. (Chapters 2 and 3)
- (iii) Detection of peptide-bacteria interaction. (Chapters 2 and 3)

- This thesis also elucidates in Chapter 4 the peptide interaction of Lactococcin G class IIb two-peptide bacteriocin in a membrane mimicking environment using molecular dynamics simulation, suggesting strategy that could be applied by different ways to explore peptide-receptor interactions of LeuA. In addition, peptide interactions of bacteriocins can provide an invaluable rational approach for the design a new class of effective therapeutic agents.

Chapter 2

Bacterial-adhesion to a Surface Tethered C-terminal 24-Amino Acid Leucocin A

2.1- Introduction

Antimicrobial peptides (AMPs) represent a wide range of short, cationic, gene-encoded peptide antibiotics that are an innate part of the immune system of many organisms [117]. Since the mid-1990s, there have been almost 1000 naturally occurring AMPs isolate and characterized [118, 119]. While it has been shown that AMP amino acid sequences are widely diverse, these peptides have been classified into relatively few conformation paradigms based on their secondary structures (i.e., α-helix, β-sheet, extended and looped) [120, 121]. Despite these structural variations, most AMPs share two distinct features, in that they are polycationic with a net positive charge and fold into amphipathic structures possessing both a hydrophobic and a hydrophilic domain. These characteristics allow them to readily interact with the negatively charged cytoplasmic membranes of most bacteria. Although the exact mechanism of action of AMPs remains a matter of controversy, there is a consensus that they exert their antimicrobial specificity and activity by binding to invariant components of microbial surfaces through specific (target specific molecules) or non-specific (electrostatic) interactions and cause membrane leakage/disruption either directly or through 'self-promoted uptake'[122-125]. Not only have AMPs been shown to

exhibit effective and rapid potency against Gram-negative and Gram-positive bacteria, but they have also been shown to have a broad-spectrum of activity against fungi, viruses, parasites and even tumour cells [126-129]. For this reason, AMPs are being intensively researched for their potential application as both diagnostic and therapeutic agents.

The availability of robust and portable biosensors to detect pathogenic bacteria is of growing importance in environmental, food and human diagnostic areas. Identification of bacteria using traditional methods, for instance culture-based and colony-counting procedures, are in most cases time-consuming, inconvenient and often require several handling steps [130]. The majority of rapid detection methods used to overcome these difficulties use antibody and nucleic acid probes for recognition, identification and quantification of the target cells [131, 132]. These techniques, including polymerase chain reaction (PCR) and immunoassays, are very powerful and versatile tools for detecting, monitoring and clinical diagnosis of pathogen infections due to their specificity and sensitivity of the biological entities employed for detection [133, 134]. However, antibody based platforms suffer from a number of potential constrains, such as lack of stability under harsh environmental conditions and the high cost of the monoclonal developments, limiting their wide scale use. Similarly, PCR techniques are at the same time very costly and often require trained personnel for the analysis [135]. On the other hand, the ease of synthesis, stability and specificity of AMPs render them a viable candidate for their use as molecular recognition entities in bio-sensing detection techniques [117, 136].

Several recent studies have explored the covalent immobilization of AMPs onto solid supports as an alternative to traditional pathogen-detection platforms [137-140]. A notable example by Mannoor et. al reports on the development of a portable, label-free, real-time sensing platform that utilizes impedance spectroscopy to distinguish pathogenic bacteria with a clinical relevant limit of 1 bacterium per microliter [140]. In their study, a semi-selective AMP magainin I was immobilized on gold microelectrodes via a C-terminal cysteine residue where they were able to selectively differentiate pathogenic and Gram-negative bacteria. However, the key to implementing the use of AMPs in bio-sensing platforms relies heavily on the ability to immobilize them on a surface in a reproducible and reliable manner. To this end, an overall understanding of AMP structure−function relationship in the tethered state is essential for the establishment of a more general approach to developing efficient, safe and long-lasting antimicrobial devices. The effects of the 'anchoring' parameters such as method for attachment of peptides to the solid support, amino acid composition, the spacer length and flexibility as well as peptide orientation at the interface on the specificity and activity of tailored surface-tethered peptides remains to be fully elucidated and is system dependent [141].

In an effort to contribute to the current understanding of the peptide-bacterial interactions of a surface immobilized peptide, we have investigated the interactions of a peptide derived from the well-known AMP Leucocin A (LeuA) with different Gram-positive bacteria. LeuA is a well-known ribosomally

synthesized class IIa bacteriocin consisting of 37 amino acid residues (**Figure 2.1**) [35].

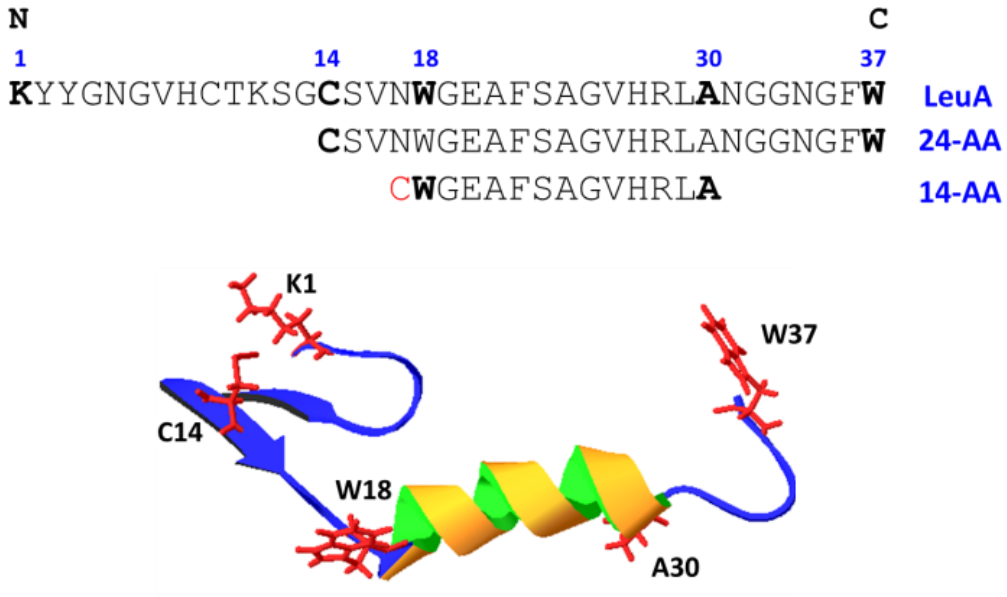

Figure 2.1. Amino acid sequences of Leucocin A (LeuA) and its derivative fragments, C-terminal fragment (24AA) and the helical fragment (14AA). The 14AA fragment has an extra cysteine group (shown in red) at the N-terminal. The three dimensional NMR solution structure of LeuA (PDB 1CW6) [35] shows the b-sheet and helical secondary structures present in the peptide. N- and C-terminus residues of LeuA and the fragments are highlighted.

Like other class IIa bacteriocins, LeuA is produced by Gram-positive lactic acid bacteria and is antilisterial peptide. It is active against *Listeria monocytogenes* in the nanomolar range (minimum inhibitory concentration or MIC 0.1 nM) [35]. It is characterized by a conserved disulfide bond and a YGNGV sequence near the N-terminus, and a C-terminal domain with an amphiphilic α-helical structure ending with a structurally extended C-terminal tail [2, 7, 29, 35, 61]. While it is suggested that the N-terminus is involved in the AMP activity, the C-terminus of the class IIa bacteriocin has been found to play a very crucial role in antimicrobial

selectivity or specificity [31-34]. Moreover, this domain is most likely involved in the binding of the AMP to the membrane-bound receptor of the target cells [2, 7, 31]. As previously mentioned the hydrophobic surface of the helix is believed to interact with a lipid membrane of the target cell and ultimately binds to a specific membrane-bound receptor, namely, mannose phosphotransferase permease (MPT) [31, 33, 34, 74, 78, 142]. We hypothesized that a peptide derived from the C-terminal region of LeuA may bind different LeuA sensitive-bacteria with same specificity as the wild type LeuA. In this study, we exploited 24-residue LeuA fragment that spans the amphipathic helical region and the C-terminal tail of the native LeuA (**Figure 2.1**). Another shorter sequence consisting of only the amphipathic helical region of LeuA, 14-residue peptide, was also used to study the interaction between these surface immobilized peptides and Gram-positive bacteria. The results highlight the feasibility of using LeuA fragment for selective detection of Gram-positive bacteria. **Figure 2.2** shows s schematic representation of the immobilized peptide-bacterial interactions.

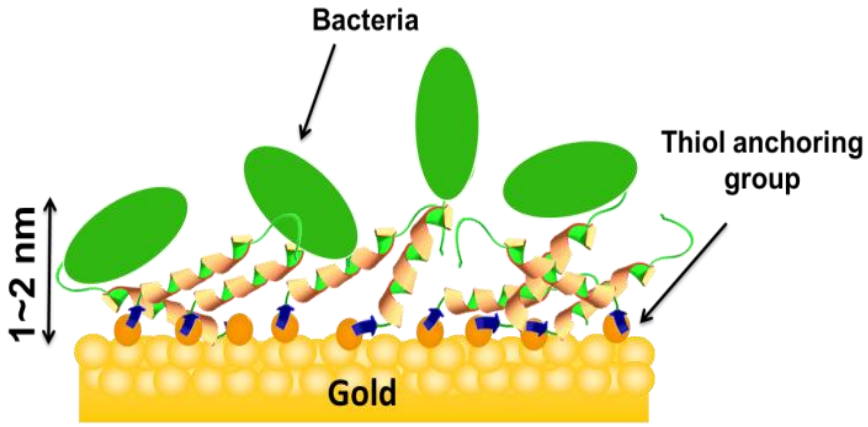

Figure 2.2. A schematic representation of the immobilized peptide-bacterial interactions. The peptide was immobilized to the gold substrate through a thiol anchoring group of the amino acid cysteine using a direct immobilization technique. Detection of bacteria is achieved via specific binding of the target cells to the immobilized peptide.

2.2 Experimental Section

2.2.1 Chemicals and Reagents

2-Chlorotrityl resin (loading 1.6 mmol/g), Fmoc-amino acids, 1-hydroxybenzotriazole (HOBt), and 2-(6-chloro-1H-benzotriazole-1-yl)-1,1,3,3 tetra methyl–aminium hexafluorophosphate (HCTU) were purchased from Novabiochem (San Diego, CA). N-methyl morpholine (NMM), diisopropylethylamine (DIPEA), triflouroaceticacid (TFA), N, N-diisopropylcarbodiimide (DIC), triflouroethanol (TFE), 1-methyl-2-pyrrolidinone (NMP), triisopropylsilane, and piperidine were purchased from Sigma-Aldrich. CyQUANT nucleic acid probe was obtained from Invitrogen (Eugene, Oregon, USA). All other commercial reagents and solvents, such as dimethylformamide (DMF), dichloromethane (DCM), and isopropyl alcohol (IPA), were analytical

HPLC grade and were purchased from Caledon Laboratories LTD (Georgetown, Ontario, Canada). Phosphate buffered saline (PBS) (Sigma-Aldrich) consists of 137 mM NaCl, 2.7 mM KCl, 4.4 mM Na_2HPO_4, and 1.4 mM KH_2PO_4 (pH 7.4). All chemical reagents were used as received without any further purification.

2.2.2 Peptide Synthesis, Purification and Characterization

2.2.2.1 Peptide Synthesis

Two LeuA derivatives composed of 14 amino acid residues (14AA LeuA, CWGEAFSAGVHRLA) and 24 amino acid residues (24AA LeuA CSVNWGEAFSAGVHRLANGGNGFW) were chemically synthesized using Fmoc solid phase peptide synthesis (Fmoc-SPPS). In the case of 14AA LeuA, an additional cysteine was added to the N-terminus of the molecule, whereas the 24AA LeuA fragment ended with its native cysteine group. Briefly, the synthesis was carried out on a 0.2 mmol scale of 2-chlorotrityl chloride resin using an automated peptide synthesizer (MPS 357, Advanced Chem-tech Inc., USA) and manual peptide synthesis methods. The first amino acid (4 equiv) was loaded manually to the resin. Initially, the resin was washed using DMF/DCM (50:50) and then swelled in DMF for 30 minutes. Fmoc-Trp (Boc)-OH (0.8 mmol, 421.28 mg) or Fmoc-Ala-OH (0.8 mmol, 249.06 mg) and DIPEA (1 mmol, 174.1 μL) dissolved in DMF (1.50 mL) were added to the swollen resin and agitated for 24 hrs at room temperature. Following the coupling step, the resin was washed with DMF, DCM and IPA. Following the coupling step, the resin was washed with DMF, DCM and IPA successively followed by a mixture of

DCM/Methanol/DIPEA (6:3:1) and finally with DMF. Fmoc was removed using 2 aliquots of a freshly prepared solution of 20% piperidine in DMF. The resin was then transferred to the peptide synthesizer collection vessel. The coupling of the Fmoc-protected amino acid residues was carried out using coupling agents DIC/HOBt in a ratio of 1:1. Acid labile side chain protections were used: Asn (Trt), Cys (Trt), Glu (tBu), His (Trt), Ser (tBu), and Trp (Boc). The synthesis protocol in the peptide synthesizer machine was optimized as follows: (**1**) 1 h each was employed for the single coupling of the first 10 amino acid residues and (**2**) double coupling of 2 h each was employed for amino acid residues 10 to 20. For each Fmoc-deprotection step, again freshly prepared 20% piperidine in DMF was used two times for 6 minutes each. The peptide was then taken off from the synthesizer and the remaining 4 amino acids of the 24-AA fragment were added manually to ensure an efficient coupling performance. The coupling was performed using 4 equiv of the amino acids and coupling reagents, HCTU (6 equiv), HOBt (4 − 5 equiv), NMM (4 − 5 equiv) in NMP were used. After each amino acid coupling the completeness of the reaction was monitored using the ninhydrine (Kaiser) test [143]. The peptide sequence was finally released from the resin with concomitant removal of acid-labile side chain protecting groups by adding a mixture of 50% TFA, 45% DCM, and 5% triisopropylsilane (~7 mL) for 90 min at room temperature with mechanical shacking. The filtrate from the cleavage reactions was concentrated in vacuum and then precipitated by adding cold diethyl ether (~15 mL). After triturating for 2 min, the peptide was collected

by centrifugation and decantation of the ether. A lyophilized crude peptide was then obtained by freeze drying the collected peptide in a lyophilizer.

2.2.2.2 Peptides Purification and Characterization

The purification and analysis of the peptides were carried out on a reversed phase HPLC (Varian Prostar 210, U.S.) using Vydac semi-preparative C18 (1 × 25 cm, 5 μm) and an analytical C8 (0.46 × 25 cm, 5 μm) column. Initially, the crude peptide was reconstituted in a 1:1 acetonitrile/water solution and then introduced to the HPLC column. The peptide was monitored at 220 nm wavelength using a linear gradient of acetonitrile/water (0.05% TFA, v/v) mixture. Peak (fraction) showing the correct mass $[M+H]^+$ was collected and evaporated on a rotary evaporator followed by lyophilization in a freeze dryer to obtain the pure peptide. The identity of the peptides was assessed by a matrix-assisted laser desorption ionizations time-of-flight (MALDI-TOF) spectrometry (page 44, Figure 2.3).

2.2.2.3 CD Spectroscopy

Circular dichroism (CD) measurements were carried out using an Olis CD spectrometer (Georgia, USA) over 190 − 260 nm in a thermally controlled quartz cell having a 0.02 cm path length. The spectra were acquired in a mixture of TFE/water (9:1) containing 0.1% TFA (pH ~ 2.5). A peptide concentration of 200 μM was used for CD measurements in order to achieve a higher structural resolution. Data was gathered every 0.05 nm with an average of eight scans. The

band width was set at 1.0 nm and the sensitivity at 5 mdeg. The baseline scans of the aqueous buffer were subtracted from the readings. The collected CD data was normalized and expressed in terms of mean residue ellipticity (deg cm^2 $dmol^{-1}$).

2.2.3 Bacterial Strains, Media and Cultural Conditions

L. monocytogenes, Listeria innocua (L .innocua), Carnobacterium divergens LV13 (*C. divergens LV13*) and *E. coli DH5α* are the bacterial strains employed in this study. The strains were grown at 37 °C overnight in APT medium, excluding *C. divergens* which was grown in APT medium and kept overnight at room temperature. All the experiments regarding the pathogenic bacterial subculture, maintenance and treatments were carried out in a level II biosafety cabinet, facility of CanBiocin Inc. (Edmonton, CA).

2.2.4 Antimicrobial Activity Assay

The activity of both the 14AA and 24AA LeuA fragments was tested against *L. monocytogenes* and *C. divergens LV13*. Peptide stock solutions were prepared in 20% acetonitrile/water and were serially diluted in sterile water to give concentrations ranging from 10 to 200 μM of the peptide. The antibacterial activity measurements were identified using the spot on lawn assay [144].

2.2.5 Peptide Surface Functionalization and Characterization

2.2.5.1 Surface Functionalization

Silicon substrates (Ultrasil, Hayward, CA) were cleaned by immersion in a freshly prepared piranha solution (1:3 30% H_2O_2/H_2SO_4 (*Caution! Piranha solution is highly reactive and must be handled with extreme care*). The clean substrates were then rinsed with excessive amounts of Milli-Q water followed by 95% ethanol and then dried under a stream of nitrogen. Gold substrates were prepared by electron beam evaporation where a titanium adhesion layer of 10 nm was first evaporated followed by a 100 nm gold layer. Both adlayers were deposited at a rate of 0.2 Å s^{-1} until the desired thickness was reached.

Peptide immobilized surfaces were prepared by immersing the freshly prepared gold substrates in a peptide solution having a concentration 100 μg mL^{-1} dissolved in dimethyl sulfoxide (DMSO ≥99%, Sigma-Aldrich). Prior to surface analysis, the substrates were removed from the solution and rinsed with copious amounts of DMSO to remove any physically adsorbed material. The samples were then dried with nitrogen and immediately analysed.

2.2.5.2 Fourier Transform Infrared Reflection Absorption Spectroscopy (FTIR-RAS)

FTIR-RAS of the surface immobilized peptides were acquired using a Nexus 670 FT-IR (Thermo Nicolet, Madison, WI) equipped with a surface grazing angle attachment (SAGA, Thermo Spectra-Tech, Shelton, CT) and a liquid-nitrogen-cooled MCT detector. The grazing angle was 75º and all spectra were averaged

over 1064 scans at a resolution of 2 cm^{-1}. Peak information was obtained using the OMNIC software provided by Thermo Nicolet. Molecular orientation of the peptide of the monolayer on the gold surface was determined from the ratio of the amide I/amide II absorbance bands in the FTIR-RAS spectra according to equation 1 under the assumption of a uniform crystal of a the peptide-thin layer [145-150].

$$\frac{I_1}{I_2} = 1.5 \times \frac{(\cos^2 \gamma - 1)(\cos^2 \theta_1 - 1) + 2}{(\cos^2 \gamma - 1)(\cos^2 \theta_2 - 1) + 2}$$

I_i, γ and θ_i (i = 1 or 2 corresponding to amide I and amide II) represent the observed absorbance, the tilt angle of the helix axis from the surface normal and the angle between the transition moment and the helix axis, respectively. The θ_1 and θ_2 are taken as 39° and 75°, respectively [151].

2.2.5.3 Ellipsometric Spectroscopy

Ellipsometry measurements were carried out using a Sopra GES5 variable angle spectroscopic ellipsometer (Sopra Inc., Palo Alto, CA) and the accompanying GESPack software package. The measurements were acquired on the gold-coated substrates before and after incubation in the peptide solution in order to determine the thickness of the chemisorbed peptide monolayer. Briefly, the spectra of the samples were scanned from 250 nm to 850 nm using an incident angle of 70° and an analyser angle at 45°. The thickness of the peptide SAM monolayer was calculated via the regression method in the Sopra WinElli software package (version 4.07) by setting the *n* and *k* values for the peptide immobilized layer as

1.45 and 0.0, respectively [152]. The results presented are the average of five measurements on individual peptide SAM substrates.

2.2.6 Adhesion and Fluorescent Microscopy

Stock solutions of the CyQUANT dye were made by dissolving CyQUANT (0.8 μL) dye reagent in HBSS buffer (200 μL, HBSS buffer was included in the CyQUANT cell proliferation kit). The solutions were stored under dark conditions at 4 ºC. Freshly prepared live cells of bacteria hydrated in PBS were then incubated with CyQUANT dye solution (100 μL) for 30 minutes at 37 ^{o}C. After the incubation, the cells were pelleted by centrifugation for the removal of the supernatant and were then re-suspended in fresh 1 × PBS buffer. Samples of stained bacterial cells (non-pathogenic *E. coli* DH5α, *C. divergens LV13, L. innocua*, and pathogenic *L. monocytogenes*) having different concentrations of 10^2, 10^4 and 10^6 cfu⁄mL were incubated independently with the immobilized peptide slides for 30 minutes under dark conditions at room temperature (T = 25 °C). Bare gold substrates (i.e., "peptide-free gold substrates") were used as a blank substrate in order to account for non-specific adsorption. After the incubation, the surface-immobilized peptide and "peptide-free" interfaces were washed several times with PBS and dried under nitrogen. The binding affinities of the different bacterial cells with the immobilized peptide were investigated using a Quorum WaveFX spinning disk confocal system (Quorum Technologies Inc., Guelph, Canada) with an oil immersion lens at a magnification 60 X/1.4. All images were recorded with a Quorum digital camera.

2.3. Results and Discussion

2.3.1 Peptide Design and Synthesis

The goal of our study was to investigate the feasibility of employing a surface-immobilized engineered peptide for the detection of potentially harmful microorganisms, specifically *L. monocytogenes*. Previous studies indicate that the α-helical C-terminus component of the AMP LeuA is predominantly responsible for bacterial cell recognition through electrostatic interactions with the cytoplasmic membrane [12]. Moreover, it has been suggested that the terminal hairpin-like structure of the AMP plays a significant role in maintaining the peptide immobilization through more direct interactions via molecular insertion into the membrane wall [61]. For these reasons, two peptides (i.e., 24AA and 14AA LeuA (**Fig. 2.1**) that span the amphipathic helical region of the wild type LeuA were synthesized using Fmoc-SPPS as described in the experimental section. Both peptides contained an N-terminus cysteine residue which readily enabled their surface 'anchoring' through well-known gold-sulfur chemistry. The peptides were purified to >95% purity as shown by analytical RP-HPLC and mass spectrometry (**Figures 2.3**). An overall yield of 60% pure peptide was achieved for the 24AA LeuA and 50% for the 14AA LeuA fragment. A lower yield for the 14AA peptide fragment was unexpected. However, the addition of the cysteine group to the 13 amino acid sequence proved problematic with regards to the coupling efficiency. During the synthesis procedure, aggregation of the peptide was noted due to insufficient coupling of the cysteine to the tryptophan residues in the 14AA LeuA peptide leading to a dramatic decrease in the overall yield. It is

well-known that the occurrence of aggregation within the peptide-resin matrix can seriously affect the reaction rates and coupling yields [153-155].

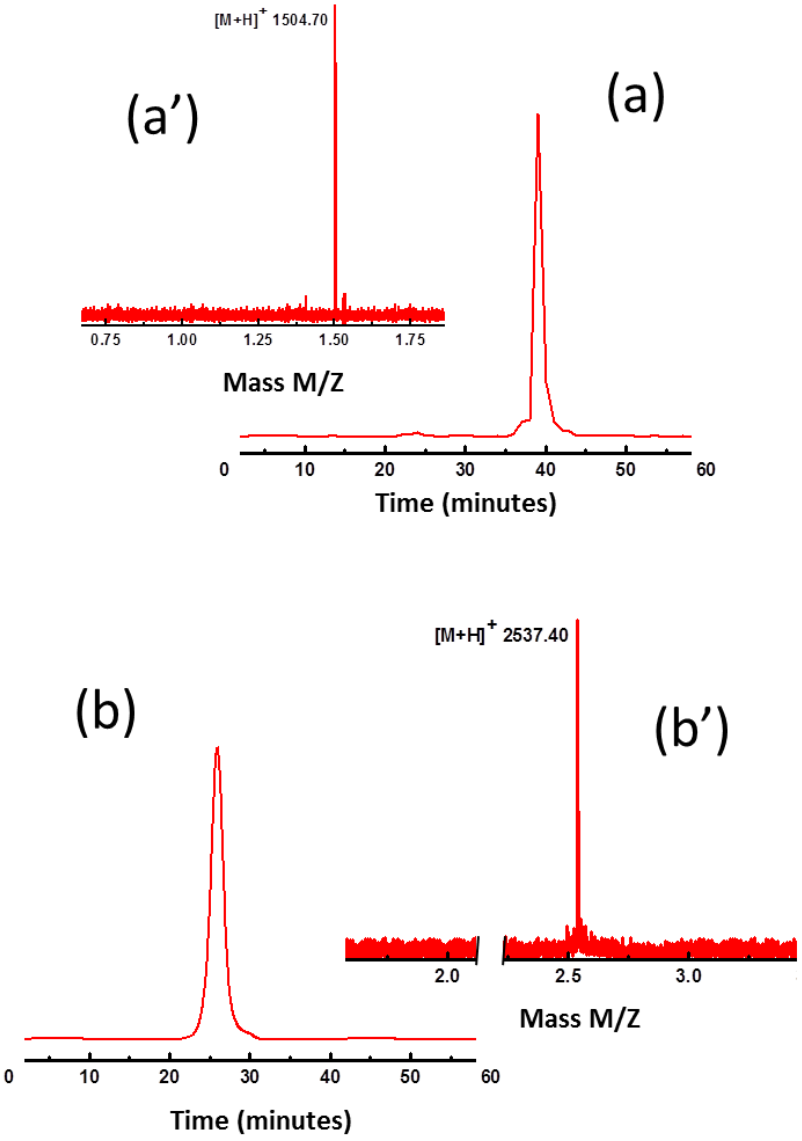

Figure 2.3. (a) HPLC chromatogram of the pure peptide (14-AA LeuA); elution time at 39 minutes, gradient was used 15 – 55% ACN/Water (0.1% TFA) in 60 min with a flow rate of 1 mL/min. **(a')** MALDI-TOF spectrum of the its observed mass; calcd mass of the peptide is 1503.7. **(b)** HPLC chromatogram of the pure peptide (24-AA LeuA); elution time at 26 minutes, gradient was used 30 – 95% ACN/Water (0.1% TFA) in 60 min with a flow rate of 2 mL/min. **(b')** MALDI-TOF spectrum of its observed mass; calcd mass of the peptide is 2536.8.

2.3.2 Conformation of Peptides in Solution

The CD spectra of the cysteine terminated 24AA and 14AA LeuA peptides are shown in **Figure 2.4**. The CD spectra of both peptides indicate significant α-helical content in TFE. This helicity is clearly indicated by the appearance of distinct negative bands at 208 nm ($\Theta = -11.4 \times 10^3$) and a negative shoulder near 220 nm. Both peptides, therefore, retain most likely the amphipathic α-helix structure which was observed previously for the wild type LeuA. [35]

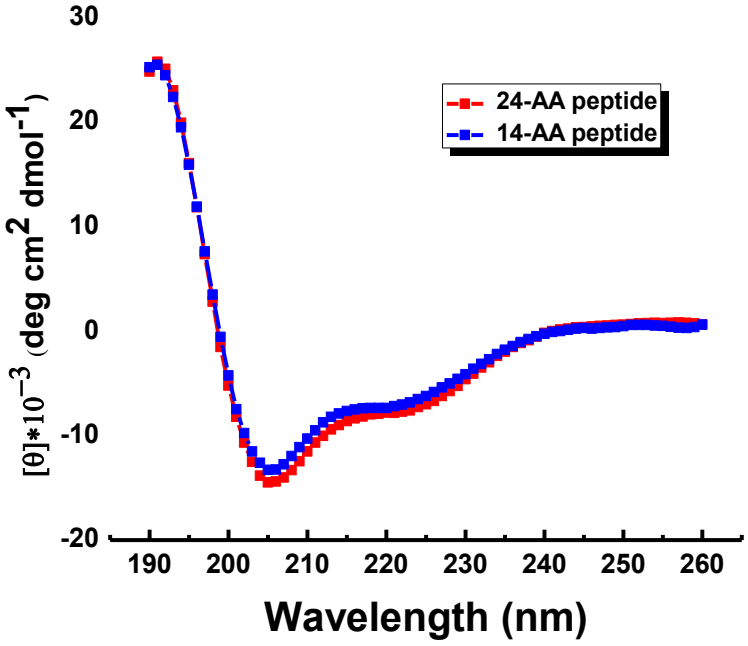

Figure 2.4. CD spectra of the 24AA and 14AA LeuA fragments in 90% TFE (0.1% TFA final concentration, pH 2.5) at 200 μM concentrations. The ellipticity was expressed as the mean residue molar ellipticity (Θ) in deg cm^2 dmol^{-1}.

2.3.3 Surface Modification and Characterization

The conformation and molecular orientation of the surface-tethered peptides can be approximated using FTIR-RAS spectroscopy. Shown in **Figure 5a** is a typical FTIR-RAS spectra observed for the surface immobilized 24AA LeuA peptide. The absorbance bands at 1670 and 1535 cm^{-1} correspond to the amide I and amide II bands, respectively. These wavenumbers are characteristic of a helical conformation [156]. Furthermore, the difference in the intensity ratio between the two peaks (amide I/amide II) can be explained in terms of the orientation of the α-helical peptide on the gold substrate with respect to the surface normal. In helical peptides, the transition moment of the amide I absorption lies nearly parallel to the helical axis and that of the amide II adsorption lies perpendicular to the helical axis [157]. The interpretation of FTIR-RAS spectra in terms of molecular orientation relies on the specific surface selection rule which connects the intensity of the bands to the orientation relative to the surface of the transition moment. Accordingly, the intensity ratio ascribed to the transition moment of amide I and amide II decreases as the tilt angle from the surface normal increases indicating that the peptide adopts a parallel orientation at the gold interface. The calculated ratio in our study of amide I and II absorbance is on the order of 1.35 which indicates that the peptide lies predominantly parallel to the gold surface in a random orientation. Furthermore, the thickness of the 24AA LeuA peptide layer was determined by ellipsometry to be 1.4 (±0.5) nm. This value also supports a flat lying configuration of the peptide SAM and is in close agreement to the predicted width (1.6 nm) of the peptide.

In the case of the 14AA LeuA peptide (**Figure 5b**), typical absorbance bands were observed at 1668, 1539 and 1409 cm^{-1} corresponding to the amide I (C=O), amide II (N-H) and amide III bands (C-N), respectively. These bands also suggest that the immobilized peptide is helical in nature at the gold interface.

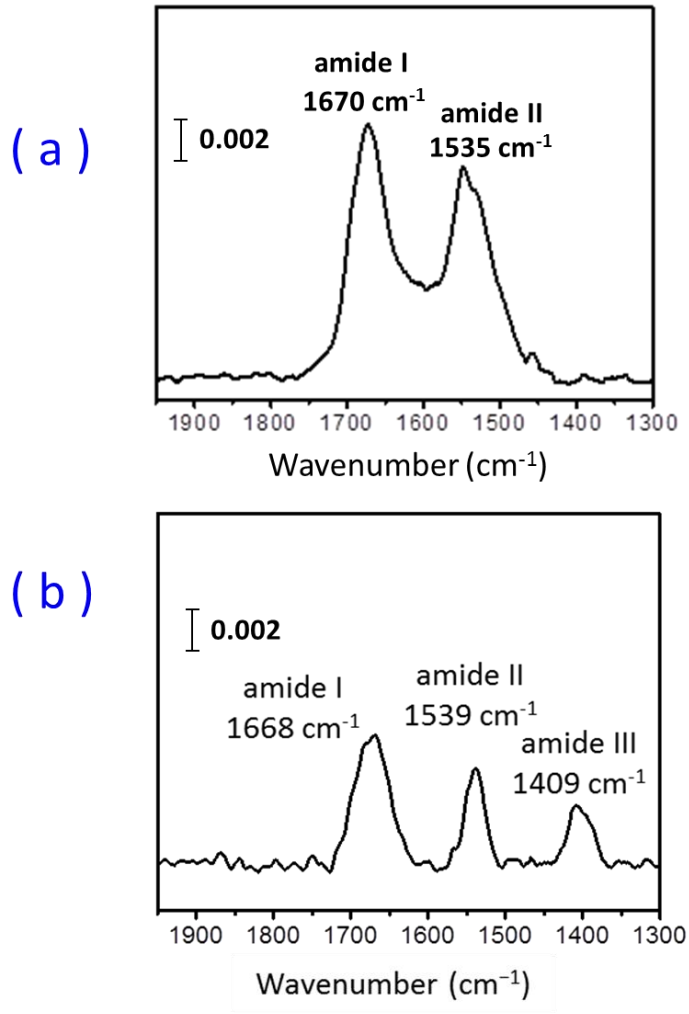

Figure 2.5. FTIR-RAS spectra of the peptide monolayers, 24AA LeuA (a) and 14AA LeuA (b) immobilized on a gold surface. The monolayer was formed from a solution of the peptide in DMSO.

2.3.4 Microscopy and Bacterial Detection

Confocal fluorescence microscopy was used to investigate the binding capabilities of the surface-immobilized peptides with bacterial cells (**Figure 2.6**). In all cases, the binding affinities of the bacterial strains were compared to control slides ("peptide-free" surfaces or non-functionalized gold substrates (Figure 2.6 A-E, top panel)). In these studies, the top panels of Figure 2.6A-E illustrate the physical adsorption of the "peptide-free" slides to the corresponding bacterial strains. Some bacteria adsorption is observed in Figure 2.6A-E (top panel) where it is attributed to the charge characteristics of both the gold interface and the peptide fragment, which will contribute to non-specific adsorption via electrostatic interactions. This non-specific interaction is not stable and can be easily removed by excessive washing of the surface. Shown in Figure 2.6 (A-D, bottom panel) are the confocal microscopy results elucidating the binding capabilities of the surface-immobilized 24AA LeuA peptide to Gram-positive bacteria (Figure 2.6A-C, bottom panel) and Gram-negative bacteria (Figure 2.6D, bottom panel); specifically, to Gram-positive non-pathogenic *C. divergens LV13* (Figure 2.6A, bottom panel), Gram-positive pathogenic *L. monocytogenes* (Figure 2.6B, bottom), Gram-positive non-pathogenic *L. innocua* (Figure 2.6C, bottom panel) and Gram-negative non-pathogenic *E. coli DH5α* strain (Figure 2.6D, bottom panel). According to Figure 2.6A-C, the results show a significant increase in the number of bacteria that bind to the peptide-coated surfaces relative to the peptide-free surfaces, whereas no notable discrepancies are apparent between the control (Figure 2.6, top panel) and the Gram-negative non-pathogenic

E. coli DH5α strain (Figure 2.6D). This was expected since LeuA is known not to exhibit any specificity or activity towards Gram-negative bacteria [158]. Moreover, the 14AA LeuA fragment, which was synthesized to consist only of the helical part of LeuA, was inactive or had limited affinity towards Gram-positive non-pathogenic *C. divergens LV13* bacteria (Figure 2.6E).

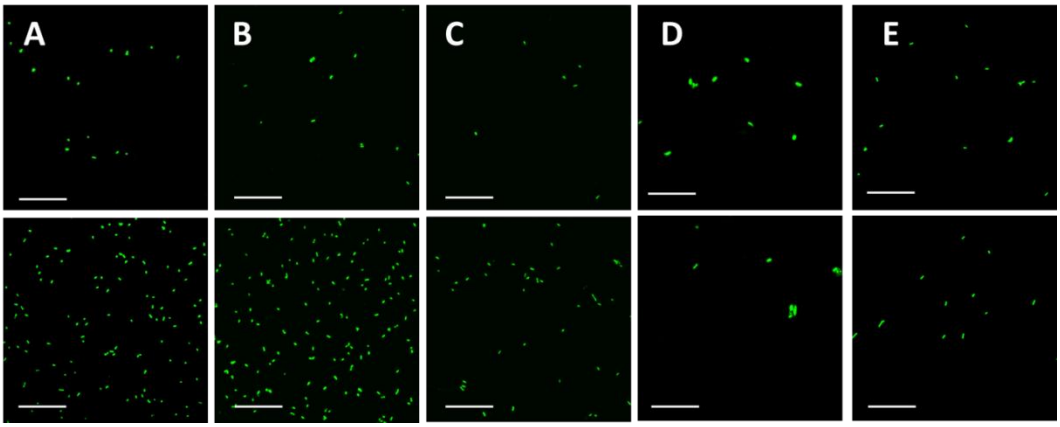

Figure 2.6. Confocal microscopic images of the selective binding of the peptide (24-AA LeuA). The top row shows the results of the incubation of peptide-free surfaces with various stained bacterial cells, while the lower row represents the selectivity binding of the peptide to various strains of bacteria at (10^6 cfu⁄mL), including (A) *C.divergens* (B) *L.monocytogenes* (C) *L.innocua and* (D) *E.coli*. Scale bars are 10 μm. Images (E) represent *C.divergens* adsorption on peptide-free surface (top image) and on 14-AA-coated surface (bottom image).

The binding affinity of the immobilized 24-AA peptide however, was varied from one bacterial strain to another. As illustrated in Figure 2.6, the highest binding affinity was observed towards *C.divergens* (Figure 2.6A) and *L.monocytogenes* (Figure 2.6B). On the other hand, a lower binding was detected against *L.inoccua* (Figure 2.6C). This degree of variation in the peptide-bacterial binding pattern between the strains is most likely due to the disparity in the degree

of exposure of the peptide to the target binding site. Furthermore, composition and number of the receptors at the cellular membrane of the target cells play significant roles in the peptide-bacterial interaction [159-161]. A recent study has shown that the antimicrobial mechanism of a class IIa bacteriocins Carnobacteriocin MB1 can be modulated by the physiological state of its target cells [162]. Furthermore, conformation and the site-specific orientation of the surface immobilized-AMP could have a substantial contribution on the peptide-bacterial binding events. Joshua Strauss et al. have reported that binding and killing of *E.coli* by cecropin CP1 is strongly dependent on the method by which the peptide is anchored to the surface [163]. In the study herein, although the direct site-specific immobilization technique was employed to anchor the peptide to the surface via the N-terminal thiol group, FTIR and ellipsometry measurements showed that the peptide most likely accommodated a random orientation at the surface. Few studies have addressed whether covalently bound peptides can bind to cells, inactivate bacteria, or distinguish between pathogenic and non-pathogenic. Recently, reports by Mello et al. found that covalently bound CP1 preferentially targeted the LPS of *E. coli* O157:H7 when compared to non-pathogenic strains of *E. coli* were achieved.[164, 165] Taitt et al. reported that when magainin I was uniformly attached to the slide a substantial improvement in the detection limits of both *Salmonella* and *E. coli* was achieved [115]. Furthermore, it was reported that if the receptor binding domains are randomly oriented or deformed, the selectivity and sensitivity of the sensor will be significantly reduced. In other words, nonspecific protein or peptide orientation

needs to be avoided or at least minimized in order to improve detection performances [166-174].

To give further insight to the selective binding of the immobilized 24-AA peptide towards various bacterial cells, the approximate numbers of the bacteria (at 10^6 cfu/mL) that bind to the immobilized-peptide were calculated and the data is plotted in **Figure 2.7.** The average number of bacteria in 10 μm^2 microscopic slide images was counted using an ImageJ 1.46 software package.

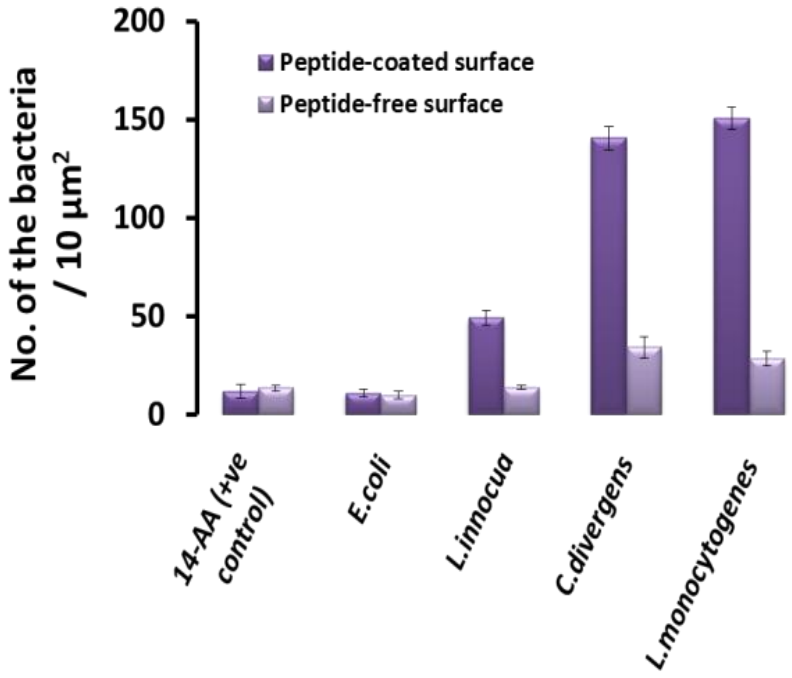

Figure 2.7. The binding affinity of the immobilized AMP (24-AA LeuA) towards various bacterial cells at 10^6 cfu/mL. Bacteria were counted using ImageJ 1.46 software package. Error bars show standard deviation based on 3 individual samples were prepared at the same conditions.

The highest binding affinity was found for *L.monocytogenes* where a surface concentration of ~156 bacteria/10 μm^2 was observed. Next, an average number of ~144 bacteria/10 μm^2 was found for *C.divergens*. Finally, surface concentrations of 46 and 11 bacteria/10 μm^2 were observed for *L.innocua* and *E.coli*, respectively. The variation in binding sensitivity of the immobilized peptide to the bacteria as discussed previously might be due to differential expression levels of the man-PT receptor from one strain to another since this variation in the receptor levels expression might also exist within the same species as it has been proposed by Morten Kjos et al.[175] Also, peptide orientation and confirmation at the surface could have a significant impact giving rise to the observed binding variations.

Figure 2.8 displays the discriminating binding affinity of the immobilized 24AA LeuA peptide towards various concentrations of *L. monocytogenes*. The measurements were performed after incubation of the immobilized peptide with pathogenic *L. monocytogenes* in concentrations ranging from 10^2, 10^4, and 10^6 cfu/mL. A blank "peptide-free surface" was employed as a control measurement. It is evident in Figure 2.8 that the different concentrations of bacterial cells have an effect on the peptide-bacterial binding affinity. The number of the bacterial cells bound to the immobilized AMP is directly proportional to the number of incubated bacterial cells. In other words, the number of bound bacteria to the immobilized AMP decreases with respect to the serially diluted bacterial concentrations.

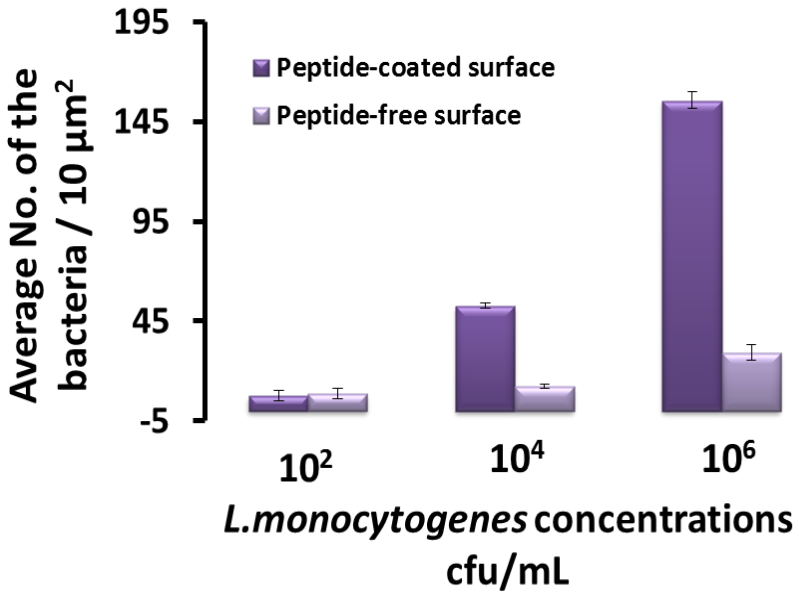

Figure 2.8. The discrimination between the binding patterns of the immobilized peptide (24-AA LeuA) towards various concentrations of *L.monocytogenes*. Error bars show standard deviation based on 3 individual samples were prepared at the same conditions.

Our results agree with the hypothesis that the amphipathic α-helix of the C-terminal region of class IIa bacteriocins is important for peptide-bacterial receptor interaction, but not itself responsible for the receptor binding and recognition. The hydrophobic face of the helical part is thought to interact with the lipid membrane and eventually react with a membrane-bound receptor of targeted bacteria.[7, 31, 32, 61, 176] Our results agree well with a recent study by Haugen et al., where it was reported that a 15-mer fragment derived from the helical region in the C-terminal half of Pediocin PA-1 inhibits the activity of Pediocin PA-1, and suggested that the corresponding residues (K20, A21, T23, N27, and A34) might be involved in interactions between Pediocin PA-1 and its receptor [33]. Furthermore, our results agree with a previous study that reported

the inhibitory action of the C-terminal LeuA (18-37) fragment to the native LeuA. In fact, the fragment portion of the LeuA (18-38) was found to inhibit the LeuA by 2 folds and suggested competitive binding of the C-terminal fragment with LeuA to a specific membrane bound receptor.[34]

Moreover, the 14-AA LeuA fragment, which was derived only from the helical part of LeuA, was inactive and had limited or no binding affinity towards the bacteria (Figure 2.6E, bottom panel). In the above mentioned previous study of the C-terminal LeuA (18-37), [34] the peptide having the hairpin-like structure at the C-terminal has shown inhibitory action of LeuA. On the other hand, the AMP having 15-amino acid residues derived only from the helical part of LeuA did not exhibit any inhibitory action [33]. These results lead us to conclude the importance of the hairpin-like structure of the C-terminal as well as the tryptophan residues at both sides of the α-helix region in receptor binding and recognition. It appears that conformation and amino acid content of the peptide play a key role in peptide binding and cell membrane interactions. As it was suggested for Pediocin PA-1, other screening studies are needed here to address the residues that play a dominant role in the peptide-receptor interactions.

2.4. Concluding Remarks

Coupling of a 24AA LeuA at a gold surface has resulted in the implementation of a label-free platform for identifying peptide-bacterial interaction. The peptide bound selectivity towards some strains in a higher degree than others. The immobilized 24AA LeuA also exhibited a specific binding towards Gram-positive bacteria with approximate sensitivity approaching 1 bacterium/μl, which is a clinical relevant concentration. On the other hand, the 14AA LeuA peptide did not show any binding, or activity towards bacterial strains. This preliminary approach addressed a future direction of developing a biosensor-based AMP for specific detection of pathogenic Gram-positive bacteria. In particularly, using immobilized LeuA fragments as a viable mechanism for the detection of *L. monocytogenes*. Our studies also have suggested the ability of the C-terminal portion of LeuA (the amphipathic helix-helix structure, beside the C-terminal hairpin-like structure) to bind to the Gram-positive bacteria.

Thus, herein our results support AMPs as interesting candidates for the use as molecular recognition elements in bio-sensing platforms. We are addressing preliminary studies towards developing a new biosensor-based antimicrobial peptide for rapid detection of pathogenic Gram-positive foodborne bacteria. A peptide based biosensor using the 24-AA LeuA as a sensing component could make detection simple and sensitive, allowing for on-site rapid detection capabilities of pathogenic foodborne bacteria.

Chapter 3

Bacterial-adhesion and viability study on surface-bio conjugated Antimicrobial Peptide Leucocin A

3.1. Introduction

As it has been introduced and discussed in Chapter one, Leucocin A (LeuA) is an antimicrobial peptide (AMP) which belongs to class IIa bacteriocins. It is a very powerful antibacterial agent against *L.monocytogenes*, which is most likely related to its binding to a target molecule on the bacterial membrane [73, 142, 177]. This receptor is suggested to be a membrane-located protein of the mannose phosphotransferase system (man-PTS). Man-PTS has been classified into four domains or subunits (i.e., IIA, IIB, IIC and IID) [76]. The first two (IIA and IIB) are found together or separated in the cytosol and are involved in the cellular uptake of glucose and mannose [76]. The last two (IID and IIC) are usually separated and are mainly involved in the phosphorylation process of the cell [76]. Only IIC and IID serve as receptors for pediocin-like bacteriocins [78]. Expression of the genes encoding these four subunits is coordinated since they are commonly clustered in one operon.

Based on some observations of mutagenesis studies, it has been strongly suggested that each individual pediocin-like bacteriocin binds to man-PTS subunits. In a competitive two-gel study, a sensitive-*Listerial* strain lacking the MptA subunit of the man-PTS became Leucocin A resistance strain [72].

Moreover, heterologous expression of the MptC subunit of the man-PTS in an insensitive strain of *Lactococcus lactis* rendered the strain sensitive to several pediocin-like bacteriocins [74]. A more recent study showed with genetic and biochemical evidence that pediocin-like bacteriocins and class IIc Lactococcin A use components of man-PTS proteins (IIC and IID) as a target receptor. It also showed that bacteriocin-immunity protein binds to the same receptor to form a complex that prevents the cells from being killed by bacteriocins [78]. Ability of pediocin-like bacteriocins to bind to a specific receptor of the target cell gives this class with enticing advantages and such unique characteristics could potentially be exploited in many ways with several benefits.

Continuing the story of the detection of foodborne bacteria, particularly *L. monocytogenes*, LeuA was employed here seeking higher selectivity and better detection limits of *L. monocytogenes*. All aforementioned positive-aspects of LeuA with regards to its specificity, selectivity and potency strongly inspired us to apply this 37 amino acid peptide for an on-site detection technique. In this chapter, Leucocin A was synthesized by two different methods and its stability was investigated in human serum and liver homogenate. Furthermore, LeuA was used to investigate bacterial adhesion and its viability when immobilized on a surface.

3.2. Material and Methods

3.2.1 Peptide Synthesis and Purification

Linear synthesis using stepwise solid phase peptide synthesis (SPPS) and peptide synthesis using native chemical ligations (NCL) were employed here to synthesize the full length LeuA (37 AA) AMP.

3.2.1.1. Linear method for peptide synthesis (37-residues LeuA)

Linear synthesis of the 37 AA LeuA (Figure 2.1) was carried out by stepwise, solid phase peptide synthesis (SPPS) using standard Fmoc-chemistry on 2-chlorotrityl chloride resin. The procedure details of the peptide synthesis using SPPS were described previously in chapters 1 and 2. The crude peptide was cleaved from the resin using triflouroacetic acid based cleavage mixture and then introduced to reversed phase HPLC (RP-HPLC) for purification. Identification of the peptide was achieved with MALDI-TOF mass spectrometry. Oxidative folding and disulfide bond formation between **Cys9** and **Cys14** was carried out on the synthesized peptide and finally the peptide was purified using RP-HPLC.

3.2.1.2. Native chemical ligation (NCL)-method

The synthesis of the full length LeuA using NCL was based on the combined synthesis of two separate fragments: one fragment containing a C-terminal

thioester (Fragment 1) and the other fragment with a N-terminal cysteine (Fragment 2). The synthetic methods used for the two fragments are outlined below.

(A) Synthesis of *Fragment 1* (1-13 AA) thioester using in situ thioesterfication on 2-chlorotriryl resin

The synthesis of Fragment 1-thioester, a 13 amino acids sequence (**KYYGNGVHCTKSG**), was carried out using Fmoc-chemistry on 2-chlorotrityl resin (loading 1.6 mmol/g). Peptide assembly on the resin was performed as has been discussed previously. The N-terminal amino acid (lysine) was Boc-protected. Synthesis of the C-terminal-thioester was carried out using in situ thioesterfication of fully protected carboxylate fragment as follows: Peptide resin (0.2 mM) was washed with DCM (3 × 3 ml) and shaken with aliquot of 1% TFA/DCM (3 × 4 ml) each for 3 minutes. The acidic supernatants were combined in the reaction vessel containing 1160 μL (6.65 mM) DIPEA to achieve a final concentration of 4 mM in peptide. To this solution was added 665 μL (6 mM, 30 equiv) methyl 3-mercatopropionate, 540 mg (4 mM, 20 equiv) HOBt, 620 μl (4 mM, 20 equiv) DIC, and 230 μl (1.33 mM) DIPEA. The mixture was stirred overnight then concentrated. The crude protected thioester-peptide was precipitated by multiple triturations with cold diethyl ether followed by centrifugation. The deprotection process (cleavage) was performed by treating the crude product with 95:5:5 TFA/TIS/H2O for 2 h at room temperature. Following this, the peptide was concentrated and isolated by precipitation with cold diethyl

ether. The crude product was purified by semi-preparative RP-HPLC as it has described previously.

(B) Synthesis of Fragment 2

Synthesis of Fragment 2, the 24-AA fragment of LeuA amino acid sequence from 14-37 (**CSVNWGEAFSAGVHRLANGGNGFW**), was carried out on 2-chlorotrityl chloride resin (0.2 mM 1.0% DVB cross-linked) by following the standard Fmoc-chemistry in peptide synthesis as described in Chapter 2. Purification and identification of the peptide were performed using a semi-preparative RP-HPLC and MALDI-TOF spectrometry.

(C) Native Chemical Ligation Procedure

The chemical ligation of the unprotected synthetic peptides (Fragments 1 and 2) was carried out by following a previous reported protocol [178]. Briefly, Fragment 1 (LeuA-thioester (1-13), 6 mg, 4 μM) and Fragment 2 (24-AA LeuA (14-37), 10 mg, 4 μM) were dissolved in a freshly degassed 0.2 M sodium phosphate buffered solution containing 6 M guanidine HCL at pH 7.5 with a final concentration of 2 mM. The ligation reaction was started by adding a mixture of thiophenol (4%)/benzyl mecaptan (4%) to the reaction vessel. The solution was stirred at 25 °C for 24 hr under argon at room temperature and monitored by semi-preparative RP-HPLC and MALDI-TOF mass spectrometry. The ligation reaction was completed after 24 hr. The precipitate was collected and then freeze dried, followed by purification and identification using RP-HPLC and MALDI-

TOF. The pure peptide then was subjected to oxidative folding (i.e., disulfide formation) as described below.

Oxidative Folding and Disulfide Bond Formation

Oxidative folding and disulfide bond formation between **Cys 9** and **Cys 14** was achieved by air oxidation in a freshly degassed 50 mM Tris buffer (pH 8.4). LeuA in reduced form (41 mg, 10.25 μmol) was dissolved in the folding buffer solution at a concentration of 1 mg/mL. 20% DMSO was added to the buffer in order to enhance peptide solubility and oxidation. The solution was gently stirred in an open-air flask for 48 h. The folding reaction was monitored using the Ellman test [179] and MALDI-TOF mass spectrometry.

3.2.2 Antibacterial Activity Assay

The biological activity of the synthetic peptide (LeuA) was tested against two bacterial strains, *C. divergens* and *L. monocytogenes*, using spot in-lawn assay. The method in detail has been discussed in the Appendix chapter (**A.2**)

3.2.3 Stability study of LeuA

3.2.3.1. Serum Stability

The proteolytic stability of the 37 amino acid residue LeuA peptide in the presence of human serum was evaluated using HPLC analysis and MALDI-TOF. Human serum (250 μL) was added to a RPMI medium (650 μL) in a 1.5 mL

Eppendorf tube to mimic a biological system. The temperature was equilibrated at 37 ± 1 °C for 15 min before adding 100 μL of peptide stock solution (1 mM solution in 10% DMSO in sterile water). The initial time was recorded at known time intervals (0, 30 min, 1h, and 24 h). An aliquot of reaction solution (100 μL) was removed and added to pure methanol (400 μL) for precipitation of serum proteins present in the human serum. The cloudy solution produced was cooled in ice at 0 °C for 15 min and then spun at 500 rpm for 15 min to pellet the serum proteins. The supernatant (50 μL) was injected into a RP-HPLC Vydac C18 column. A linear gradient from 15 − 55% ACN/Water in 45 min with a flow rate of 2 mL/min was used. The absorbance of the eluting peaks was detected @ 220 nm. The peptide was collected at an elution time of 26 minutes. The concentration of the eluted peak was measured by integrating the area under the curve and the peptide identity was definite using MALDI-TOF mass spectrometry.

3.2.3.2. In Vitro Metabolic Stability

The in vitro metabolic stability was determined by incubating LeuA with liver homogenate. The liver homogenate was prepared according to the following procedure. The liver samples were collected from male CD-1 mice. After the sample was cleaned and washed in ice-cold HEPES buffer (pH 7.4), approximately 0.98 g was transferred to a 50 mL centrifugation tube. Ice-cold HEPES buffer (5 mL) was then added and the organ was homogenized with an Ultra- Turrax (IKA, Staufen, Germany) for 1 min on ice. The homogenate was

shaken and subsequently centrifuged at 14,000 rpm for 20 min at 4 °C. Aliquots of the supernatant were transferred into microtubes and stored at -80 °C until use. Before use, the protein content of each homogenate was determined using bicinchoninic acid protein assay (BCA) to generate a stock solution with a protein concentration of 14.7 mg/mL by dilution with HEPES buffer. For the metabolic stability of the LeuA, an 100 μL aliquot of the peptide stock prepared in a 10% DMSO/water mixture (1 mM) was added to 900 μL of liver extract (200 μL of homogenate, 700 μL of RPMI medium, pH 7.4, 2.94 mg of protein in total). The mixture was incubated at 37 °C while shaking where aliquots of 100 μL were taken out at regular time intervals. The enzymatic reaction was stopped by mixing the sample with methanol (300 μL). The samples were then cooled at 0 °C for 30 min to allow precipitation of the proteins. The mixture was centrifuged at 14 000 rpm for 10 min to yield a clear supernatant that was analyzed by reversed-phase HPLC on Vydac C18 column with UV detection at 220 nm wavelength. Cleavage products were separated by analytical reversed phase HPLC using 15−55% ACN/water over 60 minutes and analyzed by MALDI-TOF mass spectrometry. Blank solutions and the control α-peptide (peptide-18) were similarly treated for comparison. The percent of hydrolysis was determined from the integration of the area under the peaks.

3.2.4 Peptide Surface Bio-conjugation

The gold substrates were cleaned and prepared as outlined in Chapter 2 section 2.5. The freshly prepared gold substrates were immersed in a binary mixture of 5 mM (25:75, 12-mercaptododecanoic acid (MUA)/6-mercapto-1-hexanol (C6OH))

in absolute ethanol for 12 h, in order to ensure an optimal homogenous formation of the adlayer [180]. The substrates were then rinsed with pure ethanol and dried with a flow of nitrogen. In order to activate the substrate-coated monolayer, the slides were treated with a solution of 10 mM *N*-hydroxysuccinimide (NHS) in DMSO for around 90 min. Following functionalization, the slides were rinsed DMSO prior to the bio-conjugation of LeuA.

LeuA immobilization was carried out by immersing the Au-modified substrates in a solution of 1 mg of LeuA in 1 mL of DMSO at room temperature for 5 h. After the immobilization step, the surfaces were vigorously rinsed in PBS with agitation and dried under a flow of dry nitrogen. **Scheme 3.1** shows a representative diagram of the peptide-surface bio-conjugation process.

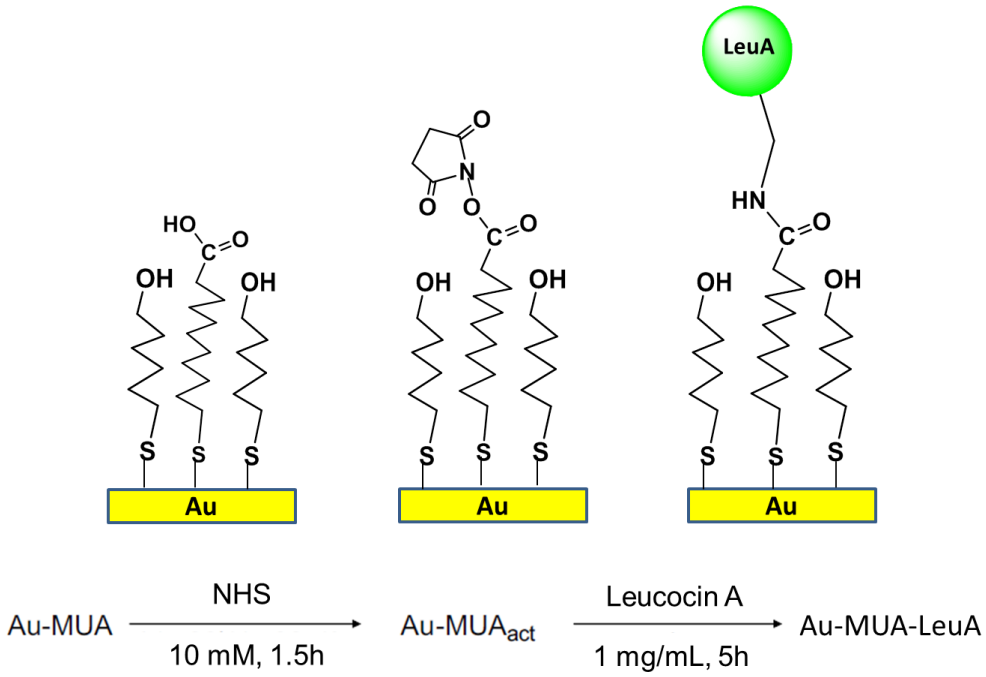

Scheme 3.1. LeuA-surface bio-conjugation**; Step 1**: SAMs formation of MUA (Au–MUA); **Step 2**: esterification (activation) of the COOH functionalities by NHS, Au–MUAact; **Step 3:** covalent binding of the LeuA, Au–MUA–LeuA.

3.2.5 Bacterial Adhesion and Confocal Imaging

The immobilized LeuA substrates were immersed in a solution of 10^6 cfu/mL of *C. divergens* in 1 mL of sterile PBS at room temperature for 3 hr. After the incubation the substrates were washed several times with PBS and allowed to dry in a sterile environment. Live/dead bacterial cell stains, CyQUANT green and propidium iodide (PI), were prepared separately with sterile water and mixed together with a ratio of 1:1. 100 μL of this mixed live/dead stain solution was incubated with the substrates in sterile vessels for 90 minutes at 37 ^{o}C. The substrates were then rinsed several times with sterile PBS and dried in sterile environment.

Peptide-bacterial interaction and bacterial viability were examined with a confocal inverted microscope, Quorum WaveFX spinning disk confocal system (Quorum Technologies Inc; Guelph, Canada). Images were acquired with an oil immersion lens at a magnification of 60 X/1.4. Multiple fluorescence signals were acquired sequentially to avoid cross talk between image channels. Fluorophores were excited with the 488 nm line of an argon laser (for CyQUANT) and the 543 nm line of a HeNe laser (for propidium iodide). The emitted fluorescence was detected through spectral detection channels between 500 – 530 nm and 555 – 655 nm for green and red fluorescence, respectively.

3.3. Results and discussion

3.3.1. Peptide Synthesis of Full Length LeuA, linear synthesis vs. NCL

3.3.1.1. Synthesis of LeuA by Linear-Stepwise SPPS

Synthesis of full length 37-residue LeuA was attempted by stepwise SPPS using standard Fmoc-chemistry on a 2-chlorotrityl chloride resin. The optimized Fmoc-chemistry described previously was used for the assembly of amino acid residues to the resin. After completion of the 37-residue chain assembly of LeuA, the crude peptide was cleaved from the resin followed by identification using MALDI-TOF and purification using RP-HPLC **(Figure 3.1)**. LeuA was obtained with an overall yield of 10% with purity of ≥ 95%.

Oxidative folding and disulfide bond formation between Cys9 and Cys14 was carried out in a buffer solution followed by purification using RP-HPLC [179, 181]. The pure oxidized LeuA was characterized by RP-HPLC and MALDI-TOF mass spectrometry.

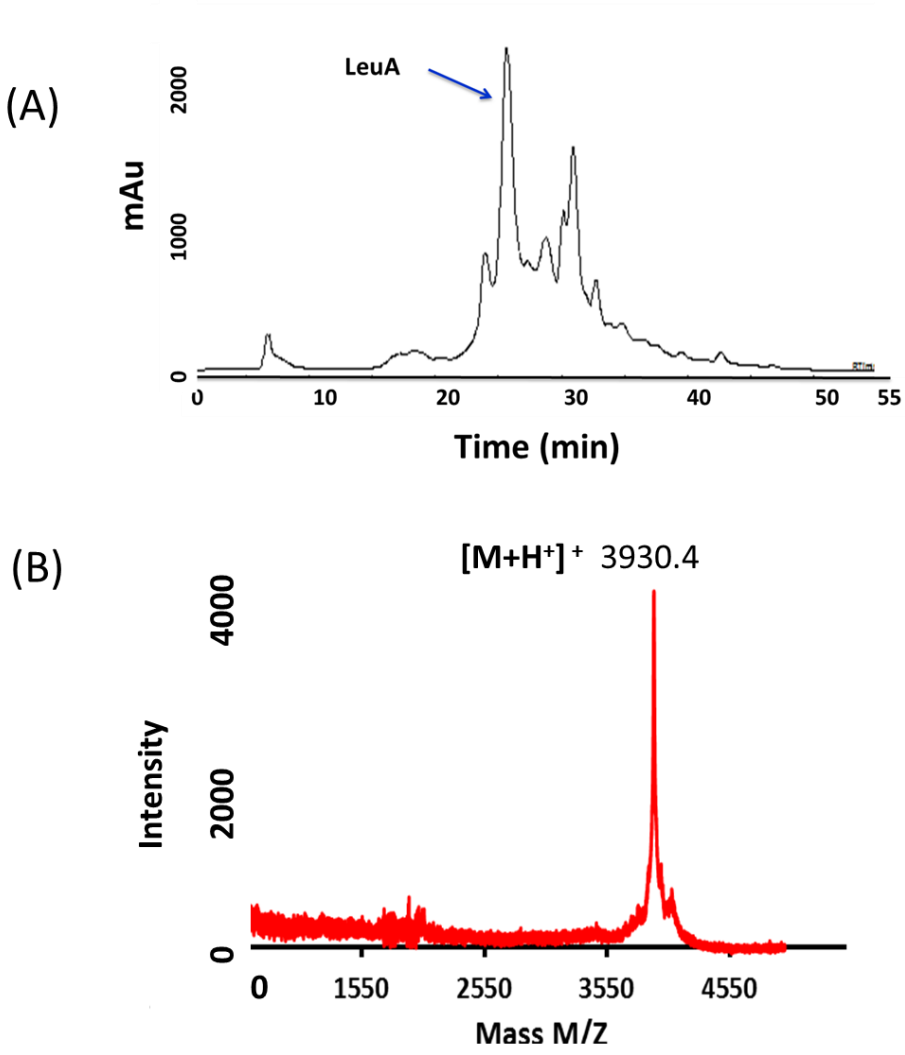

Figure 3.1. (A) The crude HPLC chromatogram of LeuA shows peptide-elution time at 26 min. (B) MALDI-TOF spectrum of LeuA shows a mass at 3930.4, calculated mass was found 3929.3.

3.3.1.2. Synthesis of LeuA by NCL

NCL has been used as an alternative technique to the stepwise SPPS for synthesis of long and difficult sequences. Peptide synthesis by NCL results in having

peptides with higher purity, yields, low racemisation, as well as a low formation of aggregated peptides. Also, it allows for the synthesis of larger peptides, protein and enzymes [86].

In NCL for LeuA, the Cys14 was chosen as the potential ligation site giving rise to two fragments, namely, 13-AA fragment 1 (1-13) and 24-AA LeuA (fragment 2) (14-37). Fragment 1 was synthesized using an in situ thioesterfication method on 2-chlrorotrityl resin and characterized using HPLC and MALDI-TOF (**Figure 3.2**). Previously, this fragment was synthesized in our lab (data not shown) using direct synthesis on sulfonamide safety catch linker resin as described by Ingenito *et al* [182]. Synthesis showed that using the in situ thioesterfication method gives higher overall yield of 33% compared to 7% using the sulfonamide safety catch linker. The 24-AA LeuA fragment 2 (14-37) was synthesized on a 2-chlorotrityl chloride resin using stepwise SPPS with an overall yield of 55% and a purity >95% (as described in chapter 2). The NCL reaction was initiated by a chemo-selective nucleophile attack of the thiol of Cys (N-terminal) of the unprotected peptide (fragment-2) on the C-terminal-thioester moiety of unprotected peptide (fragment 1). This reaction is followed by a rapid and spontaneous rearrangement through an S-N acyl shift giving rise to a ligated product.

The reaction of NCL was monitored using RP-HPLC at different time intervals (0, 24 h), where it was found that the complete reaction was obtained after 24 hr (**Figure 3.3A**). Furthermore, the presence of thiophenol with excess of

3-mercaptopropionic acid ethyl ester significantly enhanced the ligation reaction rate through nucleophile catalysis [183].

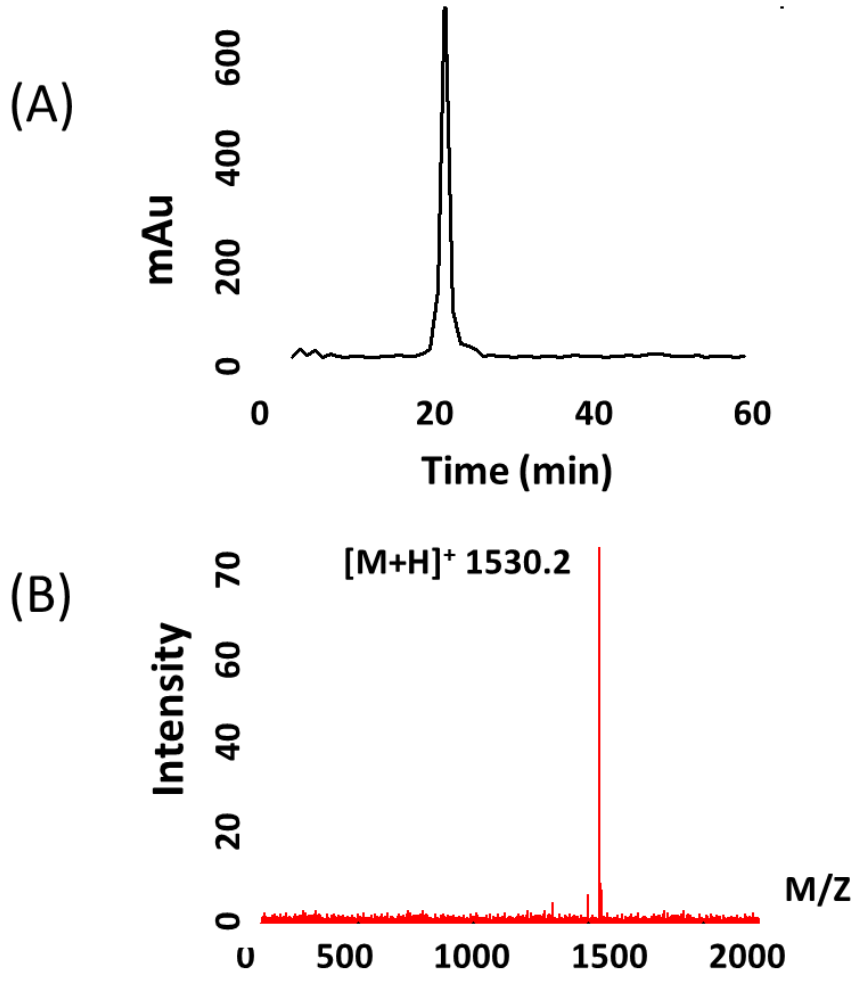

Figure 3.2. Identification and characterization of the fragment 1 (13AA), N-terminal thioester (A) HPLC chromatogram of the pure peptide, elution time at 21 min; **(B)** MALDI-TOF spectrum of the peptide shows a reduced mass at 1530, Calcd mass was found 1529.2.

The pure peptide was characterized by RP-HPLC and MALDI-TOF mass spectrometry (**Figure 3.3B**). The $[M+H]^+$ of the peptide was found to be 3930.5 (calculated $[M+H]^+$3929.3). The overall yield of the chemical ligation reaction to give the pure peptide in the reduced form was 33%. Oxidative folding and disulfide bond formation of the reduced peptide was carried out as described for the stepwise SPPS. The peptide was purified and characterized to give pure synthetic LeuA with an overall yield of 26.6% based on a 0.2 mmol scale synthesis.

Based on the use of the two synthetic methods, it is clear that using NCL to synthesize LeuA gives higher overall yield resulting in a higher purity peptide than peptide synthesis with linear-stepwise SPPS. Moreover, in situ thioesterfication method for fragment 1 (C-terminal thioester) synthesis gave a higher yield and a more pure peptide than that of linear-synthesis using sulfonamide safety catch linker resin.

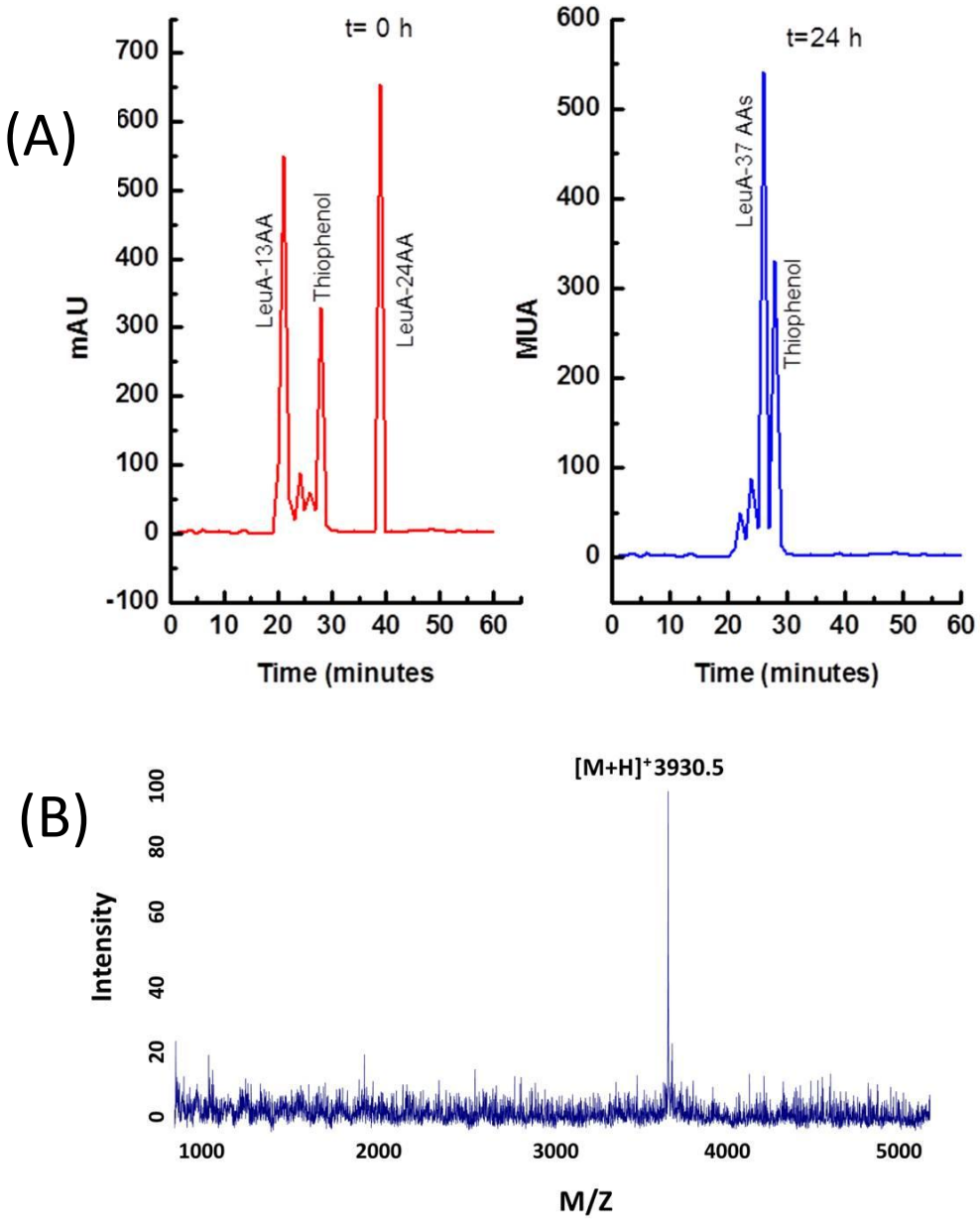

Figure 3.3. NCL monitoring of LeuA shows (A) HPLC chromatograms of NCL monitoring at zero time (t = 0 h) and after 24 h (t = 24h) and (B) MALDI-TOF spectrum of the pure peptide.

3.3.2. Proteolytic stability of LeuA

Susceptibility of LeuA to different proteolytic enzymes was investigated against human serum as well as liver homogenate. LeuA was incubated with human serum at 37 °C and aliquots were removed and analyzed at different time points up to 24 h using RP-HPLC. Figure 3.4A illustrates the complete stability of LeuA toward human serum after 24 h incubation as shown by HPLC. In contrast, LeuA exhibited proteolysis in the presence of liver homogenate within 30 minutes of incubation and complete degradation within 5 h as shown by HPLC and mass spectrometry (**Figure 3.4B**).

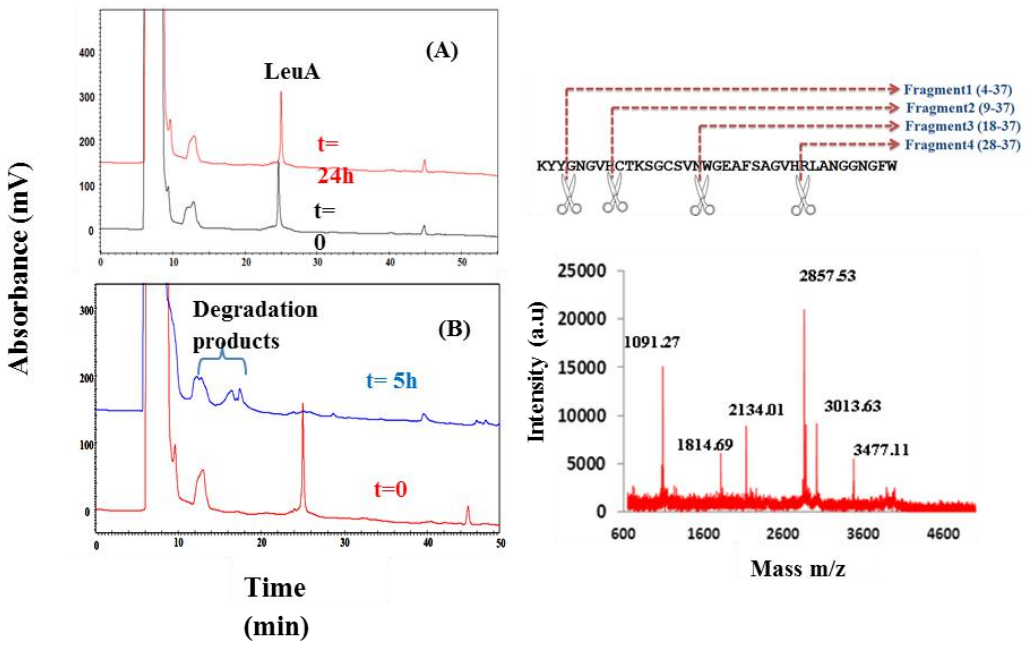

Figure 3.4. RP-HPLC chromatograms of LeuA peptide (left), after incubation with human serum **(A)** and the liver homogenate **(B)**. Peptides were incubated with the human serum or liver homogenate from mice for different time intervals 0 – 24 h, prior to HPLC analysis. LeuA elutes at 25 minutes. Degradation products from LeuA after incubation with liver homogenate appear around 14 − 17 minutes and the remaining peaks are from the medium. On the right side, LeuA sequence shows the cleavage sites on the top and the mass spectrum for the degradation products on the bottom.

The four degradation products of LeuA after incubation with liver homogenate show masses of 3477.11, 3013.63, 2857.53, and 2134.01 which correspond to cleavage at the N-terminus as well the C-terminus of the peptide. The degraded fragments 1 and 2 have been shown in a previous study when LeuA was incubated with trypsin, pepsin or chymotrypsin enzymes [35]. According to our results, it seems that LeuA is very stable in human serum. However, it is degraded into several fragments during its incubation with the liver homogenate. Our results led us to anticipate that the LeuA is mainly metabolized by liver enzymes and is not affected by the serum or its enzymes. Results suggest that if LeuA was to be used therapeutically as a substitute for antibiotics as antimicrobial agents then a higher stable form will be needed.

Table 3.1. Amino acid sequences of the main four degradation products of LeuA after incubation with live homogenate for 5 h.

Fragments #	**Sequences**	**$[M+H]^+$**
Fragment 1	GNGVHCTKSGCSVNWGEAFSAGVHRLANGGNGFW	3477.11
Fragment 2	CTKSGCSVNWGEAFSAGVHRLANGGNGFW	3013.63
Fragment 3	KYYGNGVHCTKSGCSVNWGEAFSAGVHRLANGGNGFW	2857.53
		1091.27
Fragment 4	WGEAFSAGVHRLANGGNGFW,	2134.01
	KYYGNGVHCTKSGCSVN	1814.69

3.3.3. Peptide Immobilization and Surface Characterization

The antimicrobial surface was constructed by following three steps as shown in the **scheme 3.1**. In the first step, the substrate was functionalized with a monolayer of 11-mercaptoundecanoic acid (Au–MUA). The acid functions were then activated into esters (Au–MUAact) using the activating agent NHS, in order to let Leucocin reacts via its amino groups (Au–MUA–LeuA) as a final step.

Peptide-surface characterization was performed using FTIR spectroscopy as depicted in **Figure 3.5.** The IR spectra were recorded after the successive steps of gold surface functionalization. Spectrum **(a)** has dominate intense bands assigned to CH2 chains that are recorded at 2850 and 2922 cm^{-1} suggesting a rather good crystallinity of the 11−MUA layer which is in agreement with the previous studies [184-186]

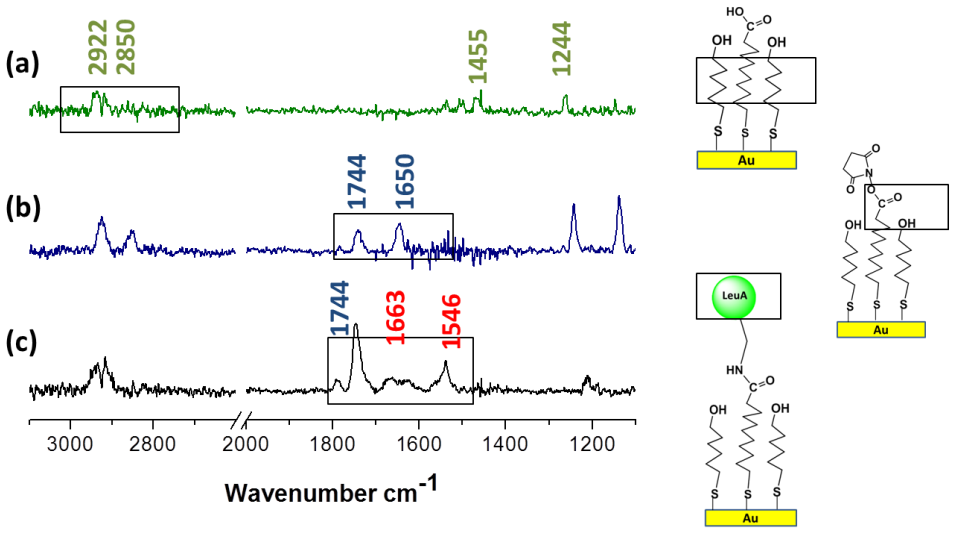

Figure 3.5. FTIR spectra of the three consecutive steps of LeuA immobilization on a gold substrate: **(a)** Au–MUA; **(b)** Au–MUAact by NHS; **(c)** covalent binding of LeuA, Au– MUA–LeuA.

The IR weak absorption at 1244 cm^{-1} is attributed to the OH deformation of the mercaptohexanol, while the weak broad peak at 1455 likely includes attribution from the scissor mode of CH_2 groups and from the symmetric COO^- stretch. A weak absorption signal at 1255 cm^{-1} is contributed to asymmetric COO^- stretch vibration confirming that some of the carboxylic acid groups are deprotonated [186]. (b) Figure 3.5b shows a signal at 1744 cm^{-1} confirming the transformation of acid groups to ester terminal groups. The peptide binding to the SAM substrate is indicated by the appearance of the bands on spectrum (C). Intense signals at 1663 and 1546 cm^{-1} are ascribed, respectively, to the amide I and amide II of the peptide bond. The band at 1738 cm^{-1} is an indication of C=O stretching of lateral chain function and of some hydrolyzed ester functions. Weak absorption signals observed at 1251 and 1457 cm^{-1} can be attributed, respectively,

to CH_2OH of the serine and O=C=OH of the glutamic acid. Note that the intensity of the observed bands depends on the peptide orientation, position and concentration on the surface-interface.

3.3.4. Confocal Study of Bacterial-adherence and Viability of the Adhered Cells

Confocal microscopy was used to detect peptide-bacterial interactions as well as study bacterial viability. In this work, the AMP activity and binding of the surface-immobilized LeuA was tested against non-pathogenic, *C. divergens LV13*. The bacteria (10^6 cfu/mL) was incubated with the functionalized slides (Au-MUA-LeuA-substrates) for 3 h at room temperature and then a solution of a live/dead stain was added for 30 minutes at 37 ^oC (see experimental section for the details).

Results showed that the number of the bacteria that bind to the functionalized surface is significantly higher as compared to the peptide-free surface. Therefore, results demonstrate ability of the surface-coated AMP to exhibit high binding to the bacteria and the ability to kill the attached bacteria at the same time. Similar experiments for comparison purposes were performed with the 24-AA fragment of LeuA that has been studied previously in chapter 2.

The live/dead stain was applied in order to understand the mode of action of the LeuA-bound to the gold substrate against the bacteria. Briefly, the live/dead stain is composed of two fluorescence dyes or DNA-probes, i.e., CyQUANT green which has ability to stain the live cells with green color and propidium

iodide (PI) which can only penetrate/cross-over damaged cell membranes resulting a red fluorescence of the bacterial cells. Thus, because PI quenches the fluorescent emission of CyQUANT, it is assumed that the green cells are alive, whereas the red cells are dead. Figure 3.6 shows the confocal microscopy images of the peptide-bacteria interaction and the live/dead cells in both surface-coated LeuA and a surface coated 24-AA LeuA. It is clear that the majority of the cells attached to the LeuA-functionalized surface carry the red color (red-stained cells) and few cells appear with the green color (green-stained cells). This means that the majority of the cells that attach to the LeuA coated surface have been killed by its contact with the AMP. On the contrary, the 24-AA-functionalized surface, which was used as a positive control, shows higher concentration of green-stained cells compared to that of red-stained cells. This is a clear indication that majority of the cells are still alive and have bound to the immobilized peptide through a specific mechanism of adhesion or receptor interaction.

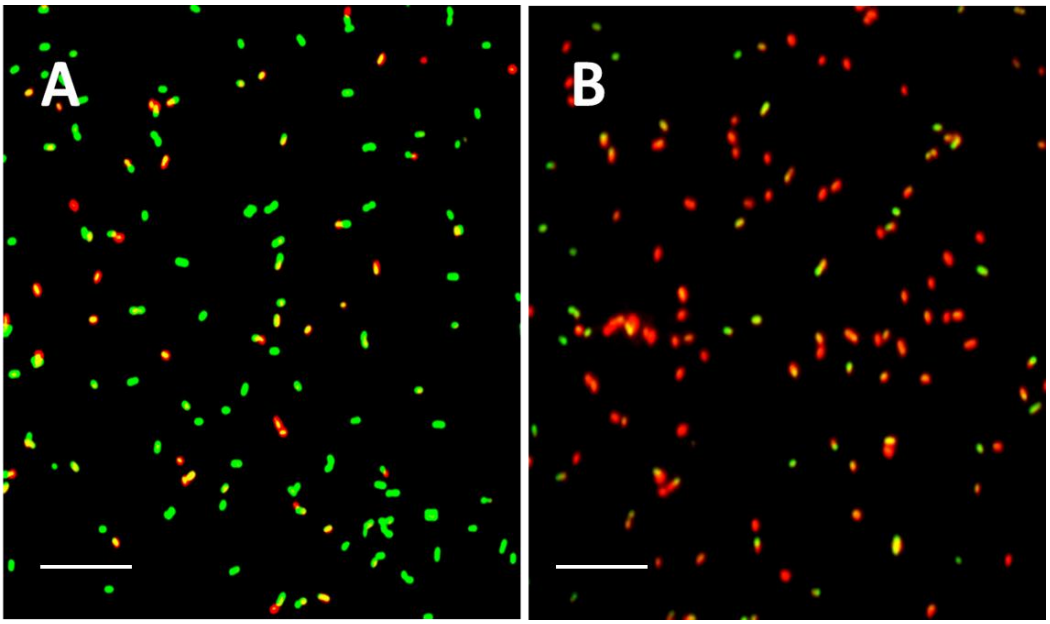

Figure 3.6. LeuA-bacterial interaction and its biological activity against *C.divergens LV13* (A) 24-AA LeuA (B) LeuA (37AA); mixture of 1:1 life/dead stain probes were incubated with the immobilized peptide. Life cells are stained in green, while dead cells have taken the red color. Scale bars are 7 μm.

Results indicate that immobilized-LeuA has the ability to kill bacterial cells. These results indicate that the bacteria adhere to the peptide-coated surface and membranes disruptions occur by the LeuA-coated surfaces which permitted the entry of propidium iodide (PI).

In this current project, further studies are under investigation, such as peptide (LeuA) selectivity, specificity and sensitivity towards other bacterial strains, such as *Listeria monocytogenes.* Also, the influence of peptide-orientations (site-specific attachment) and methods of immobilization on the peptide activity and binding-selectivity are being investigated.

3.4. Concluding remarks

This chapter has presented the synthesis of a class IIa AMP, a 37-AA Leucocin A peptide, by two methods: linear synthesis via solid phase peptide synthesis (SPPS) and native chemical ligation (NCL). It is clearly observed that NCL is the preferable method for synthesis of LeuA as well as for long peptides in general. Our studies also explored LeuA proteolytic stability in human serum as well as in liver homogenate; peptide stability was confirmed in human serum up to 24 h, while fragment degradations were apparent after 30 minutes of incubation with the live metabolizing enzymes. The antibacterial activity of the surface-immobilized LeuA by chemical bio-conjugation has been tested against Gram-positive bacteria (*C. divergens LV13*). The LeuA peptide-coated surface showed high binding affinity towards the corresponding strain, and the viability studies showed less than 20% of the cells remain alive after being in contact with the grafted LeuA. Confocal microscopy experiments and imaging results have been performed to assay the mode of action of the peptides. When LeuA is present at the surface, the bacteria that nonetheless adhered to the surface are most probably permeabilized and thus unable to grow. However, bacterial integrity is not affected on a non-LeuA functionalized surface.

Chapter 4

Molecular Dynamics Simulation study of Lactococcin G Class IIb Two-peptide Bacteriocin in a DPPC Lipid Bilayer

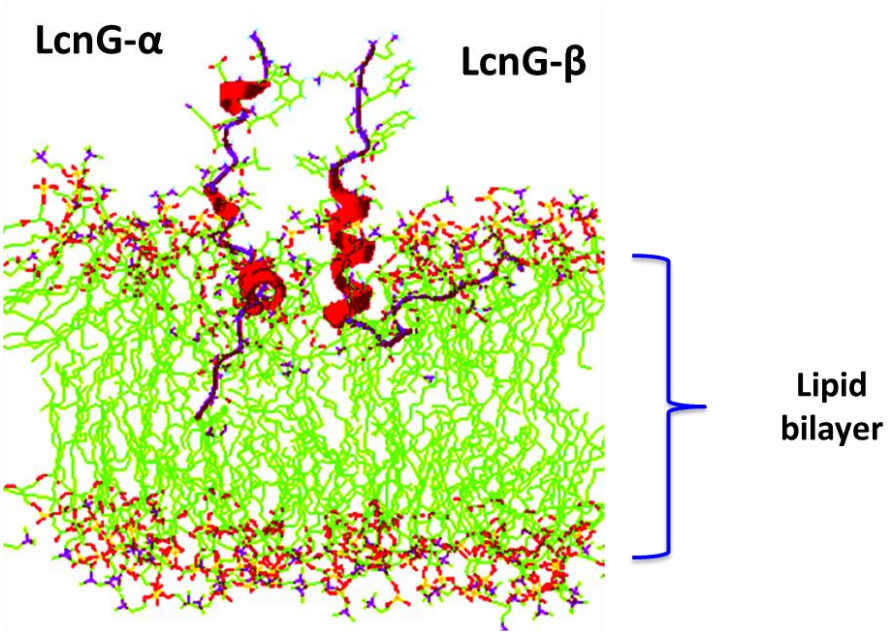

Class IIb two-peptide bacteriocin, Lactococcin G in DPPC lipid bilayer (Snapshot was taken from simulation I at 0 ns)

4.1. Introduction

Lactic acid bacteria (LAB) are potential source of several antimicrobial peptides (AMPs) that have been recognized as bacteriocins [1-5, 8, 187-189]. These AMPs possess potent activity against variety of food-borne drug resistance pathogenic bacteria. They have also been a subject of several investigations as they offer special properties as natural food preservatives, additives to animal feed, and alternatives to conventional antibacterial agent [9]. Bacteriocins are recognized as safe, heat-stable, food-grade quality agents with no toxicity to eukaryotic cells [9]. Bacteriocins are classified into several groups according to their biochemical and genetic properties [6, 17, 18]. Class I bacteriocins (Lantibiotic) are small peptides characterized by having unusual amino acids, lanthionine and β-methyllanthionine, and display broad spectrum activity against most of the gram-positive bacteria [19, 190, 191]. Class II bacteriocins (non-Lantibiotic) are small (<10 KDa), cationic antimicrobial peptides made of unmodified amino acid residues, that act at nano-pico molar concentration by inducing permeabilization on the target cell [2]. This class is further divided into other sub-classes, class IIa, class IIb, and class IIc [1, 6, 17].

Class IIa bacteriocins have been documented as one of the most interesting class of AMPs with wide-ranging applications as safe food preservatives [26]. These peptides complement antibiotics in the treatment of infectious diseases [26]. In addition, they exhibit antiviral activity to some extent [27]. Most importantly, these peptides inhibit growth of deadly gram-positive food-borne

pathogenic bacteria such as *Listeria monocytogenes*, *Bacillus cereus* and *Staphylococcus aurous* [28].

Class IIb bacteriocins consist of two complementary peptides and interestingly, these two complementary peptides act as one functional unit with an optimal antibacterial activity achieved by the presence of these two peptides together in equal amounts [8]. In other words, the two-peptides act non-separately in equal quantities to optimize the antimicrobial activity [8]. Furthermore, these peptides are generally active at pico-nano molar concentrations. Low and no activity have been observed when these two-peptides are assayed individually even at micro molar concentrations [8, 41, 42]. The mechanism of antibacterial activity is displayed by disrupting the membrane permeability of the target cell membrane [42, 43, 158].

Lactococcin G (LcnG) is the most well-studied antimicrobial peptide of the class IIb two-peptide bacteriocins [41, 44, 45, 187], and which will be the focus of this study. LcnG, isolated in 1992 by Nissen-Meyer et al [44], consists of two peptides LcnG-α and LcnG-β (**Figure. 4.1**). LcnG-α consists of 39 amino acid residues, while LcnG-β consists of 35 amino acid residues [44]. The NMR solution structure of LcnG was reported in membrane mimicking entities such as dodecylphosphocholine (DPC) micelles, as well as in triflouroethanol (TFE) [46]. The NMR studies show that the individual peptide holds into helical conformations, and circular dichroism (CD) studies show that the peptides helicity increases when these complementary peptides are present together in the solution [45]. CD study also revealed that these peptides are relatively

unstructured in water; however, they are completely structured in both TFE and DPC [45]. These results suggest direct interaction between the two-peptides. Furthermore, the genes encoding the preforms of the two-peptides are always adjacent to each other in the same operon along with the gene that encodes the immunity protein which protects the bacteriocin-producer from being killed by its own bacteriocin [7, 8]. Accordingly, these proposals reveal that the synergistic action of class IIb bacteriocin is most likely due to interaction of two-peptides with each other, and forming one antibacterial unit rather than separately acting on two different sites on the target cells [5, 7, 187].

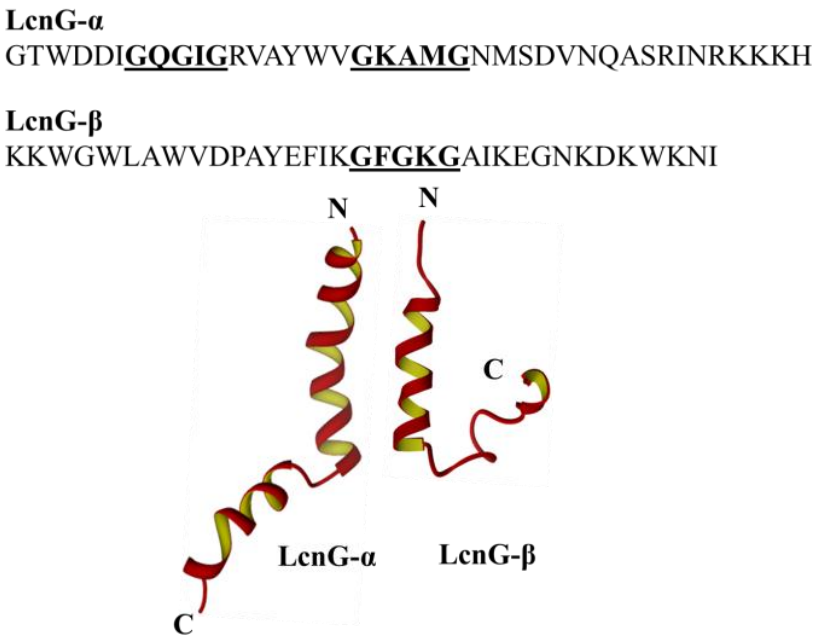

Figure 4.1 The amino acid sequence and three dimensional structure of two-peptide LcnG, LcnG-α (PDB 2JPJ) and LcnG-*β* (PDB 2JPK). The putative helix-helix GxxxG-motifs is underlined.

The sequence of class IIb two-peptide bacteriocins contain one or two conserved GxxxG motifs that most likely mediate helix-helix interactions between the two complementary peptides [192]. LcnG has three GxxxG-motifs, two in LcnG-α (G7xxxG11 and G18xxxG22) and one in LcnG-*β* (G18xxxG22). The presence of two glycine residues in each GxxxG motif is anticipated to help create flat interaction sites to allow a close contact between the two helices with hydrogen bonding and Van der Waals interactions [193-195]. Therefore, the objective of this study was to investigate the mechanism of interaction between the two LcnG peptides, LcnG-α and LcnG-*β* as well as between the peptides and a model lipid bilayer. Molecular dynamics (MD) simulations were used to explore the interaction of LcnG peptides, starting with their individual NMR solution structures, in a model zwitterionic lipid bilayer system.

4.2 Methods

4.2.1 Structure of two-peptide LcnG

The three-dimensional solution structures (NMR) of the two LcnG peptides in the presence of DPC micelles were obtained from the protein data bank (PDB) under code entries 2JPJ and 2JPK for α and *β* peptides, respectively [46]. According to the NMR solution structure, LcnG-α has a well-defined N-terminal amphipathic α-helix from residues 3 to 21 and a less well-defined hydrophilic α-helix from residues 24-34. On the other hand, LcnG-*β* has only one helical region from residue 9–19 [46]. The two GxxxG-motifs in LcnG-α are G7xxxG11 and G18xxxG22, and the one GxxxG-motif in LcnG-*β* is G18xxxG22 [45, 46].

Another important characteristic is that LcnG-α has tryptophan residues at positions 3 and 16 whereas LcnG-*β* has three tryptophan residues at the N-terminal portion, at positions 3, 5, and 8. These N-termini-tryptophans are considered to be an important factor in positioning and orienting the peptide on the membrane-water interface [196-198].

4.2.2 Lipid bilayer and simulation box construction

Lipid bilayer made of zwitterionic dipalmitoylphosphatidylcholine (DPPC) was used to mimic the cellular membrane environment. The PDB coordinate for the DPPC molecules and the bilayer composed of 64 DPPC per leaflet (128 lipid molecules) were obtained from http://moose.bio.ucalgary.ca [199]. The system was set up by placing the peptides with the DPPC arranged in a bilayer (60 molecules upper leaflet and 61 molecules lower leaflet) using Swiss-PdbViewer28 [200]. Four different systems were setup, and in all of them the peptides were embedded partially in the upper leaflets of the lipid bilayer in parallel orientations. While the C-termini were facing the hydrophobic portion of the lipid core of the system, the N-termini remained outside of the membrane as shown in **Figure. 4.2**.

In all four systems, LcnG-α peptide was fixed in the same position, whereas the position of *β*-peptide (LcnG-*β*) was changed from one system to another. In general, the peptides were placed with an average distance of 3.9 - 4.2 nm apart from each other. In the first simulation (S-I), where the peptides were 4.2 nm apart, the N-terminal residues (Gly1, Trp2, and Phe3) of α–peptide were facing N-

terminal residues, Lys2, Trp3 and Gly4, of *β*–peptide. In simulations 2 and 3 (S-II and S-III), *β*-peptides was moved slightly down with respect to α–peptide. In simulation II (S-II) with peptides at 4.0 nm apart, Lys1, Lys2 and Trp3 of *β*–peptide faced Asp4, Asp5 and Ile6 of the *a*–peptide, whereas, in simulation III (S-III), Lys1, Lys2 and Trp3 of *β*–peptide faced Trp3, and Asp4 of the *a*–peptide. Finally, in simulation 4, *β*-peptide was moved up with respect to α-peptide. Here peptides were placed 3.9 nm apart and residues Gly1, Trp2 and Phe3 of α–peptide were placed facing N-terminal residues (Trp3, Gly4, and Trp5) of *β*–peptide.

In a box with dimensions of 7 nm × 7 nm × 10 nm, the starting configurations were generated by adding SPC water molecules (~11625 ±10) on both sides of the bilayer. Sufficient counter-ions (30 Na^+, 38 Cl^-) were randomly distributed in the aqueous phase in order to render each system electrostatically neutral and obtain a final concentration of ~31 mM NaCl. The system was energy minimized before running the full simulation using 200 steps of the steepest descent energy minimization method in order to relax any steric conflicts generated during the setup. All simulations were equilibrated firstly by performing 2 ns run with a positional restrain on the peptide molecules. Following this, full MD simulations were generated for 30 ns.

4.2.3 Computational environment and simulation parameters

All molecular dynamics simulations were carried out using the GROMACS 3.3.3 simulation package and the GROMOS96 force field [201, 202] **.** The four systems were simulated in the isobaric–isothermal (NPT) ensemble at 300 K using

periodic boundary conditions**.** Weak coupling of the proteins to a solvent bath of constant temperature was maintained using the Berendsen thermostat with a coupling constant τT=0.1 ps. The pressure was controlled using the Berendsen algorithm at 1 bar with a coupling constant τP=1 ps**.** Particle Mesh Ewald (PME) algorithms was used for calculation of electrostatic interactions and a cut-off was used for van der Waals interactions [203, 204]. For all simulations, the neighbor list was updated every 10 steps, with a neighbor list cut-off distance of 1.2 nm. The Lennard–Jones interactions were truncated at a cut-off distance of 1.2 nm. The integration time step was 2 fs, and the coordinates and velocities were saved every 4 ps. The LINCS algorithm was used to restrain all bond lengths [205]. Simulations were analyzed using various GROMACS post-processing routines. Swiss-PdbViewer [200] and ViewerLite 5.0 [206] were used to visualize the systems. The GROMACS software, as well as the data analysis tools is available for free download from the internet (http://www.gromacs.org/).

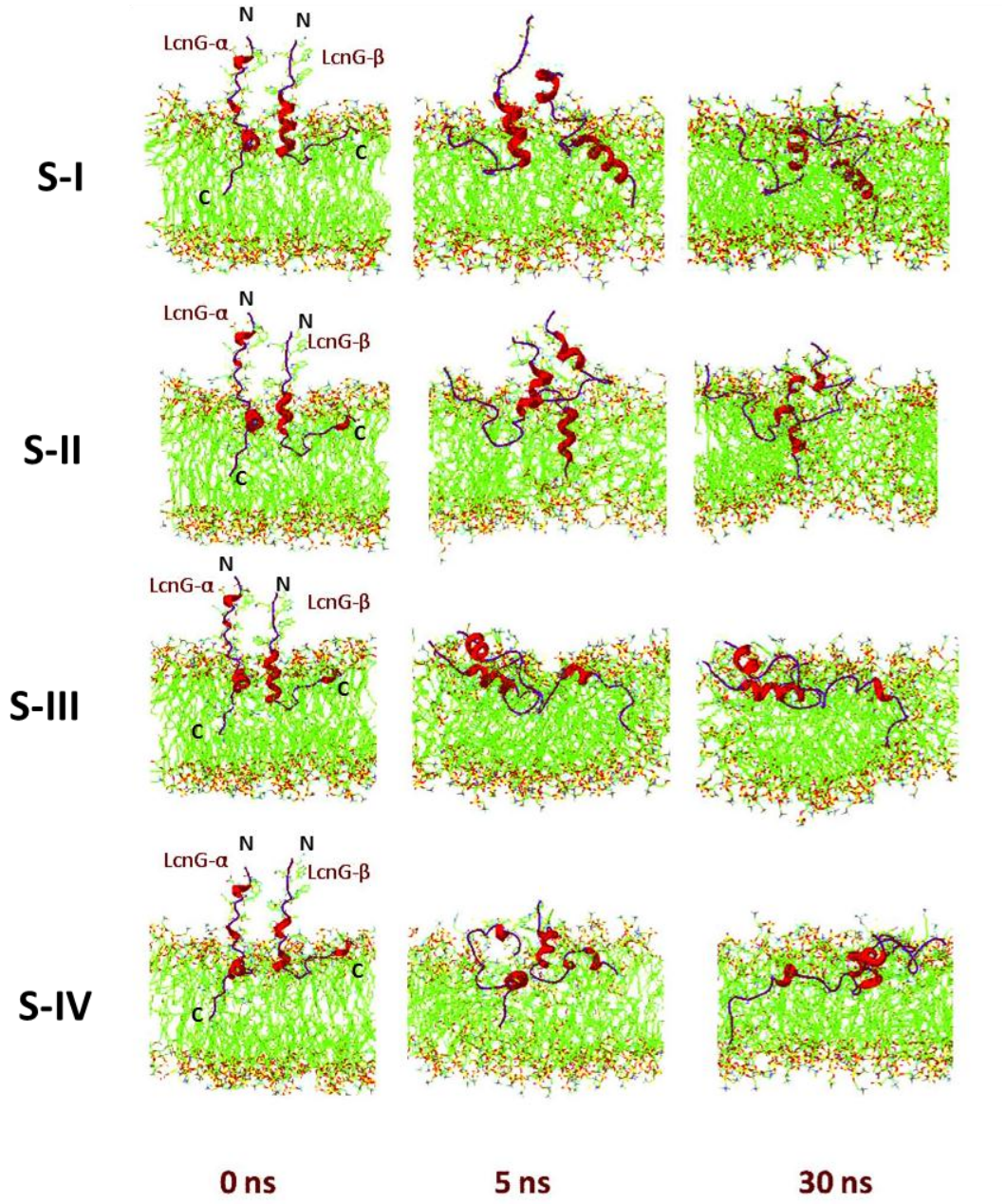

Figure 4.2 Interaction of LcnG-α and LcnG-*β* (two-peptide bacteriocin LcnG) in DPPC lipid bilayer system. Snapshots from four independent simulations I, II, III, and IV were taken at 0, 5 and 30 ns as denoted. Peptides were parallelly oriented with limited insertion of the C-termini in the lipid bilayer core and N-termini facing out toward the aqueous layer at the start of the simulations (starting orientation). For all simulations, LcnG-α had the same initial configuration whereas orientation of LcnG-*β* was changed. The lipid is shown in bond format with the hydrophobic tails in green and the polar head group in multi-colors whereas the peptides are shown as ribbon.

4.3. Results and Discussion

Four different MD simulations were conducted to investigate the mechanism of interactions of LcnG complementary peptides in DPPC bilayer. At the starting configuration, LcnG-*β* was placed in four different orientations in an aqueous bilayer system with respect to a fixed position of LcnG-α peptide as described in the experimental section (**Figure 4.2**). This allowed sampling of different peptide-peptide orientations.

4.3.1 Peptide distribution and interaction

Figure 4.2 illustrates snapshots of four independent simulations (S-I, S-II, S-II, and S-IV) at different time frames (0 ns, 5 ns, and 30 ns). The initial analysis of the trajectories of the four simulations showed complete penetration of both peptides into the lipid bilayer, and this penetration into the bilayer is most likely assisted by the partial insertion of the peptides into the upper membrane leaflet. A recent study of class IIa bacteriocin carnobacteriocin B2 has reported that a single peptide does not spontaneously penetrate lipid membranes; however, a partial insertion of the peptide into the bilayer helps a complete penetration and interaction [207]. In addition the interaction between the two corresponding peptides (LcnG-α, and LcnG-*β*) is clearly observable from the snapshot images that were taken during the simulations time.

4.3.2 Peptide-lipid interaction

A significant interaction was observed between the positively charged peptide residues and the lipid oxygen atoms. The highly charged C-terminal portion of LcnG-*β* (residues Lys34, Lys33, Lys32 and Arg31) directs the peptide toward the interface and interacts with the glycerol and the phosphorous moieties of the lipid head-groups by electrostatic interactions.

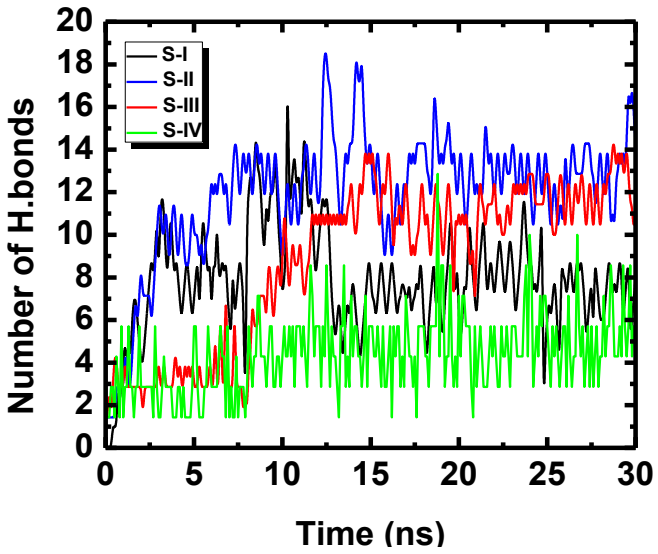

Figure 4.3 Number of hydrogen bonds between the head groups of the DPPC lipid bilayer and LcnG (LcnG-α and LcnG-β) peptide.

Peptide binding to the membrane was also investigated via analyzing the hydrogen bonding interaction between the peptide and the lipid bilayer throughout the simulations. **Figure 4.3** shows the total number of hydrogen bonds between LcnG peptides and DPPC bilayer. Hydrogen bonding interaction was found almost in all simulations between the lipid head-groups and the peptide. The average total number of the hydrogen bonds between LcnG and the lipid head-

groups during simulations was found to be around 6 ±2 in S-I, 10 ±2 bonds in S-II, 8 ±2 bonds in S-III, and only 4 ±2 in S-IV. As it is revealed in Fig. 3, the average number of the hydrogen bonds started to increase gradually as the simulation progressed and stabilized at around 15 ns.

Recent studies of piscidin 1 with DPPC have shown predominant hydrogen bonding and electrostatic interactions between piscidin positively charged residues and lipid head-groups of DPPC lipid bilayer [208], which is consistent with our investigation. Moreover, the same results were obtained by Leontiadou et al. when they studied interaction of magainin MG-H2 with the zwitterionic lipid bilayer [209]. These interactions between positively charged residues Lys34, Lys33, Lys32 and Arg31 and lipid bilayer could be dominant mechanisms by which LcnG destabilizes the membrane of the target cell.

4.3.3 Peptide orientation at the lipid-water interface

Tryptophan residues have been used to monitor the positioning of peptides at the lipid water interface [197, 210]. Both LcnG peptides LcnG-α, LcnG-β contain tryptophan residues. LcnG-α has one tryptophan (W3) and LcnG-β has three tryptophan residues W3, W5, and W8 at their N-terminal regions. The distance between these tryptophan residues and the phosphorous head-groups of upper leaflet of the lipid bilayer was used to monitor the orientation of the peptides at the lipid water interface. **Figure 4.4** shows the distance between the tryptophan residues at the N-termini of LcnG and the phosphorous head-groups of upper leaflet of the lipid bilayer, where 0 nm represents the superficial membrane-water

interface. Generally, tryptophan residues started to move closer to the bilayer since beginning of the simulations and continued declining down until the threshold distance, which is the distance where they remained with a constant space from the upper layer and positioned themselves on the outer membrane-water interface. In S-I for example, declining distance of 1.6 was observed for W3 of LcnG-α , and an average decrease of 1.75 nm, 1.8 nm, and 1.5 nm were observed relatively for W3, W5, and W8 in LcnG-*β*. In simulations S-II, S-III and S-IV, the decrease in the distance was observed for all the tryptophan residues and that is in consistence with previous studies regards behavior of the N-termini tryptophan residues of LcnG-*β* [196], and the aromatic residues generally in a membrane simulating environment [198, 211].

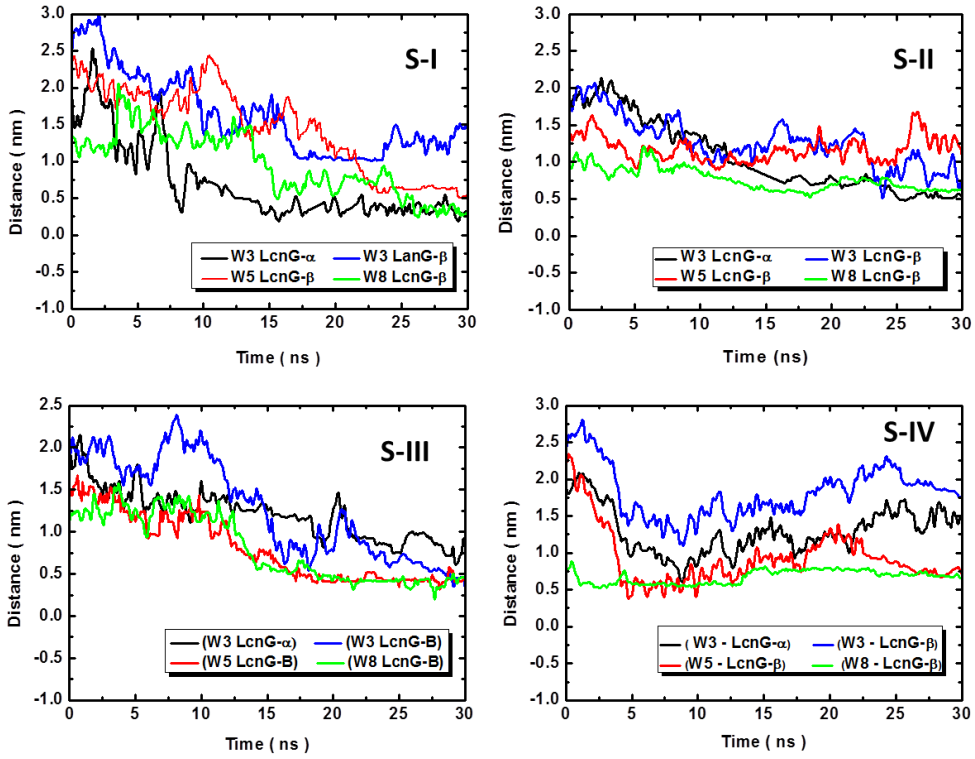

Figure 4.4. Distance between the N-termini tryptophan residues (W3 in LcnG-α and W3, W5, and W8 in LcnG-*β*) and the phosphorous group of the upper leaflet of the lipid bilayer. Black colour line represents the W3 in LcnG-α, while the Blue, red, and green colour lines corresponding to W3, W5 and W8 in LcnG-*β*, respectively. Distance at 0 nm represents to the superficial membrane-water interface.

4.3.4 Peptide-peptide interaction

The primary goal of LcnG simulations was to identify possible interaction between LcnG complementary peptides in DPPC lipid bilayer system. Although the interaction between the two-peptides can be estimated by looking at the snapshots of the simulations (**Figure 4.2**), we had paid our attention to the helixes GxxxG-motifs and the interaction that could take a place between these moieties.

Figure 4.5 (A) shows the distance between the helix-helix GxxxG-motifs of LcnG; in other words, the distance between G7xxxG11 in LcnG-α and

G18xxxG22 in LcnG-β was measured in all four simulations. Results showed that the distance between the GxxxG-motifs has decreased and it closes the two-peptides to each other. The best orientation and movement was observed in S-I, where the distance declined from 2.3 nm to reach around 1.10 nm at 15 ns. Interestingly in this simulation the distance stayed steady during all the remaining 15 ns suggesting a strong interaction between the two-peptides. Similarly, in the other simulations the distance was decreased by an average of 0.8 ± 0.2. According to the distance profiles analysis we can realize that there is a clear dropping in the distance between the GxxxG-motifs in all simulations, and that might explain their contribution in pairing the two peptides together.

Although the distance between the two attentive GxxxG-motifs of the two-peptides has decreased, it is still not close enough to form specific chemical interactions (hydrogen bonding, and/or hydrophobic interactions) between the two motifs. The trajectories analysis did not show any particular interaction between them and no indication for any sort of direct bonds. This was observed in all simulations. On the other hand, several stable hydrogen bonds were detected between the two-peptides at different amino acid residues. These hydrogen bonds were completely stable and various in their locations from one simulation to another.

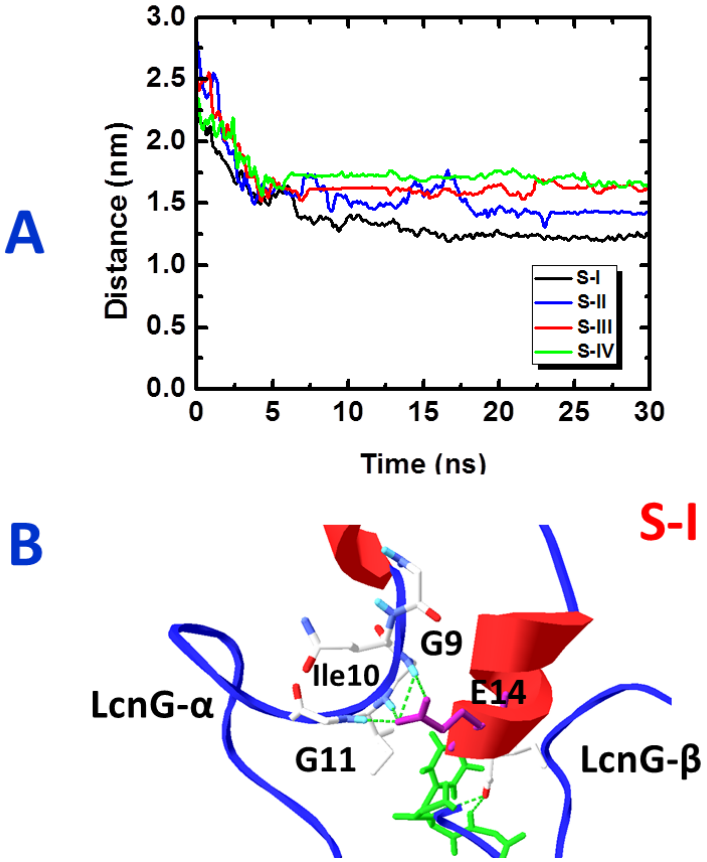

Figure 4.5. (A) The distance between helix-helix GxxxG-motifs (G7xxxG11 in LcnG-α and G18xxxG22 motif in LcnG-β) during simulations I to IV in the hydrated lipid bilayer system. **(B)** Snapshot from simulation S-I showing stable hydrogen bonding interactions between LcnG-α and LcnG-*β*. White colour chains represent the motif G7xxxG11 in LcnG-α, and the green color chains represent G18xxxG22 motif in LcnG-*β*. Pink colour chain shows amino acid Glu14.

In simulation S-I for instance, few hydrogen bonds were detected, but the most stable ones were dictated between the G9xG11 in LcnG-α, and the residues Glu14 in LcnG-*β*. These bonds were persistent during the simulation time (**Figure 5B**). In this simulation (S-I) we see the contribution of the GxxxG motif of LcnG-α in peptide interactions. The same observation was perceived in S-II, but different residues were contributed in forming the interaction; hydrogen bonds were detected between (Leu24 in LcnG-α and Glu14 in LcnG-β) and (Gly1 in

LcnG-α with Trp5 of LcnG-*β*). Three stable bonds were detected in S-III between one residue in LcnG-α (Asp5) and three residues of LcnG-*β* (Gly4, Trp5, and Ala7). Last and not the least, only one stable hydrogen bond was identified in S-IV, and that was between Gly4 in LcnG-α and Phe 2 in LcnG-*β.* We can dictate from those results that no particular interaction was repeated and neither specific site was distinguished in the peptide-peptide interactions. The only concern of our observations is that we have seen highly involvement of the amino acid glycine in bonding formation between the two-peptides. Influence of the glycine in the hydrogen bonding formation was recognizable in all simulations regardless the position of each one. We do anticipate role of amino acid glycine in pairing the peptides and that is could be as a result of closing the amino acid to the peptide's backbone. Peptide initial orientation and configuration seems to be the key for peptide-peptide and site specific interaction.

Figure 4.6A shows a hydrophobic interaction between the LcnG peptides. The distance was measured between particular hydrophobic residues that had been chosen relative to their positions during the simulation, tryptophan 3 in LcnG-α and tryptophan 8 in LcnG-*β*. We had observed intense decline of the distance between the two residues starting from the first two nano-seconds in simulations S-I and S-III (**Figure 4.6A**). Again we observe here S-I is showing the best interaction and we see that the distance was almost steady during the simulation. In simulation S-II; however, insignificant reduction was observed, and by much less degree than S-I and S-III. On the other hand, in S-IV the distance

line has not been affected, and the two residues stayed at the same initial space, apart from each other.

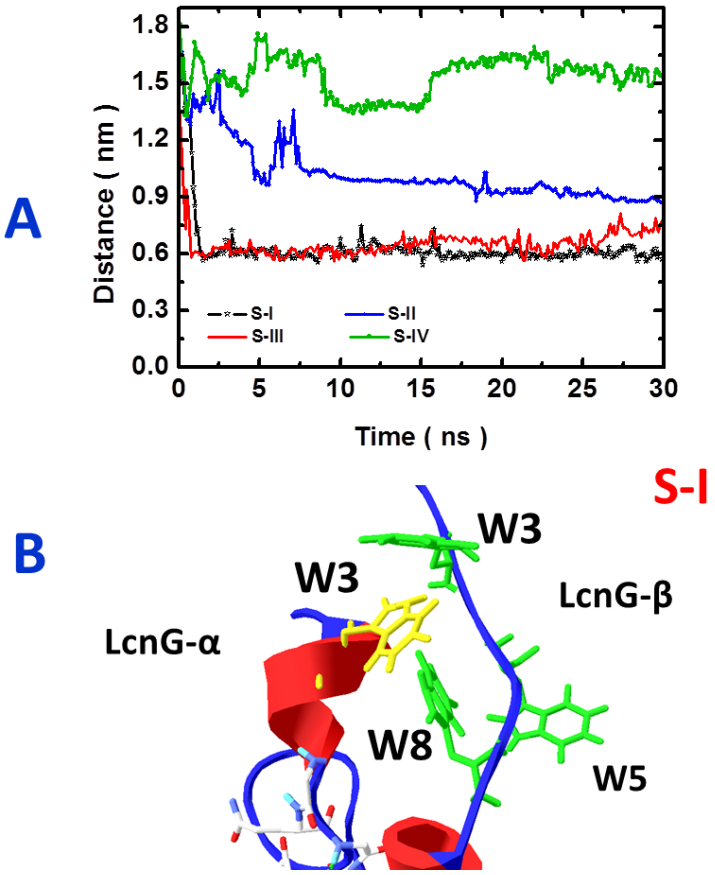

Figure 4.6. Interaction between LcnG two-peptide bacteriocin. (A) Distance with respect to time between two hydrophobic residues from LcnG-α (W3) and LcnG-*β* (W8) during the four simulations. (B) Snapshot at 7 ns shows the hydrophobic interaction between N-termini tryptophan residues in S-I.

Figure 4.6B declares position of the N-termini tryptophans from each other at 7 ns of the simulation time (S-I), and shows the hydrophobic interaction between the residues. The tryptophan residues could not be uniformly distributed through the membrane; however, they are concentrated at the top membrane-water interface. They are correctly positioned on the surface to form hydrogen

bonds with the lipid head-groups, while their hydrophobic rings come closer to each other embedding towards the lipid part to show their hydrophobic attraction. Properties of the tryptophans allow the hydrophobic interaction to take a place separated from the hydrogen bonds.

4.3.5 Peptide secondary structure

A local compute of the conformational stability of the secondary structure of the peptide is provided through assessment the helicity of the two-peptides separately. **Figure 4.7** demonstrates the % of helicity of both peptides LcnG-α and LcnG-*β* in each simulation. The % of the helicity was computed relative to the initial helicity of the peptide in DPC solution structure. **Figure 4.7A** shows % of helicity of the both peptides α and *β* in S-I and S-II. The black solid line represents the % of helicity of LcnG-α, and the black dotted line represents the LcnG-*β* in S-I. In S-II the blue solid and dotted lines represent both α and *β* peptides, respectively. Clearly, % of helicity of LcnG-α has diminished significantly comparing to % of the helicity in LcnG-*β*. Loss in secondary structure was estimated by around 55 − 65 % in LcnG-α for S-I and S-II, correspondingly, while it was decreased roughly by 30 − 40 % in LcnG-*β* for the same simulations. **Figure 4.7B** also demonstrates the loss of peptide helicity in simulations S-III (red lines) and S-IV (green lines). The average loss in the secondary structure was around 60 % for LcnG-α in both simulations (S-III, and S-IV) and approximately 35 to 40 % loss in LcnG-*β* in simulations S-III and S-IV, respectively. This estimation was calculated according to the average loss of helicity of the peptides in each simulation.

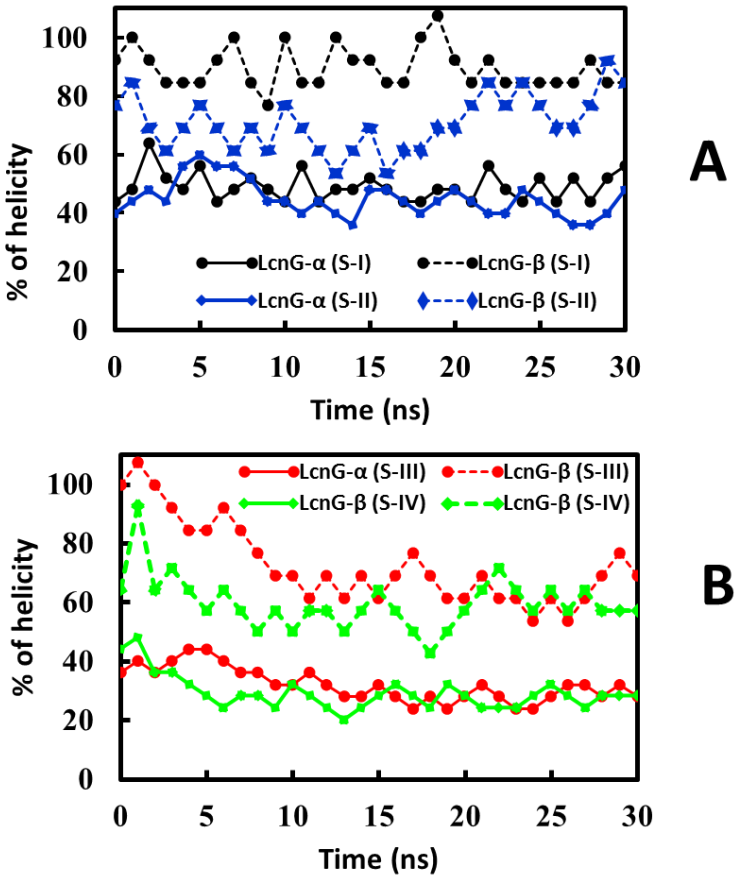

Figure 4.7. Secondary structure of LcnG during the simulations relative to the NMR solution structure (PDB codes, 2JPJ and 2JPK). **(A)** shows the secondary structure of LcnG-α (solid) and LcnG-*β* (dashed) during the first two simulations (S-I, black and S-II, blue), whereas **(B)** shows the secondary structure of LcnG-α (solid) and LcnG-*β* (dashed) during the simulations S-III (red) and S-IV (green).

Irrespective to this significant dropping in the secondary structure of the peptide during the simulations, we have found stability of the peptide helicity at specific residues. The helical part from residues 3 to 9 in LcnG-α was steady more or less entire the simulations time and the helical part from residue 26 till residue 29 also was found to be stable by 80 % along the simulations time. On LcnG-*β* peptide, the helical part from residue 9 − 14 was roughly constant and no permanent loss had appeared in this region during the simulations time. Although

there was variation in the secondary structure from residues to others; those observations were detected in all four simulations and the secondary structure was steady in each one more or less at the same regions. Helicity results are in agreement with CD studies of LcnG in present of zwitterionic dioleoylglycerophosphocholine (Ole2GroPCho) liposomes that was reported by Hauge. Havard et al 1998 [45].

4.4. Concluding remarks

MD simulations study suggests that LcnG in aqueous phase binds to the lipid head-groups via hydrogen bonding and/or electrostatic interactions. In DPPC lipid bilayer system the helix-helix GxxxG-motifs seem to play a role in pairing the two fragments to each other and that is observable from decline in the distance between the two motifs in the all conducted simulations. Furthermore, the nonspecific interaction cannot be excluded and it might be occuring depending on the peptides initial orientations as it was detected herein. Reduction in the secondary structure of the peptide was detected in all simulations; nonetheless, the stability has been witnessed in small residues with an average stability rate 90% in both α and β peptides. In consistence with previous proposal, loss in the helicity might be as a result of non-specific interaction, and that helix-helix interaction might generate and/or stabilize the helical conformation of the peptides. The N-terminus tryptophan residues in LcnG-β and the one in LcnG-α positioned themselves on the outer membrane-water interface, and they might

contribute in positioning and orientating the peptide on the aqueous-lipid bilayer system.

MD simulation study gives atomistic insight of mechanism of peptide interactions that cannot be revealed with current experimental approaches. Understanding the mechanism that governs peptide-peptide interaction is crucial for the design of a new peptide-based therapeutic agent.

Chapter 5

General Conclusion and Future Direction

5.1. General Conclusion

Foodborne illness is a significant problem that faces human health and safety. Therefore, the detection of pathogenic microorganisms in foods is essential to ensure the basic requirement of a supply of foods fit for human consumption.

The conventional bacterial detection methods currently used are slow, labor intensive and unable to meet the demands for rapid detection and food testing. Advance molecular methods, such as PCR, immunoassay, antibody and DNA based platforms are rapid, selective and specific to some extent. However, those techniques still lack the proper sensitivity, robustness, and resulted in false positive and false negative when compared to the standard culture assays. In addition, they lack the stability under harsh environmental conditions [212, 213].

The main aim of this thesis is to address a preliminary study towards developing a rapid, sensitive, and reliable method for detection of foodborne bacteria based on gold surface-immobilization of AMP LeuA. To this end, we were able to detect peptide bacterial interaction of a shorter fragment 24-AA LeuA as well as LeuA binding towards gram-positive bacteria (**chapters 2 and 3**).

Coupling of the 24-AA LeuA (C-terminal domain of Leucocin A) to a gold surface resulted in implementation of invaluable platform that can easily detect bacteria with an achievable sensitivity approaching approximately 1 bacterium/μL, which is a clinically relevant limit. This ability of the AMP-based platform to directly bind bacteria offers a promising alternative detection technique for the use of traditional culture-based assays and the other rapid detection methods such as antibody-based immunoassays. 24-AA-based platforms will also raise another advantage over the other methods as it can detect the viable cells. It can identify presence of the viable *bacteria* on the samples and overcome the drawback of false positive that resulted from using RT-PCR. We do anticipate that these results will have a positive impact on the use of the biosensor technologies to test and monitor bacteria and specially *Listeria monocytogenes* on foods, water, and other pharmaceutical products.

Food safety from farm-to-fork through the supply chain must be maintained to protect consumers from debilitating and sometimes fatal episodes of pathogen outbreaks.

MD simulation is capable to provide an atomistic perception of the peptide mechanism of interaction, and gives useful insights that are complementary to the experimental studies. Chapter 4 in the current thesis explored the peptide-peptide interaction of Lactococcin G class IIb two-peptide bacteriocin using MD simulation. LcnG is an interesting peptide consisting of two complementary peptides, LcnG-α and LcnG-β that exhibit the antibacterial activity when they are joined together and act as one functional unit. The work highlights role of the

GxxxG motifs of this class in peptide-peptide interactions and suggested its importance in maintaining the secondary structure of the peptides. Also MD simulation studies were able to explore peptide interaction with a membrane-mimicking environment (the lipid bilayer).

5.2. Future direction

The understanding of the interaction of immobilized peptides with bacteria is still at an early stage. In this regard, the first and most pertinent future direction we suggest for exploration will be understanding the effect of different immobilization methods on peptide-orientation and how it influences peptide-bacteria interactions and antibacterial activity of the immobilized peptide.

The second current goal is using the atomic force microscopy (AFM) to measure the force of adhesion between the antimicrobial peptide and bacterial strains. Furthermore, physico-chemical characterization of the microbial cell surface by AFM is under investigation, which aims to direct characterization of surface properties (i.e., morphology, molecular interactions) of microbial cells using AFM with chemically modified probes. The probing of individual interactions can be used to map cell surface receptors, and to assay the receptors' functional states, binding kinetics and elucidate an overview of cellular landscapes. This information will provide unique insight into how cells structurally and functionally modulate the molecules of their surfaces to interact with the peptide allowing for the optimization of AMP selectivity which is an

important initial step toward developing peptides-based sensors for a variety of biotechnological applications.

Further direction studies of this current project will be applying the developed technique on a sensor-device based on the immobilized-AMP for specific detection of foodborne pathogens. In other words, applying the LeuA and/or 24-AA LeuA in a sensor device and investigate the limit of bacterial detection. Recently, many methods that utilize biosensors have been applied for the detection of microorganisms. It would also be an interesting study to apply an impedance-biosensor chip for detection of *Listeria monocytogenes* based on surface-immobilization of AMP Leucocin A.

Electrochemical impedance detection techniques have been applied previously in the field of microbiology for quantifying and detect bacteria [214]. it was approved by the Association of Official Analytical Chemist International (AOAC) as a first action method for screening *Salmonella* in food samples [215]. Most of applications of impedance technology in bacterial detection have been reviewed by Silley and Forsythe (1996) and Wawerla et al. (1999) [216, 217]. The combination of impedance technique with biosensor technology has led to development of impedance biosensors that is expanding rapidly these days for bacterial detection [218]. Impedance biosensors for bacteria detection are based on impedance analysis of the electrical properties of bacterial cells when they are attached to or associated with the electrodes. Recent studies by Manu S. Mannoora et al have applied impedance biosensor for electrical detection of *E.coli* via immobilized AMP, magainin I [109].

MD simulation studies of the current thesis for LcnG class IIb two-peptide bacteriocin will allow the identification of the proper mechanism of interactions of the AMPs, and facilitate identification of new leads in the field towards developing new AMPs. This study could be further explored and supported by experiments such as synthesis of the two complementary peptides with substitutions at the GxxxG motifs, and testing their activity. Moreover, using the solid support (e.g. cellulose membrane) and testing their activity while bound to the membrane from the C and N-terminal would yield important insight into the mechanism of action of this class of AMPs. This approach will tell whether their antimicrobial activity is a surface phenomenon or whether peptides must be internalized to produce the antimicrobial toxicity. Moll et al. reveled that Lactococin G displays optimal antibacterial activity at 1:1 stoichiometry [41]. However, whether the active species is a dimer, tetramer or higher multimer complexes remains unclear. Sedimentation equilibrium experiments can be conducted to determine the actual active complex. Such studies will increase the potential use of class IIb two-peptide bacteriocins.

Bibliography

1. Cotter, P.D., C. Hill, and R.P. Ross, *Bacteriocins: developing innate immunity for food.* Nat Rev Microbiol, 2005. **3**(10): p. 777-88.
2. Drider, D., et al., *The continuing story of class IIa bacteriocins.* Microbiol Mol Biol Rev, 2006. **70**(2): p. 564-82.
3. Fimland, G., et al., *The bactericidal activity of pediocin PA-1 is specifically inhibited by a 15-mer fragment that spans the bacteriocin from the center toward the C terminus.* Appl Environ Microbiol, 1998. **64**(12): p. 5057-60.
4. Nissen-Meyer, J. and I.F. Nes, *Ribosomally synthesized antimicrobial peptides: their function, structure, biogenesis, and mechanism of action.* Arch Microbiol, 1997. **167**(2/3): p. 67-77.
5. Garneau, S., N.I. Martin, and J.C. Vederas, *Two-peptide bacteriocins produced by lactic acid bacteria.* Biochimie, 2002. **84**(5-6): p. 577-92.
6. Nes, I.F., et al., *Biosynthesis of bacteriocins in lactic acid bacteria.* Antonie Van Leeuwenhoek, 1996. **70**(2-4): p. 113-28.
7. Nissen-Meyer, J., et al., *Structure-function relationships of the non-lanthionine-containing peptide (class II) bacteriocins produced by gram-positive bacteria.* Curr Pharm Biotechnol, 2009. **10**(1): p. 19-37.
8. Oppegard, C., et al., *The two-peptide class II bacteriocins: structure, production, and mode of action.* J Mol Microbiol Biotechnol, 2007. **13**(4): p. 210-9.
9. De Vuyst, L. and F. Leroy, *Bacteriocins from lactic acid bacteria: production, purification, and food applications.* J Mol Microbiol Biotechnol, 2007. **13**(4): p. 194-9.
10. Hirsch, A.G., E.; Chapman, H. R.; Mattick, *A note on the inhibition of an anaerobic sporeformer in Swiss-type cheese by a nisin-producing streptococcus.* Journal of Dairy Research, 1951. **27**: p. 1793.
11. Rodriguez, J.M., M.I. Martinez, and J. Kok, *Pediocin PA-1, a wide-spectrum bacteriocin from lactic acid bacteria.* Crit Rev Food Sci Nutr, 2002. **42**(2): p. 91-121.
12. Ennahar, S., et al., *Class IIa bacteriocins: biosynthesis, structure and activity.* FEMS Microbiol Rev, 2000. **24**(1): p. 85-106.
13. Ryan, M.P., et al., *An application in cheddar cheese manufacture for a strain of Lactococcus lactis producing a novel broad-spectrum bacteriocin, lacticin 3147.* Appl Environ Microbiol, 1996. **62**(2): p. 612-9.
14. Dunne, C., et al., *Probiotics: from myth to reality. Demonstration of functionality in animal models of disease and in human clinical trials.* Antonie Van Leeuwenhoek, 1999. **76**(1-4): p. 279-92.
15. Tannock, G.W., *Probiotic properties of lactic-acid bacteria: plenty of scope for fundamental R & D.* Trends Biotechnol, 1997. **15**(7): p. 270-4.
16. Hickey, R.M., R.P. Ross, and C. Hill, *Controlled autolysis and enzyme release in a recombinant lactococcal strain expressing the*

metalloendopeptidase enterolysin A. Appl Environ Microbiol, 2004. **70**(3): p. 1744-8.
17. Klaenhammer, T.R., *Genetics of bacteriocins produced by lactic acid bacteria.* FEMS Microbiol Rev, 1993. **12**(1-3): p. 39-85.
18. van Belkum, M.J. and M.E. Stiles, *Nonlantibiotic antibacterial peptides from lactic acid bacteria.* Natural Product Reports, 2000. **17**(4): p. 323-335.
19. Li, B. and W.A. van der Donk, *Identification of essential catalytic residues of the cyclase NisC involved in the biosynthesis of nisin.* J Biol Chem, 2007. **282**(29): p. 21169-75.
20. Xie, L. and W.A. van der Donk, *Post-translational modifications during lantibiotic biosynthesis.* Curr Opin Chem Biol, 2004. **8**(5): p. 498-507.
21. Pag, U. and H.G. Sahl, *Multiple activities in lantibiotics--models for the design of novel antibiotics?* Curr Pharm Des, 2002. **8**(9): p. 815-33.
22. Jung, G., *Lantibiotics—Ribosomally Synthesized Biologically Active Polypeptides containing Sulfide Bridges and α,β-Didehydroamino Acids.* Angewandte Chemie International Edition in English, 1991. **30**(9): p. 1051-1068.
23. Abriouel, H., et al., *Diversity and applications of Bacillus bacteriocins.* FEMS Microbiol Rev, 2011. **35**(1): p. 201-32.
24. Diep, D.B. and I.F. Nes, *Ribosomally synthesized antibacterial peptides in Gram positive bacteria.* Curr Drug Targets, 2002. **3**(2): p. 107-22.
25. Cleveland, J., et al., *Bacteriocins: safe, natural antimicrobials for food preservation.* Int J Food Microbiol, 2001. **71**(1): p. 1-20.
26. Ingham, A., et al., *The bacteriocin piscicolin 126 retains antilisterial activity in vivo.* J Antimicrob Chemother, 2003. **51**(6): p. 1365-71.
27. Wachsman, M.B., et al., *Enterocin CRL35 inhibits late stages of HSV-1 and HSV-2 replication in vitro.* Antiviral Res, 2003. **58**(1): p. 17-24.
28. Sakayori, Y., et al., *Characterization of Enterococcus faecium mutants resistant to mundticin KS, a class IIa bacteriocin.* Microbiology, 2003. **149**(Pt 10): p. 2901-8.
29. Fimland, G., et al., *Pediocin-like antimicrobial peptides (class IIa bacteriocins) and their immunity proteins: biosynthesis, structure, and mode of action.* J Pept Sci, 2005. **11**(11): p. 688-96.
30. Uteng, M., et al., *Three-dimensional structure in lipid micelles of the pediocin-like antimicrobial peptide sakacin P and a sakacin P variant that is structurally stabilized by an inserted C-terminal disulfide bridge.* Biochemistry, 2003. **42**(39): p. 11417-26.
31. Kaur, K., et al., *Dynamic relationships among type IIa bacteriocins: temperature effects on antimicrobial activity and on structure of the C-terminal amphipathic alpha helix as a receptor-binding region.* Biochemistry, 2004. **43**(28): p. 9009-20.
32. Fimland, G., et al., *New biologically active hybrid bacteriocins constructed by combining regions from various pediocin-like bacteriocins: the C-terminal region is important for determining specificity*. Appl Environ Microbiol, 1996. **62**(9): p. 3313-8.

33. Haugen, H.S., G. Fimland, and J. Nissen-Meyer, *Mutational analysis of residues in the helical region of the class IIa bacteriocin pediocin PA-1.* Appl Environ Microbiol, 2011. **77**(6): p. 1966-72.
34. Yan, L.Z., et al., *Analogues of bacteriocins: antimicrobial specificity and interactions of leucocin A with its enantiomer, carnobacteriocin B2, and truncated derivatives.* J Med Chem, 2000. **43**(24): p. 4579-81.
35. Fregeau Gallagher, N.L., et al., *Three-dimensional structure of leucocin A in trifluoroethanol and dodecylphosphocholine micelles: spatial location of residues critical for biological activity in type IIa bacteriocins from lactic acid bacteria.* Biochemistry, 1997. **36**(49): p. 15062-72.
36. Wang, Y.J.H., M. E.; Gallagher, N. L. F.; Chai, S. Y.; Gibbs, A. C.; Yan, L. Z.; Stiles, M. E.; Wishart, D. S.; Vederas, J. C., *Solution structure of carnobacteriocin B2 and implications for structure-activity relationships among type IIa bacteriocins from lactic acid bacteria.* Biochemistry, 1999. **38**: p. 15438.
37. Haugen, H.S., et al., *Three-dimensional structure in lipid micelles of the pediocin-like antimicrobial peptide curvacin A.* Biochemistry, 2005. **44**(49): p. 16149-57.
38. Eijsink, V.G., et al., *Comparative studies of class IIa bacteriocins of lactic acid bacteria.* Appl Environ Microbiol, 1998. **64**(9): p. 3275-81.
39. Fimland, G., et al., *A C-terminal disulfide bridge in pediocin-like bacteriocins renders bacteriocin activity less temperature dependent and is a major determinant of the antimicrobial spectrum.* J Bacteriol, 2000. **182**(9): p. 2643-8.
40. Soliman, W., et al., *Structure-activity relationships of an antimicrobial peptide plantaricin s from two-peptide class IIb bacteriocins.* J Med Chem, 2011. **54**(7): p. 2399-408.
41. Moll, G., et al., *Lactococcin G is a potassium ion-conducting, two-component bacteriocin.* J Bacteriol, 1996. **178**(3): p. 600-5.
42. Moll, G.N., et al., *Complementary and overlapping selectivity of the two-peptide bacteriocins plantaricin EF and JK.* J Bacteriol, 1999. **181**(16): p. 4848-52.
43. Marciset, O., et al., *Thermophilin 13, a nontypical antilisterial poration complex bacteriocin, that functions without a receptor.* J Biol Chem, 1997. **272**(22): p. 14277-84.
44. Nissen-Meyer, J., et al., *A novel lactococcal bacteriocin whose activity depends on the complementary action of two peptides.* J Bacteriol, 1992. **174**(17): p. 5686-92.
45. Hauge, H.H., et al., *Amphiphilic α-helices are important structural motifs in the α and β peptides that constitute the bacteriocin lactococcin G.* European Journal of Biochemistry, 1998. **251**(3): p. 565-572.
46. Rogne, P., et al., *Three-dimensional structure of the two peptides that constitute the two-peptide bacteriocin lactococcin G.* Biochim Biophys Acta, 2008. **1784**(3): p. 543-54.
47. Rogne, P., et al., *Three-dimensional structure of the two-peptide bacteriocin plantaricin JK.* Peptides, 2009. **30**(9): p. 1613-21.

48. Fimland, N., et al., *Three-dimensional structure of the two peptides that constitute the two-peptide bacteriocin plantaricin EF.* Biochim Biophys Acta, 2008. **1784**(11): p. 1711-9.
49. Kawai, Y., et al., *The circular bacteriocins gassericin A and circularin A.* Curr Protein Pept Sci, 2004. **5**(5): p. 393-8.
50. Kawai, Y., et al., *Structural and functional differences in two cyclic bacteriocins with the same sequences produced by lactobacilli.* Appl Environ Microbiol, 2004. **70**(5): p. 2906-11.
51. Joerger, M.C. and T.R. Klaenhammer, *Cloning, expression, and nucleotide sequence of the Lactobacillus helveticus 481 gene encoding the bacteriocin helveticin J.* J Bacteriol, 1990. **172**(11): p. 6339-47.
52. Beukes, M., et al., *Purification and partial characterization of a murein hydrolase, millericin B, produced by Streptococcus milleri NMSCC 061.* Appl Environ Microbiol, 2000. **66**(1): p. 23-8.
53. Valdes-Stauber, N. and S. Scherer, *Isolation and characterization of Linocin M18, a bacteriocin produced by Brevibacterium linens.* Appl Environ Microbiol, 1994. **60**(10): p. 3809-14.
54. Eppert, I., et al., *Growth reduction of Listeria spp. caused by undefined industrial red smear cheese cultures and bacteriocin-producing Brevibacterium lines as evaluated in situ on soft cheese.* Appl Environ Microbiol, 1997. **63**(12): p. 4812-7.
55. Cornut, G., C. Fortin, and D. Soulieres, *Antineoplastic properties of bacteriocins: revisiting potential active agents.* Am J Clin Oncol, 2008. **31**(4): p. 399-404.
56. Chumchalova, J. and J. Smarda, *Human tumor cells are selectively inhibited by colicins.* Folia Microbiol (Praha), 2003. **48**(1): p. 111-5.
57. Hetz, C., et al., *Microcin E492, a channel-forming bacteriocin from Klebsiella pneumoniae, induces apoptosis in some human cell lines.* Proc Natl Acad Sci U S A, 2002. **99**(5): p. 2696-701.
58. Montville, T.J. and Y. Chen, *Mechanistic action of pediocin and nisin: recent progress and unresolved questions.* Appl Microbiol Biotechnol, 1998. **50**(5): p. 511-9.
59. Hechard, Y. and H.G. Sahl, *Mode of action of modified and unmodified bacteriocins from Gram-positive bacteria.* Biochimie, 2002. **84**(5-6): p. 545-57.
60. Kazazic, M., J. Nissen-Meyer, and G. Fimland, *Mutational analysis of the role of charged residues in target-cell binding, potency and specificity of the pediocin-like bacteriocin sakacin P.* Microbiology, 2002. **148**(Pt 7): p. 2019-27.
61. Johnsen, L., G. Fimland, and J. Nissen-Meyer, *The C-terminal domain of pediocin-like antimicrobial peptides (class IIa bacteriocins) is involved in specific recognition of the C-terminal part of cognate immunity proteins and in determining the antimicrobial spectrum.* J Biol Chem, 2005. **280**(10): p. 9243-50.
62. Madkour, A.E., et al., *Fast disinfecting antimicrobial surfaces.* Langmuir, 2009. **25**(2): p. 1060-7.

63. Parikh, A.N., *Membrane-substrate interface: phospholipid bilayers at chemically and topographically structured surfaces.* Biointerphases, 2008. **3**(2): p. FA22.
64. Yeaman, M.R. and N.Y. Yount, *Mechanisms of antimicrobial peptide action and resistance.* Pharmacol Rev, 2003. **55**(1): p. 27-55.
65. Remaut, H. and G. Waksman, *Protein-protein interaction through beta-strand addition.* Trends Biochem Sci, 2006. **31**(8): p. 436-44.
66. Ma, B., et al., *Protein-protein interactions: structurally conserved residues distinguish between binding sites and exposed protein surfaces.* Proc Natl Acad Sci U S A, 2003. **100**(10): p. 5772-7.
67. Kleanthous, C., *Protein-protein recognition.* 2000, Oxford University Press:Oxford; New York.
68. Brotz, H., et al., *Role of lipid-bound peptidoglycan precursors in the formation of pores by nisin, epidermin and other lantibiotics.* Mol Microbiol, 1998. **30**(2): p. 317-27.
69. Martinez, B., et al., *Specific interaction of the unmodified bacteriocin Lactococcin 972 with the cell wall precursor lipid II.* Appl Environ Microbiol, 2008. **74**(15): p. 4666-70.
70. Wiedemann, I., et al., *Specific binding of nisin to the peptidoglycan precursor lipid II combines pore formation and inhibition of cell wall biosynthesis for potent antibiotic activity.* J Biol Chem, 2001. **276**(3): p. 1772-9.
71. Dalet, K., et al., *A sigma(54)-dependent PTS permease of the mannose family is responsible for sensitivity of Listeria monocytogenes to mesentericin Y105.* Microbiology, 2001. **147**(Pt 12): p. 3263-9.
72. Gravesen, A., et al., *High-level resistance to class IIa bacteriocins is associated with one general mechanism in Listeria monocytogenes.* Microbiology, 2002. **148**(Pt 8): p. 2361-9.
73. Hechard, Y., et al., *Analysis of sigma(54)-dependent genes in Enterococcus faecalis: a mannose PTS permease (EII(Man)) is involved in sensitivity to a bacteriocin, mesentericin Y105.* Microbiology, 2001. **147**(Pt 6): p. 1575-80.
74. Ramnath, M., et al., *Expression of mptC of Listeria monocytogenes induces sensitivity to class IIa bacteriocins in Lactococcus lactis.* Microbiology, 2004. **150**(Pt 8): p. 2663-8.
75. Hechard, Y., et al., *Characterization and purification of mesentericin Y105, an anti-Listeria bacteriocin from Leuconostoc mesenteroides.* J Gen Microbiol, 1992. **138**(12): p. 2725-31.
76. Postma, P.W., J.W. Lengeler, and G.R. Jacobson, *Phosphoenolpyruvate:carbohydrate phosphotransferase systems of bacteria.* Microbiol Rev, 1993. **57**(3): p. 543-94.
77. Deutscher, J., C. Francke, and P.W. Postma, *How phosphotransferase system-related protein phosphorylation regulates carbohydrate metabolism in bacteria.* Microbiol Mol Biol Rev, 2006. **70**(4): p. 939-1031.

78. Diep, D.B., et al., *Common mechanisms of target cell recognition and immunity for class II bacteriocins.* Proc Natl Acad Sci U S A, 2007. **104**(7): p. 2384-9.
79. Fischer, E., Fourneau, E. Rer. Dtsch. , Chem. Ges, 1901. **34**: p. 2668.
80. Jones, J., *Amino Acid and Peptide Synthesis, Second edition.* Oxford Science Publications, Oxford University Press, Great Britain, 2002.
81. Doonan, S., *Peptides and Proteins*2002., Royal Society of Chemistry, Great Britain.
82. Kent, S.B.H., *Chem. Soc. Rev.* 2009. **38**: p. 338.
83. Merrifield, R.B.J.A., Chem. Soc., 1963. **85**: p. 2149.
84. Humphrey, J.M. and A.R. Chamberlin, *Chemical Synthesis of Natural Product Peptides: Coupling Methods for the Incorporation of Noncoded Amino Acids into Peptides.* Chem Rev, 1997. **97**(6): p. 2243-2266.
85. Bailey, P.D., *An Introduction to Peptide Chemistry*1990., Wiley, Germany.
86. Dawson, P.E., et al., *Synthesis of proteins by native chemical ligation.* Science, 1994. **266**(5186): p. 776-9.
87. Park, S., R.W. Worobo, and R.A. Durst, *Escherichia coli O157:H7 as an emerging foodborne pathogen: a literature review.* Crit Rev Biotechnol, 2001. **21**(1): p. 27-48.
88. Gandhi, M. and M.L. Chikindas, *Listeria: A foodborne pathogen that knows how to survive.* Int J Food Microbiol, 2007. **113**(1): p. 1-15.
89. Murphy, C., C. Carroll, and K.N. Jordan, *Environmental survival mechanisms of the foodborne pathogen Campylobacter jejuni.* J Appl Microbiol, 2006. **100**(4): p. 623-32.
90. Velusamy, V., et al., *An overview of foodborne pathogen detection: in the perspective of biosensors.* Biotechnol Adv, 2010. **28**(2): p. 232-54.
91. Wang, Y., et al., *Subtractive inhibition assay for the detection of E. coli O157:H7 using surface plasmon resonance.* Sensors (Basel), 2011. **11**(3): p. 2728-39.
92. Kiev, S.G. and L.M. John, *A review of conventional detection and enumeration methods for pathogenic bacteria in food.* Canadian Journal of Microbiology, 2004. **50**(11): p. 883-890.
93. Fung, D.Y.C., *Rapid methods and automation in food microbiology: A review.* Food Reviews International, 1994. **10**(3): p. 357-375.
94. Ibrahim, G.F., et al., *Rapid detection of salmonellae by immunoassays with titanous hydroxide as the solid phase.* Appl Environ Microbiol, 1985. **50**(3): p. 670-5.
95. Stager, C.E. and J.R. Davis, *Automated systems for identification of microorganisms.* Clin Microbiol Rev, 1992. **5**(3): p. 302-27.
96. Gracias, K.S. and J.L. McKillip, *A review of conventional detection and enumeration methods for pathogenic bacteria in food.* Canadian Journal of Microbiology, 2004. **50**(11): p. 883-890.
97. Feng, P., *Emergence of rapid methods for identifying microbial pathogens in foods.* J AOAC Int, 1996. **79**(3): p. 809-12.

98. Feng, P., *Impact of molecular biology on the detection of foodborne pathogens.* Mol Biotechnol, 1997. **7**(3): p. 267-78.
99. Curiale, M.S., M.J. Klatt, and M.A. Mozola, *Colorimetric deoxyribonucleic acid hybridization assay for rapid screening of Salmonella in foods: collaborative study.* J Assoc Off Anal Chem, 1990. **73**(2): p. 248-56.
100. Kalamaki, M., R.J. Price, and D.Y.C. Fung, *RAPID METHODS FOR IDENTIFYING SEAFOOD MICROBIAL PATHOGENS AND TOXINS1*. Journal of Rapid Methods & Automation in Microbiology, 1997. **5**(2): p. 87-137.
101. Moseley, S.L., et al., *Detection of enterotoxigenic Escherichia coli by DNA colony hybridization.* J Infect Dis, 1980. **142**(6): p. 892-8.
102. Datta, A.R., B.A. Wentz, and W.E. Hill, *Detection of hemolytic Listeria monocytogenes by using DNA colony hybridization.* Appl Environ Microbiol, 1987. **53**(9): p. 2256-9.
103. Yu, W.L. and K. Nielsen, *Review of detection of Brucella spp. by polymerase chain reaction.* Croat Med J, 2010. **51**(4): p. 306-13.
104. Ramsay, G., *DNA chips: state-of-the art.* Nat Biotechnol, 1998. **16**(1): p. 40-4.
105. Skjerve, E., L.M. Rorvik, and O. Olsvik, *Detection of Listeria monocytogenes in foods by immunomagnetic separation.* Appl Environ Microbiol, 1990. **56**(11): p. 3478-81.
106. Mercanoglu, B. and M.W. Griffiths, *Combination of immunomagnetic separation with real-time PCR for rapid detection of Salmonella in milk, ground beef, and alfalfa sprouts.* J Food Prot, 2005. **68**(3): p. 557-61.
107. Bosch, M., et al., *Recent Development in Optical Fiber Biosensors.* Sensors, 2007. **7**(6): p. 797-859.
108. Dudak, F.C. and I.H. Boyaci, *Rapid and label-free bacteria detection by surface plasmon resonance (SPR) biosensors.* Biotechnol J, 2009. **4**(7): p. 1003-11.
109. Mannoor, M.S., et al., *Electrical detection of pathogenic bacteria via immobilized antimicrobial peptides.* Proc Natl Acad Sci U S A, 2010. **107**(45): p. 19207-12.
110. Ndieyira, J.W., et al., *Nanomechanical detection of antibiotic-mucopeptide binding in a model for superbug drug resistance.* Nat Nanotechnol, 2008. **3**(11): p. 691-6.
111. Burg, T.P., et al., *Weighing of biomolecules, single cells and single nanoparticles in fluid.* Nature, 2007. **446**(7139): p. 1066-9.
112. Premasiri, W.R., et al., *Characterization of the surface enhanced raman scattering (SERS) of bacteria.* J Phys Chem B, 2005. **109**(1): p. 312-20.
113. Olofsson, A.C., M. Hermansson, and H. Elwing, *Use of a quartz crystal microbalance to investigate the antiadhesive potential of N-acetyl-L-cysteine.* Appl Environ Microbiol, 2005. **71**(5): p. 2705-12.
114. Kulagina, N.V., et al., *Antimicrobial peptide-based array for Escherichia coli and Salmonella screening.* Anal Chim Acta, 2006. **575**(1): p. 9-15.

115. Kulagina, N.V., et al., *Antimicrobial peptides for detection of bacteria in biosensor assays.* Anal Chem, 2005. **77**(19): p. 6504-8.
116. La Storia, A., et al., *Characterization of bacteriocin-coated antimicrobial polyethylene films by atomic force microscopy.* J Food Sci, 2008. **73**(4): p. T48-54.
117. Zasloff, M., *Antimicrobial peptides of multicellular organisms.* Nature, 2002. **415**(6870): p. 389-395.
118. Brogden, K.A., *Antimicrobial peptides: Pore formers or metabolic inhibitors in bacteria?* Nature Reviews Microbiology, 2005. **3**(3): p. 238-250.
119. Guani-Guerra, E., et al., *Antimicrobial peptides: General overview and clinical implications in human health and disease.* Clinical Immunology, 2010. **135**(1): p. 1-11.
120. Hancock, R.E.W., *Peptide antibiotics.* Lancet, 1997. **349**(9049): p. 418-422.
121. Yeaman, M.R. and N.Y. Yount, *Mechanisms of antimicrobial peptide action and resistance.* Pharmacological Reviews, 2003. **55**(1): p. 27-55.
122. Fantner, G.E., et al., *Kinetics of antimicrobial peptide activity measured on individual bacterial cells using high-speed atomic force microscopy.* Nature Nanotechnology, 2010. **5**(4): p. 280-285.
123. Hancock, R.E.W. and M.G. Scott, *The role of antimicrobial peptides in animal defenses.* Proceedings of the National Academy of Sciences of the United States of America, 2000. **97**(16): p. 8856-8861.
124. Shai, Y., *Mechanism of the binding, insertion and destabilization of phospholipid bilayer membranes by alpha-helical antimicrobial and cell non-selective membrane-lytic peptides.* Biochimica Et Biophysica Acta-Biomembranes, 1999. **1462**(1-2): p. 55-70.
125. Wimley, W.C., *Describing the Mechanism of Antimicrobial Peptide Action with the Interfacial Activity Model.* Acs Chemical Biology, 2010. **5**(10): p. 905-917.
126. Yount, N.Y., et al., *Advances in antimicrobial peptide immunobiology.* Biopolymers, 2006. **84**(5): p. 435-458.
127. Robinson, W.E., et al., *Anti-HIV-1 activity of indolicidin, an antimicrobial peptide from neutrophils.* Journal of Leukocyte Biology, 1998. **63**(1): p. 94-100.
128. Matanic, V.C.A. and V. Castilla, *Antiviral activity of antimicrobial cationic peptides against Junin virus and herpes simplex virus.* International Journal of Antimicrobial Agents, 2004. **23**(4): p. 382-389.
129. Hoskin, D.W. and A. Ramamoorthy, *Studies on anticancer activities of antimicrobial peptides.* Biochimica Et Biophysica Acta-Biomembranes, 2008. **1778**(2): p. 357-375.
130. Manafi, M., *Fluorogenic and chromogenic enzyme substrates in culture media and identification tests.* Int J Food Microbiol, 1996. **31**(1-3): p. 45-58.
131. Daly, P., T. Collier, and S. Doyle, *PCR-ELISA detection of Escherichia coli in milk.* Lett Appl Microbiol, 2002. **34**(3): p. 222-6.

132. Johnson, R.P., et al., *Detection of Escherichia coli O157:H7 in meat by an enzyme-linked immunosorbent assay, EHEC-Tek.* Appl Environ Microbiol, 1995. **61**(1): p. 386-8.
133. Szabo, E.A. and B.M. Mackey, *Detection of Salmonella enteritidis by reverse transcription-polymerase chain reaction (PCR).* Int J Food Microbiol, 1999. **51**(2-3): p. 113-22.
134. Rantsiou, K., et al., *Detection, quantification and vitality of Listeria monocytogenes in food as determined by quantitative PCR.* Int J Food Microbiol, 2008. **121**(1): p. 99-105.
135. Hobson, N.S., I. Tothill, and A.P. Turner, *Microbial detection.* Biosens Bioelectron, 1996. **11**(5): p. 455-77.
136. Nicolas, P. and A. Mor, *Peptides as weapons against microorganisms in the chemical defense system of vertebrates.* Annu Rev Microbiol, 1995. **49**: p. 277-304.
137. Kulagina, N.V., et al., *Antimicrobial peptides: New recognition molecules for detecting botulinum toxins.* Sensors, 2007. **7**(11): p. 2808-2824.
138. Kulagina, N.V., et al., *Antimicrobial peptide-based array for Escherichia coli and Salmonella screening.* Analytica Chimica Acta, 2006. **575**(1): p. 9-15.
139. Kulagina, N.V., et al., *Antimicrobial peptides for detection of bacteria in biosensor assays.* Analytical Chemistry, 2005. **77**(19): p. 6504-6508.
140. Mannoor, M.S., et al., *Electrical detection of pathogenic bacteria via immobilized antimicrobial peptides.* Proceedings of the National Academy of Sciences of the United States of America, 2010. **107**(45): p. 19207-19212.
141. Onaizi, S.A. and S.S.J. Leong, *Tethering antimicrobial peptides: Current status and potential challenges.* Biotechnology Advances, 2011. **29**(1): p. 67-74.
142. Ramnath, M., et al., *Absence of a putative mannose-specific phosphotransferase system enzyme IIAB component in a leucocin A-resistant strain of Listeria monocytogenes, as shown by two-dimensional sodium dodecyl sulfate-polyacrylamide gel electrophoresis.* Appl Environ Microbiol, 2000. **66**(7): p. 3098-101.
143. Kaiser, E., et al., *Color test for detection of free terminal amino groups in the solid-phase synthesis of peptides.* Anal Biochem, 1970. **34**(2): p. 595-8.
144. Tagg JR, D.A., Wannamaker LW. , *Bacteriocins of gram-positive bacteria.* Bacteriol Rev, 1976. **40**: p. 722- 756.
145. Miura, Y., et al., *Formation of oriented helical peptide layers on a gold surface due to the self-assembling properties of peptides.* Langmuir, 1998. **14**(24): p. 6935-6940.
146. Debe, M.K., *EXTRACTING PHYSICAL STRUCTURE INFORMATION FROM THIN ORGANIC FILMS WITH REFLECTION ABSORPTION INFRARED-SPECTROSCOPY.* Journal of Applied Physics, 1984. **55**(9): p. 3354-3366.

147. Boncheva, M. and H. Vogel, *Formation of stable polypeptide monolayers at interfaces: Controlling molecular conformation and orientation.* Biophysical Journal, 1997. **73**(2): p. 1056-1072.
148. Greenler, R.G., *INFRARED STUDY OF ADSORBED MOLECULES ON METAL SURFACES BY REFLECTION TECHNIQUES.* Journal of Chemical Physics, 1966. **44**(1): p. 310-&.
149. Gremlich, H.U., U.P. Fringeli, and R. Schwyzer, *CONFORMATIONAL-CHANGES OF ADRENOCORTICOTROPIN PEPTIDES UPON INTERACTION WITH LIPID-MEMBRANES REVEALED BY INFRARED ATTENUATED TOTAL REFLECTION SPECTROSCOPY.* Biochemistry, 1983. **22**(18): p. 4257-4264.
150. Worley, C.G., R.W. Linton, and E.T. Samulski, *ELECTRIC-FIELD-ENHANCED SELF-ASSEMBLY OF ALPHA-HELICAL POLYPEPTIDES.* Langmuir, 1995. **11**(10): p. 3805-3810.
151. Tsuboi, M., *INFRARED DICHROISM AND MOLECULAR CONFORMATION OF ALPHA-FORM POLY-GAMMA-BENZYL-L-GLUTAMATE.* Journal of Polymer Science, 1962. **59**(167): p. 139-&.
152. Sigal, G.B., M. Mrksich, and G.M. Whitesides, *Using surface plasmon resonance spectroscopy to measure the association of detergents with self-assembled monolayers of hexadecanethiolate on gold.* Langmuir, 1997. **13**(10): p. 2749-2755.
153. Hughes, A.B., *Amino Acids, Peptides and Proteins in Organic Chemistry, Building Blocks, Catalysis and Coupling Chemistry*2011: Wiley.
154. van Woerkom, W.J. and J.W. van Nispen, *Difficult couplings in stepwise solid phase peptide synthesis: predictable or just a guess?* Int J Pept Protein Res, 1991. **38**(2): p. 103-13.
155. Kent. S., D., C.,Hruby, V. & Kopple. K.. eds., *Peptides, Structure and Function*, 1985: Pierce Chemical Company. Rockford. IL. p. 407-414.
156. Kennedy, D.F., et al., *STUDIES OF PEPTIDES FORMING 3(10)-HELICES AND ALPHA-HELICES AND BETA-BEND RIBBON STRUCTURES IN ORGANIC SOLUTION AND IN MODEL BIOMEMBRANES BY FOURIER-TRANSFORM INFRARED-SPECTROSCOPY.* Biochemistry, 1991. **30**(26): p. 6541-6548.
157. Sakurai, T., et al., *Formation of oriented polypeptides on Au(111) surface depends on the secondary structure controlled by peptide length.* Journal of Peptide Science, 2006. **12**(6): p. 396-402.
158. Abee, T., T.R. Klaenhammer, and L. Letellier, *Kinetic studies of the action of lactacin F, a bacteriocin produced by Lactobacillus johnsonii that forms poration complexes in the cytoplasmic membrane.* Appl Environ Microbiol, 1994. **60**(3): p. 1006-13.
159. Chen, Y., R.D. Ludescher, and T.J. Montville, *Influence of lipid composition on pediocin PA-1 binding to phospholipid vesicles.* Appl Environ Microbiol, 1998. **64**(9): p. 3530-2.
160. Corbier, C., et al., *Biological activities and structural properties of the atypical bacteriocins mesenterocin 52b and leucocin b-ta33a.* Appl Environ Microbiol, 2001. **67**(4): p. 1418-22.

161. Vadyvaloo, V., et al., *Cell-surface alterations in class IIa bacteriocin-resistant Listeria monocytogenes strains.* Microbiology, 2004. **150**(Pt 9): p. 3025-33.
162. Jacquet, T., et al., *Antibacterial activity of class IIa bacteriocin Cbn BM1 depends on the physiological state of the target bacteria.* Res Microbiol, 2012. **163**(5): p. 323-31.
163. Strauss, J., et al., *Binding, inactivation, and adhesion forces between antimicrobial peptide cecropin P1 and pathogenic E. coli.* Colloids and Surfaces B: Biointerfaces, 2010. **75**(1): p. 156-164.
164. *Microbial Surfaces*. ACS Symposium Series. Vol. 984. 2008: American Chemical Society. 372.
165. Gregory, K. and C.M. Mello, *Immobilization of Escherichia coli cells by use of the antimicrobial peptide cecropin P1*. Appl Environ Microbiol, 2005. **71**(3): p. 1130-4.
166. Jonkheijm, P., et al., *Chemical strategies for generating protein biochips.* Angew Chem Int Ed Engl, 2008. **47**(50): p. 9618-47.
167. Wang, K., et al., *Molecular engineering of DNA: molecular beacons.* Angew Chem Int Ed Engl, 2009. **48**(5): p. 856-70.
168. McFadden, P., *Tech.Sight. Biosensors. Broadband biodetection: Holmes on a chip.* Science, 2002. **297**(5589): p. 2075-6.
169. Rusmini, F., Z. Zhong, and J. Feijen, *Protein immobilization strategies for protein biochips.* Biomacromolecules, 2007. **8**(6): p. 1775-89.
170. Phizicky, E., et al., *Protein analysis on a proteomic scale.* Nature, 2003. **422**(6928): p. 208-15.
171. Zhu, H., et al., *Global analysis of protein activities using proteome chips.* Science, 2001. **293**(5537): p. 2101-5.
172. Zhu, H. and M. Snyder, *Protein chip technology.* Curr Opin Chem Biol, 2003. **7**(1): p. 55-63.
173. Schweitzer, B., P. Predki, and M. Snyder, *Microarrays to characterize protein interactions on a whole-proteome scale.* Proteomics, 2003. **3**(11): p. 2190-9.
174. Balamurugan, S., et al., *Surface immobilization methods for aptamer diagnostic applications.* Anal Bioanal Chem, 2008. **390**(4): p. 1009-21.
175. Kjos, M., I.F. Nes, and D.B. Diep, *Class II one-peptide bacteriocins target a phylogenetically defined subgroup of mannose phosphotransferase systems on sensitive cells.* Microbiology, 2009. **155**(Pt 9): p. 2949-61.
176. Fimland, G., V.G. Eijsink, and J. Nissen-Meyer, *Mutational analysis of the role of tryptophan residues in an antimicrobial peptide.* Biochemistry, 2002. **41**(30): p. 9508-15.
177. Xue, J., et al., *Novel activator of mannose-specific phosphotransferase system permease expression in Listeria innocua, identified by screening for pediocin AcH resistance.* Appl Environ Microbiol, 2005. **71**(3): p. 1283-90.
178. Escher, S.E., E. Klüver, and K. Adermann, *Fmoc-based synthesis of the human CC chemokine CCL14/HCC-1 by SPPS and native chemical ligation.* Letters in Peptide Science, 2001. **8**(6): p. 349-357.

179. Boyne, A.F. and G.L. Ellman, *A methodology for analysis of tissue sulfhydryl components.* Analytical Biochemistry, 1972. **46**(2): p. 639-653.
180. Briand, E., et al., *Immobilization of Protein A on SAMs for the elaboration of immunosensors.* Colloids Surf B Biointerfaces, 2006. **53**(2): p. 215-24.
181. Lu, W.Y., M.A. Qasim, and S.B.H. Kent, *Comparative total syntheses of turkey ovomucoid third domain by both stepwise solid phase peptide synthesis and native chemical ligation.* Journal of the American Chemical Society, 1996. **118**(36): p. 8518-8523.
182. Ingenito, R., et al., *Solid Phase Synthesis of Peptide C-Terminal Thioesters by Fmoc/t-Bu Chemistry.* Journal of the American Chemical Society, 1999. **121**(49): p. 11369-11374.
183. Johnson, E.C.B. and S.B.H. Kent, *Insights into the mechanism and catalysis of the native chemical ligation reaction.* Journal of the American Chemical Society, 2006. **128**(20): p. 6640-6646.
184. Bain CD, T.E., Tao Y-T, Evall J, Whitesides GM, Nuzzo RG. , *Formulation of monolayer films by spontaneous assembly of organic thiols from solution onto gold.* J Am Chem Soc, 1989. **111**: p. 321–35.
185. Tielens F, C.D., Humblot V, Pradier C-M. , *Characterization of w-functionalized undecanethiol mixed self-assembled monolayers on Au(111) : a combined polarization modulation infrared reflection–absorption spectroscopy/X-ray photoelectron spectroscopy/periodic density functional theory study.* . J Phys Chem B, 2008. **182–90**.
186. Bertilsson L, L.B., *Infrared study of thiol monolayer assemblies on gold:preparation, characterization, and functionalization of mixed monolayers.* Langmuir, 1993. **9(1)**: p. 141–9.
187. Oppegard, C., et al., *Analysis of the two-peptide bacteriocins lactococcin G and enterocin 1071 by site-directed mutagenesis.* Appl Environ Microbiol, 2007. **73**(9): p. 2931-8.
188. Tagg, J.R., A.S. Dajani, and L.W. Wannamaker, *Bacteriocins of gram-positive bacteria.* Bacteriol Rev, 1976. **40**(3): p. 722-56.
189. Klaenhammer, T.R., *Bacteriocins of lactic acid bacteria.* Biochimie, 1988. **70**(3): p. 337-49.
190. Guder, A., I. Wiedemann, and H.G. Sahl, *Posttranslationally modified bacteriocins--the lantibiotics.* Biopolymers, 2000. **55**(1): p. 62-73.
191. Entian, K.D. and C. Klein, *[Lantibiotics, a class of ribosomally synthesized peptide antibiotics]*. Naturwissenschaften, 1993. **80**(10): p. 454-60.
192. Senes, A., M. Gerstein, and D.M. Engelman, *Statistical analysis of amino acid patterns in transmembrane helices: the GxxxG motif occurs frequently and in association with beta-branched residues at neighboring positions.* J Mol Biol, 2000. **296**(3): p. 921-36.
193. Qi, F., P. Chen, and P.W. Caufield, *The group I strain of Streptococcus mutans, UA140, produces both the lantibiotic mutacin I and a nonlantibiotic bacteriocin, mutacin IV.* Appl Environ Microbiol, 2001. **67**(1): p. 15-21.

194. Senes, A., D.E. Engel, and W.F. DeGrado, *Folding of helical membrane proteins: the role of polar, GxxxG-like and proline motifs.* Curr Opin Struct Biol, 2004. **14**(4): p. 465-79.
195. Senes, A., I. Ubarretxena-Belandia, and D.M. Engelman, *The Calpha --- H...O hydrogen bond: a determinant of stability and specificity in transmembrane helix interactions.* Proc Natl Acad Sci U S A, 2001. **98**(16): p. 9056-61.
196. Oppegard, C., et al., *Mutational analysis of putative helix-helix interacting GxxxG-motifs and tryptophan residues in the two-peptide bacteriocin lactococcin G.* Biochemistry, 2008. **47**(18): p. 5242-9.
197. de Planque, M.R., et al., *Different membrane anchoring positions of tryptophan and lysine in synthetic transmembrane alpha-helical peptides.* J Biol Chem, 1999. **274**(30): p. 20839-46.
198. Ridder, A.N., et al., *Analysis of the role of interfacial tryptophan residues in controlling the topology of membrane proteins.* Biochemistry, 2000. **39**(21): p. 6521-8.
199. Feller, S.E.V., R. M.; Pastor, R. W., *Computer simulation of a DPPC phospholipid bilayer: Structural changes as a function of molecular surface area.* Langmuir, 1997. **13**: p. 6555.
200. Guex, N. and M.C. Peitsch, *SWISS-MODEL and the Swiss-PdbViewer: an environment for comparative protein modeling.* Electrophoresis, 1997. **18**(15): p. 2714-23.
201. Lindahl, E., B. Hess, and D. van der Spoel, *GROMACS 3.0: a package for molecular simulation and trajectory analysis.* Journal of Molecular Modeling, 2001. **7**(8): p. 306-317.
202. D.V. Spoel, A.R.v., E. Apol, P.J. Meulenhoff, D.P. Tieleman, A.L.T.M. Sijbers, B. Hess, K.A. Feenstra, E. Lindahl, R. vanDrunen, H. J.C. Berendsen, Gromacs User Manual Version 3.1.1, Nijenborgh4, 9747 AG Groningen, The Netherlands, Internet: www.gromacs.org, 2002.
203. T. Darden, D.Y., and L. Pedersen. , J Chem Phys, 1993. **98**: p. 10089-10092.
204. H. J. C. Berendsen, J.P.M.P., W. F. van Gunsteren, A. Di Nola, and J. R. Haak., J Chem Phys, 1984. **81**: p. 3684-3690.
205. B. Hess, H.B., H.J.C. Berendsen, J. Fraaije, LINCS: a linear constraint solver for molecular simulations, J. Comp. Chem., 1997. **18**: p. 1463–1472.
206. MSI. Molecular Simulations Inc., U., (http://molsim.vei.co.uk/weblab/) 1998.
207. Soliman, W., S. Bhattacharjee, and K. Kaur, *Interaction of an antimicrobial peptide with a model lipid bilayer using molecular dynamics simulation.* Langmuir, 2009. **25**(12): p. 6591-5.
208. Mehrnejad, F. and M. Zarei, *Molecular dynamics simulation study of the interaction of Piscidin 1 with DPPC bilayers: structure-activity relationship.* J Biomol Struct Dyn, 2010. **27**(4): p. 551-60.
209. Leontiadou, H., A.E. Mark, and S.J. Marrink, *Antimicrobial peptides in action.* J Am Chem Soc, 2006. **128**(37): p. 12156-61.

210. Killian, J.A. and G. von Heijne, *How proteins adapt to a membrane-water interface.* Trends Biochem Sci, 2000. **25**(9): p. 429-34.
211. Schiffer, M., C.H. Chang, and F.J. Stevens, *The functions of tryptophan residues in membrane proteins.* Protein Eng, 1992. **5**(3): p. 213-4.
212. Espy, M.J., et al., *Real-time PCR in clinical microbiology: applications for routine laboratory testing.* Clin Microbiol Rev, 2006. **19**(1): p. 165-256.
213. McKillip, J.L. and M. Drake, *Real-time nucleic acid-based detection methods for pathogenic bacteria in food.* J Food Prot, 2004. **67**(4): p. 823-32.
214. Yang, L. and R. Bashir, *Electrical/electrochemical impedance for rapid detection of foodborne pathogenic bacteria.* Biotechnol Adv, 2008. **26**(2): p. 135-50.
215. AOAC, *Salmonella in food, automated conductance methods: AOAC official method 991.38. Official Methods of Analysis of AOAC International, 16th ed.,* . Association of Official Analytical Chemists International; Gaithersburg, MD, 1996.
216. Silley, P. and S. Forsythe, *Impedance microbiology--a rapid change for microbiologists.* J Appl Bacteriol, 1996. **80**(3): p. 233-43.
217. Wawerla, M., et al., *Impedance microbiology: applications in food hygiene.* J Food Prot, 1999. **62**(12): p. 1488-96.
218. Ruan, C., L. Yang, and Y. Li, *Immunobiosensor chips for detection of Escherichia coil O157:H7 using electrochemical impedance spectroscopy.* Anal Chem, 2002. **74**(18): p. 4814-20.

Appendix

A.1. Protocol for LeuA Synthesis on the Automated Peptide Synthesizer MPS 357 FOR AMINO ACIDS 2-11:-

1. Fill CV with 100 ml of DMF
2. Mix for 20.0 minute(s) on speed 5
3. Empty collection vessel
4. Fill CV with 2.0ml of AA
5. Fill CV with 2.0ml of DIC
6. Mix both for 60.0 minute(s) on speed 5
7. Empty collection vessel
8. Fill CV with 5.0 ml of DMF
9. Mix both for 2.0 minute(s) on speed 5
10. Empty collection vessel
11. Fill CV with 2.0ml of AA
12. Fill CV with 2.0ml of DIC
13. Mix both for 60.0 minute(s) on speed 5
14. Empty collection vessel
15. Fill CV with 5.0 ml of DMF
16. Mix both for 2.0 minute(s) on speed 5
17. Empty collection vessel
18. Fill CV with 5.0 ml of DCM
19. Mix both for 2.0 minute(s) on speed 5
20. Empty collection vessel
21. Fill CV with 5.0 ml of DMF
22. Mix both for 2.0 minute(s) on speed 5
23. Empty collection vessel
24. Fill CV with 3.0 ml of PIP
25. Fill CV with 1.0 ml of HoBt
26. Mix both for 8.0 minute(s) on speed 5
27. Empty collection vessel
28. Repeat from step 25, 1 time(s)
29. Fill CV with 5.0 ml of DMF
30. Mix both for 2.0 minute(s) on speed 5
31. Empty collection vessel
32. Fill CV with 5.0 ml of DCM
33. Mix both for 2.0 minute(s) on speed 5
34. Empty collection vessel
35. Fill CV with 5.0 ml of DMF
36. Mix both for 2.0 minute(s) on speed 5
37. Empty collection vessel
38. End 83

THE PROTOCOL FOR AMINO ACIDS 11-20:-

1. Fill CV with 100 ml of DMF
2. Mix for 20.0 minute(s) on speed 5
3. Empty collection vessel
4. Fill CV with 2.0ml of AA
5. Fill CV with 2.0ml of DIC
6. Mix both for 60.0 minute(s) on speed 5
7. Empty collection vessel
8. Fill CV with 5.0 ml of DMF
9. Mix both for 2.0 minute(s) on speed 5
10. Empty collection vessel
11. Fill CV with 2.0ml of AA
12. Fill CV with 2.0ml of DIC
13. Mix both for 60.0 minute(s) on speed 5
14. Mix both for 60.0 minute(s) on speed 5
15. Empty collection vessel
16. Fill CV with 5.0 ml of DMF
17. Mix both for 60.0 minute(s) on speed 5
18. Empty collection vessel
19. Fill CV with 5.0 ml of DCM
20. Mix both for 2.0 minute(s) on speed 5
21. Empty collection vessel
22. Fill CV with 2.0 ml of NMM
23 Fill CV with 2.0 ml of HBTU (this is acetic anhydride in the bottle)
24. Mix both for 10.0 minute(s) on speed 5
25. Repeat from step 18, 1 time(s)
26. Empty collection vessel
27. Fill CV with 5.0 ml of DMF
28. Mix both for 60.0 minute(s) on speed 5
29. Empty collection vessel
30. Fill CV with 5.0 ml of DCM
31. Mix both for 2.0 minute(s) on speed 5
32. Empty collection vessel
33. Fill CV with 3.0 ml of PIP
34. Fill CV with 1.0 ml of HoBt
35. Mix both for 8.0 minute(s) on speed 5
36. Empty collection vessel
37. Repeat from step 25, 1 time(s)
38. Fill CV with 5.0 ml of DMF
39. Mix both for 60.0 minute(s) on speed 5
40. Empty collection vessel
41. Fill CV with 5.0 ml of DCM
42. Mix both for 2.0 minute(s) on speed 5
43. Empty collection vessel
44. Fill CV with 5.0 ml of DMF 84

45. Mix both for 2.0 minute(s) on speed 5
46. Empty collection vessel
47. End

Procedure A.2: Measuring the Peptide Biological Activity antibacterial Using Agar-plate Assay (Spot in Lawn Assay).

Materials used:

Agar, APT broth, Disposable culture tubes, sterile Petri dishes, sterile glass bottles for preparation of culture media, and sterile tips

Bacterial Indicators:

Carnobacteriocin divergens LV13 (or UAL9) and *Listeria monocytogenes*

Protocol:

- **Plate media:** Dissolve 4.62 gm of APT broth in 100 mL of MilliQ water at room temperature, add 1.5% agar (1.5 gm/100mL), and shake gently.
- **Soft agar:** Dissolve 4.62 gm of APT broth in 100 mL of water; add 0.75% agar (0.75 gm/100 mL).
- **Culture media:** dissolve 4.26 APT/100 mL of water; pour them in the culture tubes (6mL/tube).
- Autoclave the above three preparations for 15 min at 121^0C (don't overheat or leave longer)
- While hot, pour the hard agar (in a biosafety cabinet or near the flame) 10 mL/plate.
- Pour the soft agar, while hot, in sterile tubes 6mL/tube, leave it to dry.
- Keep all in the fridge till use (plated are kept upside down)

- **Indicator subculture:** using the inoculating lobe or sterile tips, touch it in the frozen bacteria and put it in the culture media (APT broth), leave in the incubator at 37^0 overnight.

- **Bioactivity test:**

✓ Mark the plate with numbers at the bottom side
✓ Spot the peptides on the agar plate and then leave the spots to dry.
✓ Take one APT soft agar tube (which was heated to liquefy) leave it till worm (around 45 ^{0}C), quickly add 60 μL of the indicator stain, shake gently and then pour on the plate.
✓ Let the plate dry, incubate at 37 ^{0}C overnight.

A.3. Confocal Microscopy Images of Peptide-bacterial Interactions.

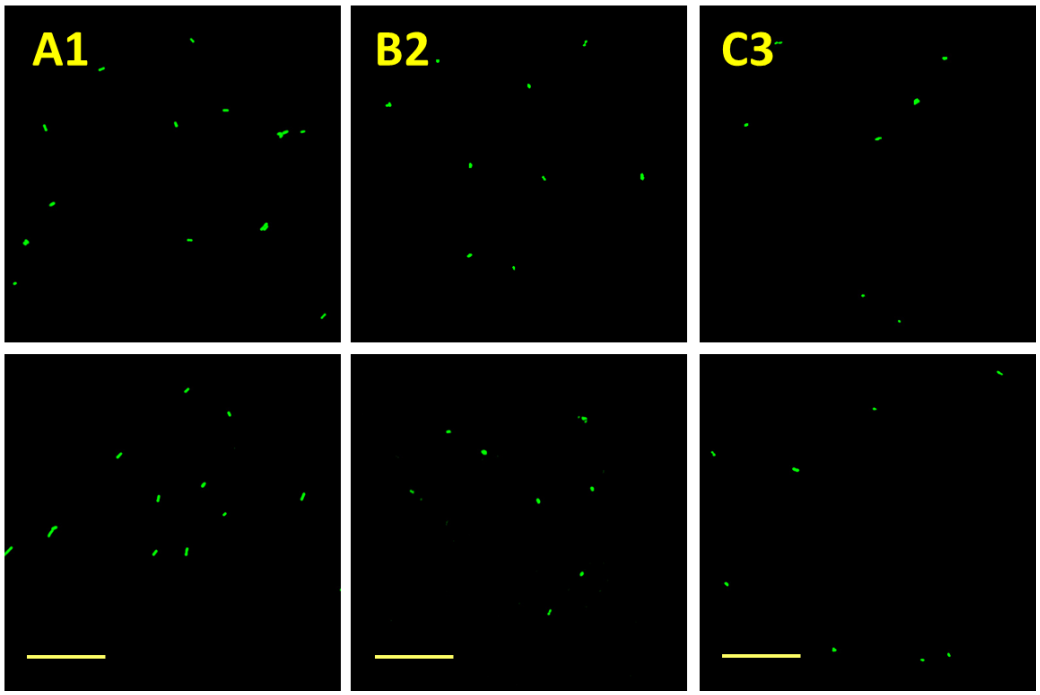

A.3a. Confocal microscopy images of the bacterial adsorption. Top row is a demonstration of peptide-free surfaces A1, B1 and C1 were incubated with three different bacterial concentrations respectively as 10^6, 10^4, and 10^2 cfu/mL. Bottom row shows adsorption of the bacteria (*C.divergens*) at 14-AA-coated surfaces at three different bacterial concentrations, 10^6, 10^4, and 10^2 cfu/mL for A2, B2, and C2, respectively. Scale bars are 10 μm.

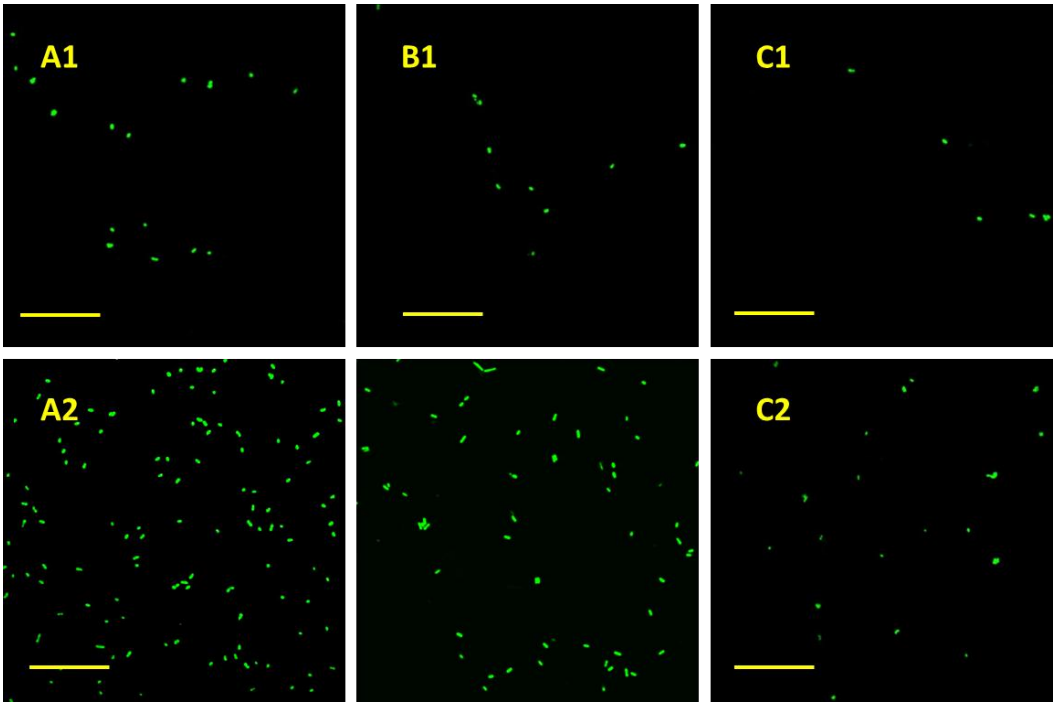

A.3b. Confocal microscopy of the selective binding of peptide (24 AAs LeuA). **Up row** is a demonstration of peptide-free surfaces as negative controls A1, B1 and C1 were incubated with three different concentrations of C.divergens respectively as 10^6 , 10^4, and 10^2 cfu/mL. **Bottom row** shows binding of the immobilized peptide to stained bacterial cell (*C.divergens*) at three different concentrations, 10^6, 10^4, and 10^2 cfu/mL for A2, B2, and C2, respectively. Scale bars are 10 μm.

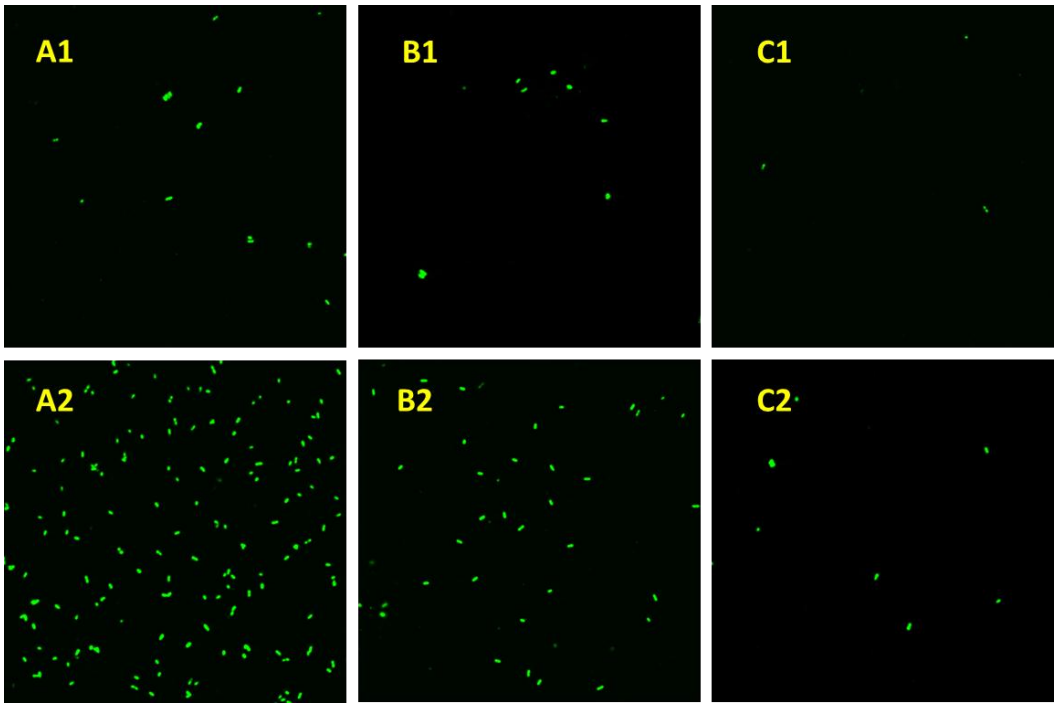

A.3c. Confocal microscopy of the selective binding of peptide (24 AAs LeuA). **Up row** is a demonstration of peptide-free surfaces as negative controls A1, B1 and C1 were incubated with three different concentrations of *L.monocytogenes* respectively as 10^6, 10^4, and 10^2 cfu/mL. **Bottom row** shows binding of the immobilized peptide to stained bacterial cell (*L.monocytogenes*) at three different concentrations, 10^6, 10^4, and 10^2 cfu/mL for A2, B2, and C2, respectively. Scale bars are 10 μm.

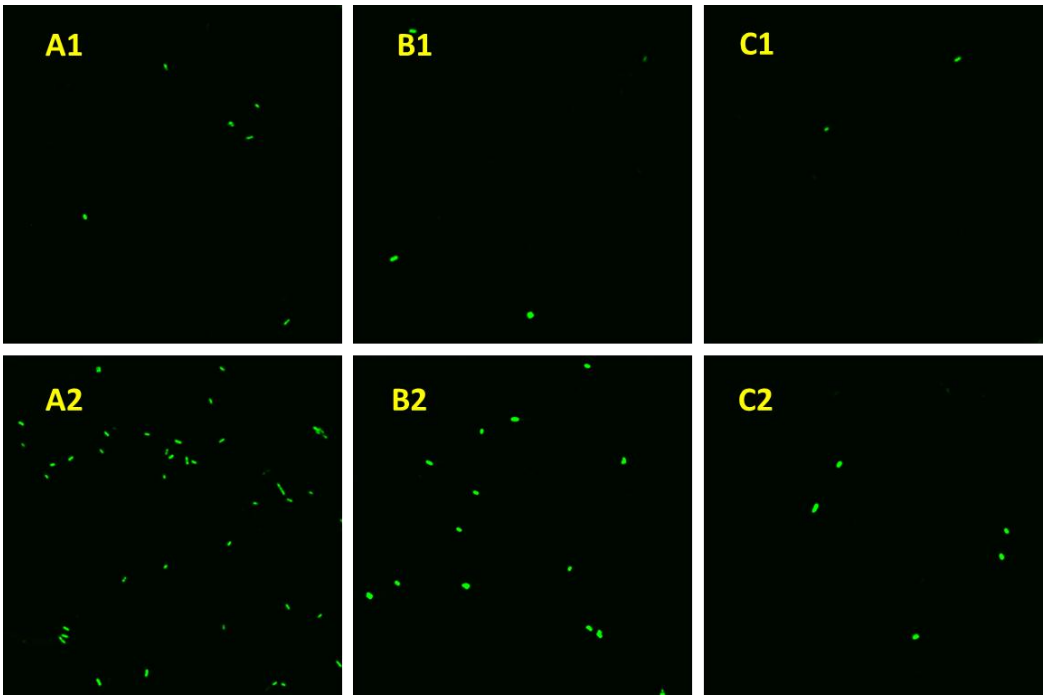

A.3d. Confocal microscopy of the selective binding of peptide (24 AAs LeuA). **Up row** is a demonstration of peptide-free surfaces as negative controls A1, B1 and C1 were incubated with three different concentrations of *L.innocua* respectively as 10^6 , 10^4, and 10^2 cfu/mL. **Bottom row** shows binding of the immobilized peptide to stained bacterial cell (*L.innocua*) at three different concentrations, 10^6, 10^4, and 10^2 cfu/mL for A2, B2, and C2, respectively. Scale bars are 10 μm.

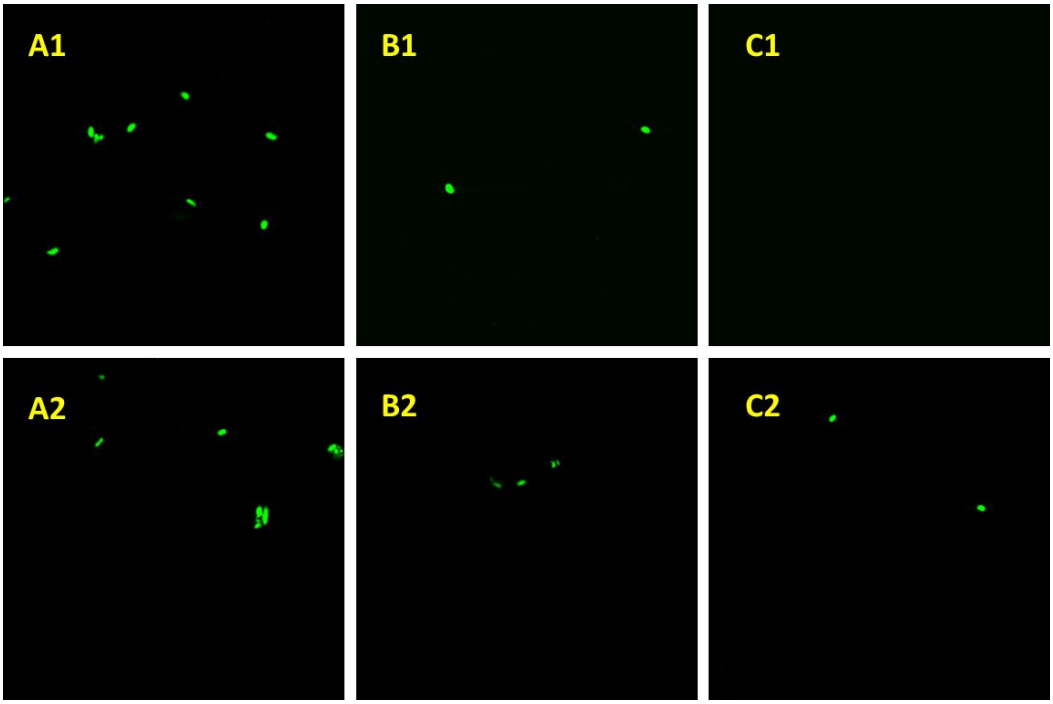

A.3e. Confocal microscopy of the binding of peptide (24 AAs LeuA). **Up row** demonstration of peptide-free surfaces as negative controls A1, B1 and C1 were incubated with three different bacterial concentrations respectively as 10^6, 10^4, and 10^2 cfu/mL. **Bottom row** adsorption of the bacteria (E.coli) on 24-AA-coated surfaces at three different bacterial concentrations, 10^6, 10^4, and 10^2 cfu/mL for A2, B2, and C2, respectively. Scale bars are 10 μm.